Black Holes, Black Rings and their Microstates

Iosif Lucian Răzvan Bena

Institut de Physique Théorique, CEA/Saclay
F-91191 Gif-sur-Yvette CEDEX

Abstract

In this thesis we describe some of the recent progress towards the construction and analysis of three-charge configurations in string theory and supergravity, and discuss the implications of the existence of these solutions for the physics of black holes. We begin by describing the Born-Infeld construction of three-charge supertubes with two dipole charges, and then discuss the general method of constructing three-charge solutions in five dimensions. We explain in detail the use of these methods to construct black rings, black holes, as well as smooth microstate geometries with black hole and black ring charges, but with no horizon. We present arguments that many of these microstate geometries are dual to boundary states that belong to the same sector of the D1-D5-P CFT as the typical states. We then discuss scaling microstate solutions, that are smooth, horizonless, and can classically have a throat of infinite size. We address several puzzles related to the physics of these solutions. In the final part of the thesis we analyze supertube that probe microstate solutions. We argue that generically supertubes give rise to smooth horizonless geometries, and that the entropy of these supertubes is much larger than that of supertubes in flat space, and might have a growth with the charges similar to that of a black hole.

Contents

1 Introduction

Black holes are very interesting objects, whose physics brings quantum mechanics and general relativity into sharp contrast. Perhaps the best known, and sharpest, example of such contrast is Hawking's information paradox [1]. This has provided a very valuable guide and testing ground in formulating a quantum theory of gravity. Indeed, it is one of the relatively few issues that we know *must* be explained by a viable theory of quantum gravity.

String theory is a quantum theory of gravity, and has had several astounding successes in describing properties of black holes. In particular, Strominger and Vafa have shown [2] that one can count microscopic configurations of branes and strings at zero gravitational coupling, and exactly match their statistical entropy to the Bekenstein-Hawking entropy of the corresponding black hole at large effective coupling.

Another way to understand the Strominger-Vafa entropy matching is via the *AdS*-CFT correspondence[1] [3]. One can make a black hole in string theory by putting together D5 branes and D1 branes and turning on momentum along the direction of the D1's. If one takes a near horizon limit of this system, one finds a bulk that is asymptotic to $AdS_3 \times S^3 \times T^4$, and which contains a BPS black hole. The dual boundary theory is the two-dimensional conformal field theory that lives on the intersection of the D1 branes and the D5 branes and is known as the D1-D5-P CFT. If one counts the states with momentum N_p and R-charge J in this conformal field theory, one obtains the entropy

$$S = 2\pi\sqrt{N_1 N_5 N_p - J^2}\ , \tag{1}$$

which precisely matches the entropy of the dual black hole [4] in the bulk.

A very important question, with deep implications for the physics of black holes, is: *"What is the fate of these microscopic brane configurations as the effective coupling becomes large?"* Alternatively, the question can be rephrased in *AdS*-CFT language as: *"What is the gravity dual of individual microstates of the D1-D5-P CFT?"* More physically, *"What do the black-hole microstates look like in a background that a relativist would recognize as a black hole?"*

1.1 Two-charge systems

These questions have been addressed for the simpler D1-D5 system[2] by Mathur, Lunin, Maldacena, Maoz, and others, [5, 6, 7, 8, 10, 11], see [13] for earlier work in this direction, and [14] for a review of that work. They found that the states of that CFT can be mapped into two-charge supergravity solutions that are asymptotically $AdS_3 \times S^3 \times T^4$, and have

[1] Historically the AdS-CFT correspondence was found later.

[2] Throughout this thesis we will refer to the D1-D5 system and its U-duals as the "two-charge system", and to the D1-D5-P system and its U-duals as the "three-charge system".

no singularity. These supergravity solutions are determined by specifying an arbitrary closed curve in the space transverse to the D1 and D5 branes, and have a dipole moment corresponding to a Kaluza-Klein monopole (KKM) wrapped on that curve[3]. Counting these configurations [5, 21] has shown that the entropy of the CFT is reproduced by the entropy coming from the arbitrariness of the shape of the closed curve.

While the existence of such a large number of two-charge supergravity solutions might look puzzling – again, these BPS solutions are specified by arbitrary *functions* – there is a simple string-theoretic reason for this. By performing a series of S and T dualities, one can dualize the D1-D5 configurations with KKM dipole charge into configurations that have F1 and D0 charge, and D2-brane dipole moment. Via an analysis of the Born-Infeld action of the D2 brane, these configurations were found by Mateos and Townsend to be supersymmetric, and moreover to preserve the same supersymmetries as the branes whose asymptotic charges they carry (F1 and D0 charge), independent of the shape of the curve that the D2 brane wraps [22, 23, 24]. Hence, they were named "supertubes." Alternatively, one can also dualize the D1-D5 (+ KKM dipole) geometries into F1 string configurations carrying left-moving momentum. Because the string only has transverse modes, the configurations carrying momentum will have a non-trivial shape: Putting the momentum into various harmonics causes the shape to change accordingly. Upon dualizing, the shape of the momentum wave on the F1 string can be mapped into the shape of the supertube [25].

Hence, for the two-charge system, we see that the existence of a large number of supergravity solutions could have been anticipated from the earlier work on microscopic two-charge stringy configurations (supertubes or F1 string carrying left-moving momentum). In Section 3 we will consider three-charge supertubes and discuss how their physics anticipated the discovery of some of the corresponding supergravity solutions that are discussed in Section 4.

1.2 Mathur's Conjecture (or the "Fuzzball Proposal")

An intense research programme has been unfolding over the past few years to try to see whether the correspondence between D1-D5 CFT states and smooth bulk solutions also extends to the D1-D5-P system. The crucial difference between the two-charge system and the three-charge system (in five dimensions) is that in the regime of parameters where all the branes backreact on the geometry, the latter generically has a macroscopic horizon, whereas the former only has an effective horizon at the Planck or string scale.

Indeed, historically, the link between microstate counting and Bekenstein-Hawking entropy (at vanishing string coupling) was first investigated by Sen [26] for the two-charge system. While this work was extremely interesting and suggestive, the result

[3]A system that has a prescribed set of charges as measured from infinity often must have additional dipole charge distributions. We will discuss this further in Section 3, but for the present, one should note the important distinction between asymptotic charges and dipole charges.

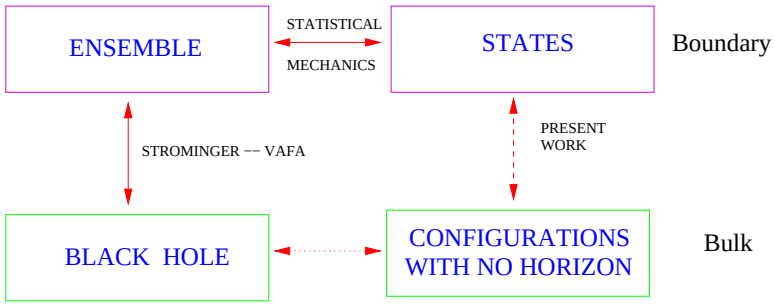

Figure 1: An illustrative description of Mathur's conjecture. Most of the present research efforts go into improving the dictionary between bulk and boundary microstates (the dotted arrow), and into constructing more microstate geometries.

became compelling only when the problem was later solved for the three-charge system by Strominger and Vafa [2]. Similarly, the work on the microstate geometries of two-charge systems is extremely interesting and suggestive, but to be absolutely compelling, it must be extended to the three-charge problem. This would amount to establishing that the boundary D1-D5-P CFT microstates are dual to bulk microstates – configurations that have no horizons or singularities, and which look like a black hole from a large distance, but start differing significantly from the black hole solution at the location of the would-be horizon.

String theory would then indicate that a black hole solution of classical general relativity should not be viewed as a fundamental object in quantum gravity, but rather as an effective "thermodynamic" description of an ensemble of horizonless configurations with the same macroscopic/asymptotic properties. (See Fig. 1.) The black hole horizon would be the place where these configurations start differing from each other, and the classical "thermodynamic" description of the physics via the black hole geometry stops making sense.

An analogy that is useful in understanding this proposal is to think about the air in a room. One can use thermodynamics and fluid mechanics to describe the air as a continuous fluid with a certain equation of state. One can also describe the air using statistical mechanics, by finding the typical configurations of molecules in the ensemble, and noticing that the macroscopic features of these configurations are the same as the ones found in the thermodynamic description. For most practical purposes the thermodynamic description is the one to use; however, this description fails to capture the physics coming from the molecular structure of the air. To address problems like Brownian motion, one should not use the thermodynamic approximation, but the statistical description. Similarly, to address questions having to do with physics at the scale of the horizon (like the information paradox) one should not use the thermodynamic approximation (given by the classical black hole solution), but one should use the statistical description, given

by the microstate configurations.

This dramatic shift in the description of black holes, has been most articulately proposed and strongly advocated by Mathur, and is thus often referred to as "Mathur's conjecture" or the "fuzzball proposal." In fact, one should be careful and distinguish two variants of this conjecture. The weak variant is that the typical microstates are horizon-sized stringy configurations that have unitary scattering, but have generically large curvature (Planck scale), and hence cannot be described accurately using the supergravity approximation. The strong form of Mathur's conjecture, which is better defined and easier to prove or disprove, is that the Hilbert space of *typical* black hole microstates is spanned by smooth solutions that can be described using supergravity.

In either form, Mathur's conjecture represents quite a drastic departure from classical wisdom about black holes. Indeed, in classical general relativity one constructs black hole solutions, and then argues that the curvature at the black hole horizon is small, and hence there is no reason for the region around the black hole horizon, and the inside of the black hole in general, not to be accurately described by classical relativity. Indeed, at the black hole singularity the curvature becomes large, classical relativity breaks down and quantum gravity effects become important. However, because the singularity of the black hole is far away from (and for non-extremal black holes also in the future of) the horizon, these quantum effects are not expected to drastically affect the physics at the horizon. The larger the black hole, the smaller the curvature at the horizon is, and the larger the distance (or time) from the horizon to the singularity. Hence, using a plastic expression, one can say that somebody could fall through the horizon of a huge black hole (with a small horizon curvature) drinking his coffee, and would have no idea it fell through a horizon before it would realize, much later, that it is approaching a singularity that cannot be avoided.

Mathur's conjecture (or at least the author's reading of this conjecture) implies this picture is false – if the classical black hole solution breaks down at the horizon, and the description in terms of a huge number of microstates takes over, then this region is not accurately described any more by classical general relativity. Quantum effects are not localized at the black hole singularity, but rather spread over a very large distance, all the way to the black hole horizon. The essential reason for this is that the degrees of freedom available at the singularity can have a very low mass, and hence by the uncertainty principle can spread over a very large distance. This mechanism is well understood for BPS black holes, and can be argued to extend to non-BPS black holes as well – more details on this can be found in the review articles [14].

In fact, the resolution of a singularity via low-mass modes that affect the physics on a *macroscopic* scale, that is much larger than the size of the region of high curvature near the singularity is nothing new in string theory: The best-known examples are the Polchinski-Strassler configurations dual to vacua of the $\mathcal{N} = 1^*$ theory, and the LLM solutions, which can be thought of as resolutions of singular giant gravitons. The only difference between those systems and extremal black holes is that the timelike singularity is not cloaked by

a horizon. However, it is quite unclear why the size of the region over which the timelike singularity is resolved has anything to do with the presence of a horizon; indeed, our work indicates that for the timelike singularity corresponding to extremal black holes, this size is also much larger than the size of the large-curvature region, and is in fact given by the horizon size. [4] Furthermore, as we will argue in Subsection 1.5, and will see from the explicit construction in Section 10, quantum effects might in fact affect not only solutions with a horizon, but even smooth horizonless-solutions that have the same asymptotics a black hole !

One should also mention that the idea that quantum effects could extend all the way to the black hole horizon has been popping up here and there in the work of many people studying black holes and quantum gravity. Indeed, replacing the black hole by a horizon-sized chunk of absorbing "stuff" would automatically solve Hawking's information paradox, and hence is a rather seducing idea, which has been at times embraced not only by string theorists, but by people studying quantum field theory in curved space (the gravastars of Mazur and Mottola are perhaps the best-known candidates [120]) or Loop-Quantum-Gravity [121].

The main problem with all these "black hole replacements" is that they are supposed to have the same size as the black hole. If one thinks about this a bit, this is a very stringent requirement: if gravity becomes stronger the black hole horizon grows ! In contrast, the size of all the objects we are familiar with (like stars or planets) and in general of any object supported against gravitational collapse by a non-gravitational force becomes smaller and smaller as gravity becomes stronger.

In the author's opinion, Mathur's conjecture is the string-theoretic version of these proposals. It's key advantage is that – unlike in the other proposals – one can honestly construct and analyze the microstate geometries that are supposed to replace the black hole, one can argue that there is a huge number of such geometries, and one can prove that the size of these geometries has the same growth with Newton's constant as the size of the black hole horizon, thus solving the problem discussed in the previous paragraph (to our knowledge, the correct growth with Newton's constant has not been established in the other proposals to replace the black hole).

The purpose of my research over the past few years has been to construct very large families of horizonless configurations (both in string theory and in supergravity) that have the same charges and the same mass as a classical black hole. Of course, these configurations are classical, and oftentimes have a moduli space. Hence, classically, there is an infinite number of such configurations, that need to be quantized before one can call them *micro*states in the strictest sense of the word. In the analogy with the air in a room, these geometries correspond to classical configurations of molecules. Classically there is an infinite number of such configurations, but one can quantize them and count them to

[4] It is well-possible that for non-extremal black holes the singularity-resolution mechanism might be different - this will be discussed below.

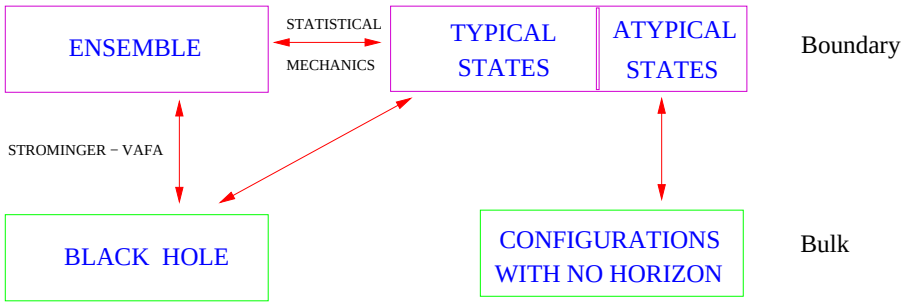

Figure 2: An schematic description of Possibility 1.

find the entropy of the system.

1.3 Three possibilities for the physics of black holes

Our purpose throughout this thesis will be to show that string theory contains a huge number of smooth configurations that have the same charges and asymptotics as the three-charge BPS black hole in five dimensions, and to argue that counting these configurations, or relating them to the states of the boundary CFT will indicate that black holes in string theory are not fundamental objects, but rather a statistical way to describe an ensemble of black-hole-sized configurations with no horizon and with unitary scattering. Nevertheless, even in the absence of a definitive proof of this, the current understanding of black hole microstates makes it well worth exploring in more detail the three logical possibilities about what the physics of three-charge black hole is, or otherwise, the three possible answers to the question: "What is the bulk AdS dual to an individual CFT pure microstate":

Possibility 1: One bulk solution dual to many boundary microstates

It is possible that some of the states of the CFT, and in particular the typical ones (whose counting gives the black hole entropy) do not have individual bulk duals, while some other states do. However this runs counter to all our experience with the AdS-CFT correspondence: In all the examples that have been extensively studied and well-understood (like the D1-D5 system, Polchinski-Strassler [99], giant gravitons and LLM [102, 95], the D4-NS5 system [104]) the AdS-CFT correspondence relates boundary states to bulk states and boundary vacua to bulk vacua.

It is logically possible that, for the D1-D5-P system only, the path integrals in the bulk and on the boundary are related in the standard way via the AdS-CFT correspondence, and yet all the boundary states that give the CFT entropy are mapped into one black hole solution in the bulk. This possibility is depicted in Fig. 2. However, this possibility raises a lot of questions. First, why would the D1-D5-P system be different from all the

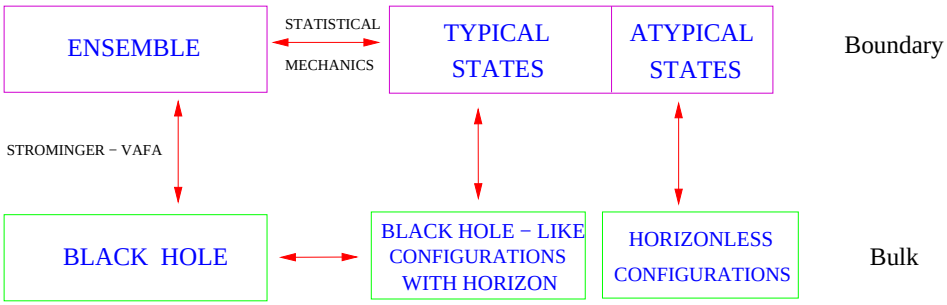

Figure 3: An schematic description of Possibility 2.

other systems mentioned above. Moreover, from the microscopic (or CFT) perspective, there is nothing special about having three charges: One can map the boundary states in the D1-D5-KKM system in *four* dimensions to the corresponding bulk microstates [35, 105, 106]. The only reason for which the D1-D5-P system would be different from all the other systems would be the fact that it has the right amount of charges to create a macroscopically-large event horizon in five dimensions. To have such divergently different behavior for the D1-D5-P system in five dimensions would be, depending on one's taste, either very deep or, more probably, very bizarre.

Even if the typical states of the three-charge system correspond to one single black hole, we have seen that besides this black hole there exists a huge number of smooth solutions that also are dual to individual states of this CFT. Hence, according to Possibility 1, some states of the CFT would have individual bulk duals and some others would not (they would be dual as an ensemble to the black hole). This distinction is very unnatural. One might explain this if the states dual to the black hole and the ones dual to microstate geometries are in different sectors of the CFT, but this is simply not the case. As we will see in Section 9.6, the deep bulk microstates correspond to boundary states that have one (or several) long component string(s). Hence, they belong to the same CFT sector as the typical microstates. If typical microstates did not have individual bulk duals, then in the same sector of the CFT we would have both states with a bulk dual and states without one. While not obviously wrong, this appears, at least, dubious and unjustifiable from the point of view of the CFT.

Possibility 2: Typical bulk microstate very similar to black hole.

It is possible that all the states of the CFT are dual to geometries in the bulk, but the typical states are dual to geometries that have a horizon, and that only differ from the classical black hole by some Planck-sized fuzz near the singularity. This situation is depicted in Fig. 3.

This also has a few problems. First, there are arguments, [14], that if the microstates of the black hole only differ from the classical geometry near the singularity, this does

not solve the information paradox. Putting such arguments on one side, there is a more obvious objection: Possibility 2 means that typical microstates would have horizons, and so it would seem that one would have to ascribe an entropy to each microstate, which violates one of the principles of statistical mechanics. A counterargument here is to observe that one can always ascribe an ad hoc entropy to a microstate of any system simply by counting the number of states with the same macroscopic properties. What really distinguishes a microstate from an ensemble is that one has complete knowledge of the state of the former and that one has lost some knowledge of the state in the latter. The counterargument asserts that the presence of the horizon does not necessarily indicate information loss, and that the complete information might ultimately be extracted from something like the Hawking radiation. Thus microstates could have a horizon if information is somehow stored and not lost in the black hole. This is a tenable viewpoint and it is favored by a number of relativists but it defers the issue of how one decodes the microstate information to some unknown future physics whereas string theory appears to be pointing to a very interesting answer in the present.

There is also one of the objections raised in possibility 1: We have seen that some CFT states corresponding to long component strings are dual to deep microstates, that have no horizon. If the second possibility is correct, then other states in *the same sector* of the CFT would be dual to geometries that have a horizon and a singularity, and are therefore drastically different. Moreover, for extremal black holes, the distance to the horizon is infinite, while the distance to the cap of the microstates is finite (though divergent in the classical limit). Hence, in the same sector of the CFT, some states would be dual to supergravity solutions with an infinite throat, while others would be dual to solutions with a finite throat. This again appears quite dubious from the point of view of the CFT.

One can also think about obtaining the bulk microstate geometries by starting from a weak-coupling microstate (which is a certain configuration of strings and branes) and increasing the string coupling. During this process, we can imagine measuring the distance to the configuration. If a horizon forms, then this distance would jump from being finite to being infinite. However, for the smooth microstates, this distance is always a continuous function of the string coupling, and never becomes infinite. While the infinite jump of the length of the throat is a puzzling phenomenon, equally puzzling is the fact that only some microstates would have this feature, while some very similar ones would not[5].

Possibility 3: Typical bulk microstates differ from black hole at the scale of the horizon.

It is possible that all boundary microstates are dual to horizonless configurations. The classical black hole geometry is only a thermodynamic description of the physics, which stops being valid at the scale of the horizon, much like fluid mechanics stops being a good description of a gas at scales of order the mean free path. For physics at the horizon

[5]We thank Samir Mathur for pointing out this argument to us.

scale, one cannot rely on the thermodynamic description, and has to use a "statistical" description in terms of a large number of microstates. This possibility is depicted in Fig. 1.

Since these microstates have no horizon, they have unitary scattering but it takes a test particle a very long time to escape from this microstate. Hence, if this possibility is correct, the information paradox is reduced to nothing but an artifact of using a thermodynamic description beyond its regime of validity. This possibility now splits into two options, having to do with the appropriate description of the typical black hole microstates:

Possibility 3A: Typical microstates have curvature of order the Planck scale, and therefore cannot be described in supergravity and require the full force of string theory.

Possibility 3B: Typical microstates have curvature smaller than the Planck scale, and therefore can be described in supergravity.

As we cannot, yet, explore or count large strongly-interacting horizon-sized configurations of branes and strings using our current string theory technology, Possibility 3A would be more challenging to establish or analyze. We therefore need to examine Possibility 3B in great detail to see if it is true, or at least determine the extent to which supergravity can be used. One way to do this is by counting the microstates, using for example counting techniques of the type used in [21]. Another approach is to find the exact (or even approximate) dictionary between the states of the CFT and the bubbled geometries in the bulk. Anticipating (or perhaps speculating) a bit, one could imagine that, as a result of this investigation, one could relate the number of bubbles of a deep microstate to the distribution of the momentum on the long component string of the dual CFT state. Such a relation (which could in principle be obtained using scattering experiments as in [7, 31]) would indicate whether typical bulk microstates have large bubbles or Planck-sized bubbles, and would help distinguish between Possibilities 3A and 3B.

One of the interesting questions that needs to be addressed here is: *What about non-extremal black holes?*. All the arguments presented in this thesis in favor of the third possibility have been based on supersymmetric black holes, and one can legitimately argue that even if these black holes describe an ensemble of smooth horizonless configurations, it may be that non-supersymmetric black holes (like the ones we have in the real world) are fundamental objects, and not ensembles. The arguments put forth to support Possibility 3 for non-extremal black holes are rather more limited. Indeed, on a technical level, it is much more difficult to find non-supersymmetric, smooth microstate geometries, but some progress has been made [83]. There are nevertheless some interesting physical arguments based primarily on the phenomenon of charge fractionation.

The idea of charge fractionation [107, 108] is most simply illustrated by the fact that when you put N_1 D1 branes (or strings) in a periodic box of length L, then the lowest mass excitation carried by this system is not of order L^{-1}, but of order $(N_1 L)^{-1}$. The explanation is that the branes develop multi-wound states with the longest effective length

being of order $N_1 L$. Similarly, but via a rather more complex mechanism, the lowest mass excitations of the D1-D5 system vary as $(N_1 N_5)^{-1}$. This is called charge fractionation. It is this phenomenon that leads to the CFT mass gap given in (264). The other important consequence of fractionation is that the corresponding "largest" natural physical length scale of the system grows as $N_1 N_5$. One of the crucial physical questions is how does the "typical" length scale grow with charge. That is, what is the physical scale of the most likely (or typical) configuration. It is believed that this will grow as some positive power of the underlying charges, and this is the fundamental reason why it is expected that microstate geometries are "large" compared to the Planck scale and that microstate geometries are not just relevant within a few Planck units of the singularity, but extend to the location of the classical horizon.

This argument can be extended to non-BPS systems. Configurations of multiple species of branes also exhibit fractionation. For this reason, it is believed that, given a certain energy budget, the way to get most entropy is to make brane-antibrane pairs of different sorts[6]. Putting together these different kinds of branes creates a system with very light (fractionated) modes, whose mass is much much lower than the Planck scale. These modes can then "extend" all the way to the horizon, and have to be taken into account when discussing physics at this scale.

One of the counterarguments to the third possibility is that one can collapse a shell of dust and create a horizon at very weak curvatures, long before the black hole singularity forms. Moreover, the larger the mass, the longer will be the time elapsed between the formation of the horizon and the singularity. Hence, it naively appears that the horizon cannot possibly be destroyed by effects coming from a singularity that is so far away. Nevertheless, if fractionation gives the correct physics, then one can argue that as the mass of the incoming shell increases, the number of brane-antibrane pairs that are created becomes larger, and hence the mass of the "fractionated" modes becomes smaller; these modes will then affect the physics at larger and larger scales, which can be argued to be of order the horizon size. In this picture the collapsing shell would reach a region where a whole new set of very light degrees of freedom exist. Since these "fractionated" degrees of freedom have a much larger entropy, the shell will dump all its energy into these modes, which would then expand to the horizon and destroy the classical geometry up to this scale. More details in support of these arguments can be found in [14].

On the other hand, one may hope to preserve the status quo for non-extremal black holes by arguing that fractionation is a phenomenon that is based on weakly coupled D-brane physics, and is not necessarily valid in the range of parameters where the black hole exists. This, however, leaves one with the problem of explaining why fractionation appears to be occurring in extremal black holes and why non-BPS black holes should be

[6]This idea has been used in formulating microscopic brane-antibrane models for near-BPS black holes [109] and for black branes [110], and has recently received a beautiful confirmation in the microscopic calculation of the entropy of extremal non-BPS black holes [111]. It has also been applied to cosmology [112] and to understanding the Gregory Laflamme instability [113] microscopically [114, 115].

any different. Indeed, if the classical solution for the extremal black hole is proven to give an incorrect description of the physics at the horizon when embedded into a quantum theory of gravity, it is hard to believe that other similar, non-extremal solutions will give a correct description of the physics at the horizon. It will be much more reasonable to accept that all the classical black hole solutions are thermodynamic descriptions of the physics, which break down at the scale of the horizon.

The most direct support for the smooth microstate structure of non-extremal black holes would be the construction and counting of smooth, non-extremal geometries generalizing those presented here, like those constructed in [83]. Such constructions are notoriously difficult and, barring a technical miracle in the construction of non-BPS solutions, it is hard to hope that there will be a complete classification of such geometries in the near future. On the other hand, it is instructive and encouraging to recall the developments that happened shortly after the original state counting arguments of Strominger and Vafa for BPS black holes: There was a lot of analysis of near-BPS configurations and confirmation that the results could be generalized perturbatively to near-BPS states with small numbers of anti-branes. This might prove fruitful here and would certainly be very useful in showing that generic smooth microstate geometries are not special properties of BPS objects. It would thus be interesting to try, either perturbatively, or perhaps through microstate mergers, to create near-BPS geometries.

Finally, the fact that the classical black hole solution does not describe the physics at the scale of the horizon seems to contradict the expectation that this solution should be valid there since its curvature is very small. There are, however, circumstances in which this expectation can prove wrong. First, if a solution has a singularity, it oftentimes does not give the correct physics even at very large distance away from this singularity because the boundary conditions at the singularity generate incorrect physics even in regions where the curvature is very low. Such solutions therefore have to be discarded. A few examples of such solutions are the Polchinski-Strassler flow [99] without brane polarization [100], or the singular KK giant graviton [102, 103]. The reason why we do not automatically discard black hole solutions is that their singularities are hidden behind horizons and sensible boundary conditions can be imposed at the horizon. However, this does not imply that all solutions with singularities behind horizons must be good: It only shows that they should not be discarded *a priori*, without further investigation. What we have tried to show is that if the third possibility is correct then the investigation indicates that the classical BPS black-hole solution should not be trusted to give a good description of the physics at the scale of the horizon.

1.4 A simple analogy

To understand Possibility 3 and Mathur's conjecture in general a little better, it is instructive to recall the physics of a gas, and to propose an analogy between the various descriptions of a black hole and the various descriptions of this gas.

For scales larger than the mean free path, a gas can be described by thermodynamics, or by fluid mechanics. At scales below the mean free path, the thermodynamic description breaks down, and one has to use a classical statistical description, in which one assumes all the molecules behave like small colliding balls. When the molecules are very close to each other, this classical statistical description breaks down, and we have to describe the states of this gas quantum mechanically. Moreover, when the temperature becomes too high, the internal degrees of freedom of the molecules become excited, and they cannot be treated as small balls. There are many features, such as shot noise or Brownian motion, that are not seen by the thermodynamic description, but can be read off from the classical statistical description. There are also features that can only be seen in the full quantum statistical description, such as Bose-Einstein condensation.

For black holes, if Possibilities 3A or 3B are correct, then the AdS-CFT correspondence relates quantum states to quantum states, and we expect the bulk dual of a given boundary state to be some complicated quantum superposition of horizonless configurations. Unfortunately, studying complicated superpositions of geometries is almost impossible, so one might be tempted to conclude that even if Possibilities 3A or 3B are correct, there is probably no new physics one can learn from it, except for an abstract paradigm for a solution to the information paradox. Nevertheless, we can argue by analogy to a gas of particles that this is not the case.

Consider a basis for the Hilbert space of the bulk configurations. If this basis is made of coherent states, some of the states in this basis will have a semiclassical description in terms of a supergravity background. This would be very similar to the situation explored in [95], where bubbled geometries correspond to coherent CFT states. The supergravity solutions we have discussed in these notes are examples of such coherent states. The main difference between the Possibility 3A and 3B has to do with whether the coherent states that form a basis of the Hilbert space can be described using supergravity or whether one has to use string theory to describe them. By analogy with the gas, this is the difference between the regime where the simple "colliding ball" model is valid, and the regime where one excites internal degrees of freedom of the molecules.

If supergravity is a good description of most of the coherent states, we can argue that we have constructed the black hole analogue of the classical statistical description of an ideal gas. Even if most of the coherent states can only be described in a full string-theoretic framework, one can still hope that this will give the analogue of an, albeit more complicated, classical statistical description of the gas. Both these descriptions are more complete than the thermodynamic description, and for the gas they capture physics that the thermodynamic description overlooks. Apart from solving the information problem, it would be very interesting to identify precisely what this physics is for a black hole. Indeed, as we will explain below, it might lead to some testable signature of string theory.

On the other hand, the black-hole analogue of the quantum statistical description involves a complicated and hard-to-study quantum superposition of microstates, and is therefore outside our present theoretical grasp. One can speculate, again in analogy with

the ideal gas, that there are probably interesting physical phenomena that can only be captured by this description, and not by the classical statistical description.

We should also note that in [10] it has been argued that from the point of view of the dual CFT, the difference between the typical microstates and the classical black hole solution can only be discerned by doing a very atypical measurement, or waiting for a very long time[7]. This is analogous to the case of a gas, where if one waits for a very long time, of order the Heisenberg recurrence time, one will observe spikes in the pressure coming from very unlikely events, such as a very large number of molecules hitting the wall at the same time. In the thermodynamic approximation one ignores the small energy gap between microstates, and such phenomena are not visible. The fact that the classical black hole geometry has an infinite throat and no mass gap implies that this geometry will not display such fluctuations at very large time-scales. Since the CFT does have a mass gap, and fluctuations at large scales occur, one can argue [116] that the black hole gives a thermodynamic description of the physics, and not a microscopic one.

Since, by standard AdS-CFT arguments, a long time on the boundary corresponds to a large distance into the bulk, one can argue that atypical CFT measurements involving very long times correspond in the bulk to propagators that reach very close to the black hole horizon [10]. Hence, this supports the intuition that one can distinguish between different microstates by making experiments at the scale of the horizon. Moreover, in a gas one can distinguish between the ensemble and the microstates by making experiments at scales smaller than the mean free path. At this scale the thermodynamic description breaks down, and new phenomena that cannot be captured by thermodynamics appear. By analogy, for the black hole we have argued that the scale where thermodynamics breaks down is that of the horizon. Therefore, both our arguments and the arguments of [10] indicate that experiments made *at the scale of the horizon* should distinguish between a microstate and the classical solution. While from the point of the dual CFT these experiments appear to be very atypical, they might not be so atypical from the point of view of the dual bulk. It would certainly be very interesting to propose and analyze in more detail such gedanken experiments, and explore more thoroughly the implications of this fact.

1.5 The size of quantum effects

As we have explained in Subsection 1.2, the essence of Mathur's conjecture is that quantum effects from the black hole singularity extend over a macroscopic scale, all the way to the black hole horizon, and invalidate the classical geometric description of the physics in the region between the horizon and the singularity. Hence, one could say plastically that quantum effects should "destroy the geometry" between the horizon and the singularity.

Our work on black hole and black ring microstates, summarized in Section 10, hints

[7] See [117] for other interesting work in this direction.

that quantum effects might be even more powerful than that - in certain circumstances they could even destroy a very large chunk of a classical horizonless low-curvature supergravity solution !

In that section we construct smooth microstate geometries that have the same charges, dipole moments and angular momenta as black rings with a macroscopically large horizon area, first found in [43]. These solutions are identical to black-ring solutions, both in the asymptotic region, and in the near-horizon region, but instead of having the infinite throat of classical BPS black rings, they have a very deep throat that ends in a smooth cap. All the charges of the solution come from fluxes threading topologically non-trivial cycles at the bottom of the throat.

If we impose $U(1) \times U(1)$ symmetry on the solutions then the depth of the throat is naturally limited by the size of the flux quanta and, as discussed in Section 9 [42], we expect the red-shift of low-energy excitations near the bottom of the throat to yield an energy that matches the mass gap of the dual CFT.

The striking result of Section 10 is that there exist solutions that do not have a $U(1) \times U(1)$ isometry, and that can have a throat whose length depends both on the fluxes, and on geometric moduli of the base space. Most particularly, we construct *abyssal* solutions in which the depth of the throat can be made arbitrarily large by tuning certain angles on the base space! In these scaling solutions, the size of all the cycles remains finite as the length of the throat becomes larger and larger, and hence the solutions can be described using supergravity for arbitrarily lengths of the throat. While we only discuss abyssal solutions corresponding to black rings, it is pretty clear that black hole microstates with this feature could also be constructed this way. From a four-dimensional perspective, these solutions correspond to D6–$\overline{\text{D6}}$ solutions that have closed quivers, and hence the branes appear to get arbitrarily close to each other [80]. Nevertheless, that perspective is misleading: when considering the full five-dimensional solution, the physical distances between the GH points corresponding to the D6 branes remains *finite* throughout the scaling. Moreover, unlike their four-dimensional counterparts, the solutions that we consider are smooth.

The fact that one can construct smooth horizonless solutions that have arbitrarily long throats poses interesting questions for the interpretation of microstate geometries from the point of view of the AdS/CFT correspondence. Since these geometries are dual (up to $1/N$ corrections) to states of the boundary CFT, it appears naively that these states will have an arbitrarily small mass-gap, as well as a whole tower of excitations that can be made arbitrarily light, contradicting expectations for a quantum theory in a box. Moreover, since the geometries we construct are supersymmetric and have very large cycles, and hence very low curvatures, one can imagine perturbing them slightly by adding a suitably small box of gas with some entropy, and doing this without significantly disturbing the geometries. If one then dials the length of the throat to become arbitrarily large one will obtain a system that has the entropy of the gas, but has an energy arbitrarily close to the BPS bound. We believe it is important to refine these puzzles and discuss

some possible resolutions.

1.5.1 The spectrum and mass gaps in AdS/CFT: The puzzle

The best-studied theory that is holographically dual to the geometries we consider is the D1-D5 CFT. At strong coupling this CFT is dual to string theory on $AdS_3 \times S^3 \times T^4$. Even though our geometries are constructed in eleven-dimensional supergravity, it is elementary to dualize them to the appropriate IIB frame. One then obtains a solution in which the D1 and D5 branes are wrapped on a common circle, C . To obtain a solution that is asymptotic to $AdS_3 \times S^3 \times T^4$ one must also drop the constant terms in the harmonic functions associated with the D1-brane and D5-brane charges [45, 63]. In doing this, the circle, C, decompactifies and becomes part of the AdS_3 [8].

It is often useful to consider the D1-D5 field theory in a finite-sized "box" and one of the simplest ways to do this is to restore the constants to the harmonic functions so that the supergravity solution is asymptotically flat and the common circle, C, has a radius, R. At weak coupling, the perturbative string excitations must be quantized in mass units of $\frac{1}{N_1 N_5 R}$ and so one expects the mass gap and the typical energy gap between states to be of this order. There are some issues as to whether this approach is well-defined in the strict sense of the AdS/CFT correspondence (see below); a more careful approach would be to introduce a UV cut-off in the radial direction of AdS_3. The effect of this is, once again, to introduce a scale in the bulk. More generally, anything that sets a finite scale for the spatial volume of the field theory direction at infinity also sets a mass scale for that theory.

Three-charge solutions that are asymptotically $AdS_3 \times S^3 \times T^4$ also have additional, intermediate scales. For both black holes and black rings, there exists a scale $r_p \sim \sqrt{Q_P}$ associated to the total momentum. This scale is set by the equal balance of the terms in the momentum harmonic function $Z_P \approx 1 + Q_P/r^2$. For black rings there are also scales set by the radius of the ring and by the dipole charges.

Since the AdS/CFT correspondence relates smooth, horizonless, asymptotically AdS solutions to states of the dual field theory, one can calculate, both in the bulk and on the boundary, the spectrum of non-BPS excitations above a given BPS state, and try to identify the boundary dual of a certain state by matching these spectra. These calculations have been very successful both for two-charge solutions [5, 7], and for simple three-charge solutions [31]. This has allowed precise matching of bulk solutions with boundary states.

A rougher way to estimate the non-BPS mass gaps in the spectrum of excitations above a certain asymptotically-flat bulk solution is to consider the lowest energy oscillations localized in the throat of this solution. The corresponding mass gap, and indeed typical energy separation of states, in the holographic dual theory is then obtained by calculating

[8] One should not confuse this AdS_3 with that of the near-horizon limit of the supertube in M-theory: They are different, and the AdS_3 of the IIB theory emerges non-trivially via the T-dualities.

the red-shifted energy of these excitations at infinity in the asymptotically flat solution[9]. For the D1-D5-P system, introducing a cut-off for evaluating the energy of excitations is not even necessary since the bulk solution already contains a scale associated to the momentum charge Q_P. The bulk energies redshifted to this scale correspond on the boundary to the ratio between the energy of the excitations and the energy coming from the total momentum.

For the deep microstate geometries, the non-BPS excitations about these states generically have a mass gap, and typical energy separation between states, that vary inversely with the depth of the throat in the bulk. For the $U(1) \times U(1)$ invariant microstates, the spectrum coming from the deepest possible throats matches the lowest bound on the mass gap expected from the orbifold point description of the CFT, namely, $E_0 = \frac{1}{N_1 N_5 R}$ [42]. Although we have not checked this explicitly, we also expect the mass gap of the deepest $U(1) \times U(1)$ black ring microstates to match the mass gap expected from the orbifoled point description of black rings [45].

For microstates that do not have a $U(1) \times U(1)$ invariance, we have the "abysses" in which the throat can become arbitrarily deep as a function of moduli. As the throat becomes deeper and deeper, all the excitations at the bottom of the throat became lighter and lighter, and the field theory spectrum approaches what looks like a continuum spectrum. Nevertheless, one does not expect this of a quantum theory that is confined in a box, however large. Since we are comparing spectra at different values of the coupling constants, and one might argue that strong coupling effects do not modify the spectrum of $U(1) \times U(1)$ invariant configurations, but will modify the spectrum of the configurations with less symmetry, and allow states whose energy separations are much smaller than the expected weak-coupling value. However, for excitations above a given BPS state, these energy separations will not become arbitrarily small if the size of the box is kept fixed. Using condensed-matter language, when the mass of a very large number of excitations goes to zero one approaches a quantum critical point, and one does not expect to find quantum critical points in systems of finite size.

1.5.2 A possible resolution: Quantizing the moduli space

The simplest and most straightforward resolution of this abyssal conundrum would be to find a way of cutting off the throats of the scaling solutions at some finite value.

As we have already noted, the modulus in our example must be extremely finely tuned in order to obtain a very deep throat. In string theory, and even in supergravity, this moduli space will be quantized. Indeed, one can try to quantize it by considering the effective action for slow motions on the moduli space and then apply quantum mechanics

[9]Alternatively, one can work entirely with an asymptotically AdS solution, that is cut off at a large, but finite distance, $r = \frac{1}{\epsilon}$, and impose appropriate boundary conditions on this surface [9]. The red-shifted bulk energy evaluated at the cutoff $r = \frac{1}{\epsilon}$ can then be matched to the energy in the boundary theory placed in a box of size $\frac{1}{\epsilon}$.

(where Planck's constant will be related to $\frac{1}{N}$ effects). This will mean that there will be limits on our ability to precisely localize GH points on the GH base metric and thus localize the moduli sufficiently well to generate very deep throats. The effectiveness of this will depend on the details of the correct physical metric on the phase-space of the theory. If the metric on the moduli space comes from the positions in the $\mathbb{R}^3$ base of the GH geometry, then it may well provide an effective and useful cut-off. On the other hand, the phase space measure may well be related to the complete physical metric and it is hard to imagine how a quantization principle could cut-off a throat that is several megaparsecs long.

Putting this more graphically, suppose that one is given a smooth, horizonless, classical solution of arbitrarily low curvature and g_s, and that has a length 10^{10} times larger than the maximum value consistent with mass gaps on the boundary theory, it is very hard to imagine that quantum effects, which are intrinsically of order $1/N$, will be able to destroy it. Note that the puzzle is *not* about destroying the very large throats by throwing particles from infinity. For an arbitrarily deep throat this can always be done, as any particle thrown in from infinity will eventually be blue-shifted enough going down the throat to destroy it. From the boundary perspective the very deep throats correspond to very finely tuned superpositions of eigenstates, and generic interactions with other states can easily destroy them. The fact that particles thrown in from infinity destroy the states does not make them physically irrelevant[10] (though it will probably imply that non-BPS microstates will not have arbitrarily long throats – see the discussion below). The puzzle comes from the *existence* and the physics of BPS microstates of arbitrary long throats, and the fact that the excitations that live at the bottom of the throat appear virtually massless from the point of view of the boundary theory.

Despite the concerns over "quantizing away" macroscopic geometries, there are natural ways in which this might be realized. For example, the angles on the base space could well be quantized because of the quantization of angular momentum. Given a certain bubbling solution, the value of J_R is determined entirely by the quantized fluxes on the bubbles (151), and hence it is automatically quantized. The angular momentum, J_L, defined in (152) and (150), not only depends upon the quantized flux but also upon the orientations of the bubbles. Continuously varying an angle will therefore generically yield non-integer values of J_L. While this is certainly true of the simple example considered in Section 10, and indeed will be true if one varies a single modulus in almost any solution, one can easily construct solutions in which there are moduli that do not change the total value of J_L. For example, one could make a scaling solution with two identical bubbling black rings on opposite planes; alternatively one could consider a $\mathbb{Z}_2$ symmetric bubbling black hole (like the "pincer" solution studied in [42] and discussed in Section 9). These configurations, which have $J_L = 0$ because of symmetry, can still become arbitrarily deep

[10] In the same way in which the fact that one can throw elephants and destroy a resonant cavity does not make the study of the modes of the cavity irrelevant.

and it seems unlikely that any quantization coming from the *total* angular momentum could stop that.

On the other hand, one should also have some notion of a local quantization of the angular momentum. This is because, in some circumstances, it is possible to separate different components of a scaling solution in such a manner that it can be decomposed into separate classical objects; the J_L of each component must be quantized. It thus seems plausible that the individual contributions, $\vec{J}_{L\,ij}$ in (154), coming from each bubble should be quantized. The *magnitude* of the $\vec{J}_{L\,ij}$ is already quantized because of the quantization of fluxes, and so the non-trivial content of this statement lies in the quantization of the direction of $\vec{J}_{L\,ij}$. In such a picture, the total J_L in (276) would then be obtained by the standard rules for the addition of spins in quantum mechanics. If this picture were correct, then the ability to classically orient an individual bubble would be limited by the inverse of the magnitude of the flux that it carries. The fine tuning needed to create abysses would thus be limited.

Another possibility is that even if abysses exist, it does not make sense to talk about their mass gaps because even a very small particle at the bottom of a throat could have a large effect on the geometry and prevent the throat from becoming arbitrarily long. An example of this can occur in the "doubly-infinite" AdS_2 throats that are encountered in the near-horizon geometry of black holes and black rings. As discussed in [52][11], such infinite throats can by destroyed by the energy-momentum tensor coming from a very small perturbation.

Since the throats of our solutions are capped, the metric near the cap is no longer of $AdS \times S$ form. Therefore, extending the calculation of [52] to our solutions is not straightforward. If we naively assume equation (2.16) of [52] captures the essential physics, one can extend that analysis to our case. We find that a non-trivial energy-momentum tensor can be accommodated on top of our solutions provided the sphere shrinks to zero size at the cap. Fortunately, this is already happening even in the smooth BPS solutions, and is indeed a necessary feature of all the capped microstates. Hence, the obvious extension of the argument in [52] does not rule out abyssal throats. It would be very interesting to see if one can construct an argument in a similar spirit that would cut off an abyss.

It is interesting to note that a three-center solution that contains D6, anti-D6 and D0 branes has been quantized recently by [122], using the relation between such solutions and the quiver quantum mechanics describing these branes in the regime of parameters where they do not backreact on the geometry. This quantization has shown that for this configuration the scaling stops, at a depth whose mass-gap is the same as that of the typical states, much like for $U(1) \times U(1)$ solutions constructed in Section 9. It is possible that for the three-center solution the scaling stops because of the quantization of total angular momentum (which is always nonzero for three-center configurations), and that

[11] See equations (2.15) to (2.17) of that paper for more details.

upon quantizing multicenter solutions of zero angular momentum the scaling would not stop. Another possibility is that the scaling is always stopped.

Summarizing this sub-section, it appears difficult to logically exclude the existence of some quantum mechanism that limits the depth of a throat. On the other hand, if this were to happen, as suggested by [122], this would be a rather remarkable first example of quantum effects destroying a very large portion of a smooth, horizonless, low-curvature, asymptotically-flat classical geometry.

1.5.3 Another possible resolution: Stringent constraints on the duality

Another possible resolution of the problem is to take the more "stringent" view that the AdS/CFT correspondence only relates field theories in an infinite volume to asymptotically AdS solutions without a cutoff. In this context calculations of mass gaps, times of flights, or energy spectra are, at best, of limited validity and, at worst, meaningless. From this perspective, the only thing one can meaningfully compute in the bulk are N-point functions. Indeed, by computing one-point functions in certain two-charge geometries and relating them to vev's in the boundary theory it is possible to obtain a very precise mapping between bulk solutions and their dual boundary states [12], without appealing to spectra and mass-gaps.

This view poses the opposite problem: Why were mass-gap calculations in the D1-D5 system in a finite box so successful? One possible answer is that all these calculations were done for $U(1) \times U(1)$ invariant microstates, and the extra symmetry "protects" the calculations done on the two sides of the duality, even if the duality is not strictly valid. Conversely, the microstates that do not have a $U(1) \times U(1)$ invariance are not protected, and there is no reason why the calculations done in two inequivalent theories should agree. This answer is also consistent with the fact that mass-gaps computed in $U(1) \times U(1)$ invariant three-charge microstates cannot be less than the smallest mass gap expected from the free (orbifold point) description of the CFT [42]. If this view is correct then one needs to understand what this protection mechanism is and why it works and why it fails.

There is also another rather puzzling feature of this perspective: While the D1-D5 system does not have a scale, the D1-D5-P system does have a scale set by Q_P. Even if it does not make sense to talk about the energy of excitations of arbitrarily deep throats by themselves, it does make sense to talk about the ratio between this excitation energy and the energy coming from the total momentum, Q_P. We therefore find that the energies of excitations in an abyss are going to zero compared to the energy of the momentum excitations that are ultimately responsible for making the classical horizon area macroscopic. It would therefore seem that one could store very large amounts of entropy in such massless excitations.

1.6 Entropy elevators and non-BPS microstates.

As we have seen, we have two distinct, though logically possible outcomes, both of which are physically unexpected and both of which hint at tantalizing new phenomena. If abysses are cut off by quantum effects then these quantum effects can remove macroscopic portions of a low-curvature asymptotically-flat solution, and if the abysses are not cut off, then we appear to have a quantum critical point.

In trying to understand both of these possibilities it is useful to introduce the idea of "entropy elevators." Consider a small sub-system of non-BPS excitations and then adiabatically lower that sub-system into very deep throats so that the energy is red-shifted to the value determined by the depth of the throat and yet the entropy in the non-BPS excitations remains constant. There are two ways that one could imagine controlling such an elevator: Either by lowering the elevator using a massless cable or, as we prefer here, constructing the non-BPS excitations in a "shallow cap" and then adiabatically changing the modulus so that the cap descends to the bottom of a deep throat. If the moduli space is quantized then the elevator is only allowed to go to discrete floors and there is a lowest possible floor, but in an abyss there is no lower limit and all the excitations of that sub-system will become massless in the limit when the length of the throat approaches infinity. Hence, at the critical point the system has new massless modes.

For a given smooth cap there will be a limit on the size of the non-BPS sub-system: It must not significantly alter the physics of the cap and radically modify the elevator. In the limit when the throat is infinite, the extra mass will be zero and the state will, once again be (arbitrarily close to) BPS, and yet there will still be entropy in this sub-system. The solution will also be (arbitrarily close to) the classical BPS black hole. Hence, it is possible that one can only use microstate geometries to account for the entropy of the BPS black hole by considering all the throats that can act as "entropy elevators" that carry massive sub-systems of finite entropy to an infinite throat depth, where their mass becomes zero.

The entropy that a certain "elevator" can carry is limited by the requirement that the non-BPS sub-system added on does not destroy the solution. Note that this requirement has nothing to do with the energy seen from infinity, but rather with the effect of the sub-system on the bubbles that form the cap of the solution. Whether the sub-system destroys a certain cap, or not, has nothing to do with the length of the throat at whose end the cap is. The sub-system should only care about the local geometry of the cap and its presence should not limit the ability of the elevator to descend. The only effect of the throat is to make the energy of the sub-system as seen from infinity larger or smaller. Thus, for every cap we can associate a maximal "local" energy E_c that is the maximal energy that does not destroy it, and a certain entropy S_c. The mass above the BPS bound as seen from infinity is $E_\infty = E_c\sqrt{g_{00}^{min}}$ where g_{00}^{min} is the value of g_{00} at the bottom of the throat. As the throat length approaches infinity, the elevator associated with each deep throat contributes with S_c to the entropy of the black hole. It is tempting to conjecture

that the entropy of the BPS black holes comes entirely from these entropy elevators[12].

The idea of lowering boxes containing entropy into black holes and studying the entropy in the process is not new in General Relativity and has led to apparent paradoxes and beautiful resolutions. See, for example, [18, 19] and for recent work see also [20]. However, entropy elevators have two very different features. The first is that the box is lowered on top of a horizonless, BPS solution, and there is no Hawking radiation from the horizon to keep the box in equilibrium, or to allow the creation of box - anti-box pairs. The second is that the entropy in the elevators never goes into the entropy of a black hole: As the elevators descend, the solution always remains horizonless. Indeed, we will see below that as an elevator carrying a box of a certain "local" energy, E, descends, the energy as seen from infinity decreases, and the horizon of the corresponding black hole also descends at the same rate.

The idea of entropy elevators also has some interesting consequences for near-BPS black holes. These black holes have a finite throat depth, set by the non-extremality parameter. In the elevator picture, to create a finite amount of non-extremality one must add a finite amount of energy, ΔE, above the BPS bound. To create this amount of energy at infinity by putting a non-BPS sub-system on an elevator means that the amount of energy on the elevator must be $E_{local} = \Delta E/\sqrt{g_{00}}$. At a certain depth this energy will exceed the energy, E_c, needed to destroy the cap. Thus there is a limit to which the entropy elevator can descend for a given amount of non-extremality.

If the entropy elevators can be used to create near-BPS black hole microstates, the depth of the entropy elevators that carry most of the entropy should match the depth of the horizon of the near-BPS black hole. While a perfect matching of these two quantities is not possible without constructing the solutions corresponding to the elevators, one can check that the depth of the elevators and the "depth" of the horizon scale in the same way with the energy above extremality, which is a rather non-trivial check.

Indeed, given a certain energy, ΔE, above the BPS bound, one can construct shallow entropy elevators, that have a sub-system of energy a few times ΔE, as well as deeper elevators, that have a sub-system of energy $E_{local} = \Delta E/\sqrt{g_{00}^{\rm bottom}}$. Clearly, the deeper elevators will carry a bigger system, and will have more entropy. If we make E_{local} bigger than the maximal energy a cap can support, E_c, then the elevator will be destroyed. Hence, most entropy will come from the elevators of depth corresponding to

$$g_{00}^{\rm bottom} = (Z_1 Z_2 Z_3)^{-2/3} = \frac{(\Delta E)^2}{E_c^2}. \tag{2}$$

We can compare the depth of these elevators to the depth of the horizon of a near-BPS black hole. The easiest measure of the depth of that throat are the values of the three

[12]This would imply that the entropy of the D1-D5-P CFT at strong coupling has "accumulation points," corresponding to the abysses.

harmonic functions at the horizon, which in the near-BPS limit are given by:

$$Z_i \approx \frac{Q_i}{\Delta E} \tag{3}$$

Hence, the depth of the elevators and the depth of the near-BPS black hole horizon have the same dependence on ΔE. This is a necessary feature if elevators are to give the microstates of the non-extremal black holes, and its confirmation is encouraging. It would be interesting to analyze in more detail the amount of energy, E_c, that a certain cap can carry, and see if its dependence on the charges also matches that predicted by equations (2,3).

Hence, if this idea of entropy elevators is correct, one should think about elevators that descend to an infinite depth as giving the entropy of the extremal black holes, and the elevators that descend to a finite depth as giving the entropy of the non-extremal black holes.

1.7 Observational Implications

The whole problem with finding experimental or observational tests of string theory is that the string scale and the Planck scale are so far out of reach of present accelerations. However, the ideas of fractionation and the present ideas about the microstate structure of black holes show us that we can get stringy effects on very large length scales. It would obviously be very exciting if we could make black holes at the LHC and thereby test these ideas, but even if this were not to happen, we may still be able to see some signature of stringy black holes within the next decade. Indeed, the gravitational wave detectors LIGO and LISA are very likely to detect the gravitational "ring-down" of merging black holes within the next few years and, while the underlying computations will be extremely difficult, one might reasonably hope that the microstate structure arising from string theory could lead to a new, detectable and recognizable signature in the LIGO or LISA data.

One of the most fascinating aspects of this picture of black holes is that it might have experimentally-observable consequences in several situations, such as the collision of two black holes, the ring-down of a black hole, the radiation emitted from the center of an accretion disk, or the possible production of black holes in particle accelerators.

In the case of astrophysical black holes, the departures from general relativity predicted by this picture might result in different gravity wave patterns in black hole collisions, that could be measured with the gravity wave detector LISA. Indeed, if classical generality breaks down at the black hole horizon, and there are new light degrees of freedom, which might take away the non-sphericity of the black hole resulting after a merger much faster than predicted in general relativity.

Also, if the bulk gravity scale and the TeV scale are the same (as some models of physics beyond the Standard Model suggest), then black holes could be produced at the

upcoming Large Hadron Collider. If the picture of black hole discussed above is correct, the objects produced would not be black holes, but black hole microstates. They would have a spectrum similar to black holes, but will probably have different branching ratios, and hence produce experimentally different signatures.

2 Summary of the author's work and its presentation.

Per Kraus and the author have been the first to construct three-charge brane configurations that have the right properties to correspond to the microstates of three-charge black holes [27]. We have found a very large number of such configurations, given by several arbitrary closed curves. This work is presented in Section 3.

The author then solved (together with Nick Warner) the rather challenging problem of constructing the supergravity solutions sourced by arbitrary-shaped configurations, and found that the most general solutions can be obtained by solving three *linear* equations [53, 55]. We illustrated this method by constructing the first explicit solutions describing circular supersymmetric black rings with three arbitrary charges and three dipole charges (these solutions were also found in parallel by [63] and [64]). These solutions (whose existence was first conjectured by Per Kraus and the author [27, 55]) produce an infinite violation of black hole uniqueness in five dimensions. We have also constructed the first three-charge supersymmetric black Saturn (a black ring with a black hole in the center), as well as more complicated solutions where the black hole is displaced away from the center of the ring [75].

The author has found (with Per Kraus) the first microscopic descriptions of black rings, by relating them to four-dimensional black holes, and by analyzing them in the two-dimensional D1-D5 conformal field theory [45]. The relation between five-dimensional supertubes and black rings and four-dimensional multi-center black hole configurations (reviewed in subsection 6.6) is an important feature of the so-called 4D-5D connection, which the author's papers [45, 35, 69], together with [68, 67] were the first to point out.

Per Kraus and the author have also been the first to construct microstates of four-dimensional black holes, by analyzing the D1-D5-KK-P system. The author then then combined the knowledge of these microstates with the physics of black rings to find (together with Nick Warner) the largest existing class of solutions corresponding to microstates of five-dimensional black holes. These solutions (reviewed in Sections 6, 7) have topologically-nontrivial cycles wrapped by fluxes, and have no horizons [36].

As we will see in Section 8 most of the solutions in this class have charges and angular momenta corresponding to black rings and black holes of zero horizon area [40]. This has been a limitation for this research programme, which the author has overcome (with N. Warner and his student C.-W. Wang), by finding the first solutions in the literature that are microstates of five-dimensional black holes and black rings that have a classically large

horizon area [42, 43]. These solutions (reviewed in Sections 9 and 10) are dual to states of the dual conformal field theory that belong to the same sector as the typical black hole microstates, and their finding is a very important step towards proving that black holes in string theory are ensembles of horizonless configurations.

The black ring microstate solutions found in [43] also display a very puzzling feature - they are smooth solutions that have low curvature, but can have a throat that classically can have an arbitrary length. If the length of the throat is capped off by quantum fluctuations, as the recent analysis of [122] indicates, this would be the first circumstance where quantum effects could wipe away a large region of a smooth horizonless low-curvature geometry, and would signal that certain regimes supergravity is no longer a low-energy effective theory of string theory.

The author has also found (together with N. Warner, N. Bobev and his PhD student C. Ruef) a mechanism by which one can generate smooth black hole microstate geometries that are parameterized by arbitrary functions (and hence depend on an infinite number of continuous parameters) [130]. These entropy coming from these geometries appears to be of the same order as entropy of the corresponding black hole [123], which further strengthens the evidence for the picture of black holes presented above.

Before beginning we should emphasize that the work that we present is part of a larger effort to study black holes and their microstates in string theory. Many groups have worked at obtaining smooth microstate solutions corresponding to five-dimensional and four-dimensional black holes, a few of the relevant references include [30, 31, 32, 33, 34, 35, 36, 37, 38, 39, 40, 41, 42, 44, 128]. Other groups focus on improving the dictionary between bulk microstates and their boundary counterparts, both in the two-charge and in the three-charge systems [8, 45, 11]. Other groups focus on small black holes[13] and study their properties using the attractor mechanism [47], or relating them to topological strings via the OSV conjecture [48]. Reviews of this can be found in [49], and a limited sample of work that is related to the exploration presented here can be found in [50].

2.1 Outline

In order to construct families of solutions that have no horizon have the same charges and asymptotics of black holes, the first step is to try to construct large numbers of microscopic stringy three-charge configurations. These configurations (discussed in section 3) were constructed in [27], and are called three-charge supertubes. Like their two-charge cousins, these supertubes depend on arbitrary continuous functions, and hence have a

[13]These black holes do not have a macroscopic horizon, but one can calculate their horizon area using higher order corrections [46]. This area agrees with both the CFT calculation of the entropy, and also agrees (up to a numerical factor) with the counting of two-charge microstates. Hence, one could argue (with a caveat having to do with the fact that small black holes in IIA string theory on T^4 receive no corrections) that small black holes, which from the point of view of string theory are in the same category as the big black holes, are, in fact, superpositions of horizonless microstates.

classical moduli space of infinite dimension.

In Section 4 we present the construction of three-charge supergravity solutions corresponding to arbitrary superpositions of black holes, black rings, and three-charge supertubes of arbitrary shape. We construct explicitly a solution corresponding to a black hole at the center of a black ring, and analyze the properties of this solution. This construction and the material presented in subsequent sections can be read independently of Section 3.

Section 5 is a geometric interlude, devoted to Gibbons-Hawking metrics and the relationship between five-dimensional black rings and four-dimensional black holes. Section 6 contains the details of how to construct new microstate solutions using an "ambipolar" Gibbons-Hawking space, whose signature alternates from $(+,+,+,+)$ to $(-,-,-,-)$. Even though the sign of the base-space metric can flip, the full eleven-dimensional solutions are smooth.

In Section 7 we discuss geometric transitions, and the way to obtain smooth horizonless "bubbling" supergravity solutions that have the same type of charges and angular momenta as three-charge black holes and black rings. In Section 8 we construct several such solutions, finding in particular microstates corresponding to zero-entropy black holes and black rings.

In Section 9 we use mergers to construct and analyze "deep microstates," which correspond to black holes with a classically large horizon area. We find that the depth of these microstates becomes infinite in the classical (large charge) limit, and argue that they correspond to CFT states that have one long component string. This is an essential (though not sufficient) feature of the duals of typical black-hole microstates (for reviews of this, see [28, 29]). Thus the "deep microstates" are either typical microstates themselves, or at least lie in the same sector of the CFT as the typical microstates.

In Section 10 we construct smooth horizonless solutions that are microstates of three-charge black rings. We also find that there exist scaling solutions that can have a throat whose length can be dialed to be of arbitrary length. The puzzles raised by this fact were discussed in Subsection 1.5, and their most obvious resolution is that quantum effects can destroy a very large portion of a classical low-curvature horizonless geometry.

Finally, in Section 11 we study fluctuating two-charge supertubes in three-charge geometries. We show that the entropy of these supertubes is determined by their locally-defined *effective* charges, which differ from their asymptotic charges by terms proportional to the background magnetic fields. When supertubes are placed in deep, scaling microstate solutions, these effective charges can become very large, leading to a much larger entropy than one naively would expect. Since fluctuating supertubes source smooth geometries in certain duality frames, we propose that such an entropy enhancement mechanism might lead to a black-hole like entropy coming entirely from configurations that are smooth and horizonless in the regime of parameters where the classical black hole exists.

3 Three-charge microscopic configurations

Our purpose here is to follow the historical path taken with the two-charge system and try to construct three-charge brane configurations using the Born-Infeld (BI) action. We are thus considering the intrinsic action of a brane and we will not consider the back-reaction of the brane on the geometry. The complete supergravity solutions will be considered later.

There are several ideas in the study of D-branes that will be important here. First, one of the easiest ways to create system with multiple, different brane charges is to start with a higher-dimensional brane and then turn on electromagnetic fields on that brane so as to induce lower-dimensional branes that are "dissolved" in the original brane. We will use this technique to get systems with D0-D2-D4-D6 charges below.

In constructing multi-charge solutions, one should also remember that the equations of motion are generically non-linear. For example, in supergravity the Maxwell action can involve Chern-Simons terms, or the natural field strength may involve wedge products of lower degree forms. Similarly, in the BI action there is a highly non-trivial interweaving of the Maxwell fields and hence of the brane charges. In practice, this often means that one cannot simply lay down independent charges: Combinations of fields sourced by various charges may themselves source other fields and thus create a distribution of new charges. In this process it is important to keep track of asymptotic charges, which can be measured by the leading fall-off behaviour at infinity, and "dipole" distributions that contribute no net charge when measured at infinity. When one discusses an N-charge system one means a system with N commuting asymptotic charges, as measured at infinity. For microstate configurations, one often finds that the systems that have certain charges will also have fields sourced by other dipole charges. More precisely, in discussing the BI action of supertubes we will typically find that a given pair of asymptotic charges, A and B, comes naturally with a third set of dipole charges, C. We will therefore denote this configuration by A-$B \to C$.

3.1 Three-charge supertubes

The original two-charge supertube [22] carried two independent asymptotic charges, D0 and F1, as well as a D2-brane dipole moment; thus we denote it as a F1-D0 $\to$ D2 supertube. It is perhaps most natural to try to generalize this object by combining it with another set of branes to provide the third charge[14]. Supersymmetry requires that this new set be D4 branes. To be more precise, supertubes have the same sypersymmetries as the branes whose asymptotic charges they carry and so one can naturally try to put together

[14]One might also have tried to generalize the F1-P dual of this system by adding a third type of charge. Unfortunately, preserving the supersymmetry requires this third charge to be that of NS5 branes and, because of the dilaton throat of these objects, an analysis of the F1-P system similar to the two-charge one [5] cannot be done.

F1-D0 → D2 supertubes, F1-D4 → D6 supertubes, and D0-D4 → NS5 supertubes, and obtain a supersymmetric configuration that has three asymptotic charges: D0, D4 and F1, and three dipole distributions, coming from D6, NS5 and D2 branes wrapping closed curves. Of course, the intuition coming from putting two-charge supertubes together, though providing useful guidance, will not be able to indicate anything about the size or other properties of the resulting three-charge configuration.

To investigate objects with the foregoing charges and dipole charges one has to use the theory on *one* of the sets of branes, and then describe all the other branes as objects in this theory. One route is to consider tubular D6-branes[15], and attempt to turn on world-volume fluxes to induce D4, D0 and F1 charges. As we will see, such a configuration also has a D2 dipole moment. An alternative route is to use the D4 brane non-Abelian Born-Infeld action. Both routes were pursued in [27], leading to identical results. Nevertheless, for simplicity we will only present the first approach here.

One of the difficulties in describing three-charge supertubes in this way is the fact that the Born-Infeld action and its non-Abelian generalization cannot be used to describe NS5 brane dipole moments. This is essentially because the NS5 brane is a non-perturbative object from the perspective of the Born-Infeld action [99]. Thus, our analysis of three charge supertubes is limited to supertubes that only have D2 and D6 dipole charge. Of course, one can dualize these to supertubes with NS5 and D6 dipole charges, or to supertubes with NS5 and D2. Nevertheless, using the action of a single brane it is not possible to describe supertubes that have three charges and three dipole charges. For that, we will have to wait until Section 4, where we will construct the full supergravity solution corresponding to these objects.

3.2 The Born-Infeld construction

We start with a single tubular D6-brane, and attempt to turn on worldvolume fluxes so that we describe a BPS configuration carrying D4, D0 and F1 charges. We will see that this also necessarily leads to the presence of D2-brane charges, but we will subsequently introduce a second D6-brane to cancel this.

The D6-brane is described by the Born-Infeld action

$$S = -T_6 \int d^7\xi \, \sqrt{-\det(g_{ab} + \mathcal{F}_{ab})}, \tag{4}$$

where g_{ab} is the induced worldvolume metric, $\mathcal{F}_{ab} = 2\pi F_{ab}$, T_6 is the D6-brane tension and we have set $\alpha' = 1$. The D6 brane also couples to the background RR fields through the Chern-Simons action:

$$S_{CS} = T_6 \int \exp(\mathcal{F} + B) \wedge \sum_q C^{(q)} \,. \tag{5}$$

[15]Tubular means it will only have a dipole charge just like any loop of current in electromagnetism.

By varying this with respect to the $C^{(q)}$ one obtains the D4-brane, D2-brane and D0-brane charge densities:

$$\begin{aligned} Q_4 &= 2\pi\, T_6\, \mathcal{F} && (6)\\ Q_2 &= 2\pi\, T_6\, (\tfrac{1}{2}\, \mathcal{F}\wedge\mathcal{F}) && (7)\\ Q_0 &= 2\pi\, T_6\, (\tfrac{1}{3!}\, \mathcal{F}\wedge\mathcal{F}\wedge\mathcal{F})\,. && (8) \end{aligned}$$

To obtain the quantized Dp-brane charges, one takes the volume p-form on any compact, p-dimensional spatial region, R, and wedges this volume form with Q_p and integrates over the spatial section of the D6 brane. The result is then the Dp-brane charge in the region R.

The F1 charge density can be obtained by varying the action with respect to the time-space component of NS-NS two form potential, B. Since B appears in the combination $\mathcal{F}+B$, one can differentiate with respect to the gauge field:

$$Q_1 \;=\; \frac{\partial\mathcal{L}}{\partial B_{0i}} \;=\; \frac{\partial\mathcal{L}}{\partial F_{0i}} \;=\; \frac{\partial\mathcal{L}}{\partial\dot{\vec{A}}} \;=\; \vec{\pi}\,, \qquad (9)$$

which is proportional to the canonical momentum conjugate to the vector potential, $\vec{A}$.

Our construction will essentially follow that of the original D2-brane supertube [22], except that we include four extra spatial dimensions and corresponding fluxes. We take our D6-brane to have the geometry $\mathbb{R}^{1,1}\times S^1\times T^4$ and we choose coordinates (x^0,x^1) to span $\mathbb{R}^{1,1}$ and (x^6,x^7,x^8,x^9) to span the T^4. The S^1 will be a circle of of radius r in the (x^2,x^3) plane and we will let θ be the angular coordinate in this plane. We have also introduced factors of 2π in (6), (7), (8), (9) to anticipate the fact that for round tubes everything will be independent of θ and so the integrals over θ will generate these factors of 2π. Thus the D-brane charge densities above are really charge densities in the remaining five dimensions, and the fundamental string charge is a charge density per unit four-dimensional area. Note also that the charges, Q, are the ones that appear in the Hamiltonian, and are related to the number of strings or branes by the corresponding tensions. These conventions will be convenient later on.

Since the S^1 is contractible and lies in the non-compact space-time, any D-brane wrapping this circle will not give rise to asymptotic charges and will only be dipolar. In particular, the configuration carries no asymptotic D6-brane charge due to its tubular shape. To induce D0-branes we turn on *constant* values of $\mathcal{F}_{1\theta}$, $\mathcal{F}_{67}$, and $\mathcal{F}_{89}$. Turning on $\mathcal{F}_{1\theta}$ induces a density of D4-branes in the (x^6,x^7,x^8,x^9) plane, and since these D4 branes only wrap the T^4, their charge can be measured asymptotically. The fields $\mathcal{F}_{67}$, and $\mathcal{F}_{89}$ similarly generate dipolar D4-brane charges. To induce F1 charge in the x^1 direction we turn on a constant value of $\mathcal{F}_{01}$. It is also evident from (7) that this configuration carries asymptotic D2-brane charges in the (x^6,x^7) and (x^8,x^9) planes and dipolar D2-brane charge in the (x^1,θ) direction. The asymptotic $D2$-brane charges will eventually

be canceled by introducing a second D6-brane. This will also cancel the dipolar D4-brane and D2-brane charges and we will then have a system with asymptotic F1, D0 and D4 charges and dipolar D2 and D6 charges.

With these fluxes turned on we find

$$S = -T_6 \int d^7\xi \, \sqrt{(1-\mathcal{F}_{01}^2)r^2 + \mathcal{F}_{1\theta}^2}\sqrt{(1+\mathcal{F}_{67}^2)(1+\mathcal{F}_{89}^2)}\,, \tag{10}$$

where we use polar coordinates in the (x^2, x^3) plane, and the factors of r^2 come from $g_{\theta\theta}$. By differentiating with respect to $\mathcal{F}_{01}$ we find

$$Q_1 = 2\pi T_6 \frac{\mathcal{F}_{01} r^2}{\sqrt{(1-\mathcal{F}_{01}^2)r^2 + \mathcal{F}_{1\theta}^2}} \sqrt{(1+\mathcal{F}_{67}^2)(1+\mathcal{F}_{89}^2)}. \tag{11}$$

The key point to observe now is that if we choose

$$\mathcal{F}_{01} = 1 \tag{12}$$

then r^2 drops out of the action (10). We will also choose

$$\mathcal{F}_{67} = \mathcal{F}_{89}\,. \tag{13}$$

We can then obtain the energy from the canonical Hamiltonian:

$$\begin{aligned} H &= \int Q_1 \mathcal{F}_{01} - L & (14)\\ &= \int \left[Q_1 + 2\pi T_6 |\mathcal{F}_{1\theta}| + 2\pi T_6 |\mathcal{F}_{1\theta}\mathcal{F}_{67}\mathcal{F}_{89}| \right] & (15)\\ &= \int \left[Q_1 + Q_4 + Q_0 \right]. & (16) \end{aligned}$$

The last two integrals are taken over the coordinates $(x^1, x^6, x^7, x^8, x^9)$ of the D6-brane. The radius of the system is determined by inverting (11):

$$r^2 = \frac{Q_1}{2\pi T_6} \frac{\mathcal{F}_{1\theta}}{1+\mathcal{F}_{67}\mathcal{F}_{89}} = \frac{1}{(2\pi T_6)^2} \frac{Q_1 Q_4^2}{Q_0 + Q_4}. \tag{17}$$

If we set $Q_0 = 0$ then (17) reduces (with the obvious relabeling) to the radius formula found for the original D2-brane supertube [22]. From (16) we see that we have saturated the BPS bound, and so our configuration must solve the equations of motion, as can be verified directly.

Supersymmetry can also be verified precisely as for the original D2-brane supertube [22]. The presence of the electric field, $\mathcal{F}_{01} = 1$, causes the D6-brane to drop out of the equations determining the tension and the unbroken supersymmetry. Indeed, just like the two-charge system [23], we can consider a D6-brane that wraps an *arbitrary* closed curve

in $\mathbb{R}^4$; the only change in (10) and (11) is that r^2 will be replace by the induced metric on the D6 brane, $g_{\theta\theta}$. However, when $\mathcal{F}_{01} = 1$ this does not affect equations (15) and (16), and therefore the configuration is still BPS. Moreover, if $\mathcal{F}_{1\theta}$ is not constant along the tube, or if $\mathcal{F}_{67}$ and $\mathcal{F}_{89}$ remain equal but depend on θ the BPS bound is still saturated.

Hence, classically, there exists an infinite number of three-charge supertubes with two dipole charges, parameterized by several arbitrary functions of one variable [27]. Four of these functions come from the possible shapes of the supertube, and two functions comes from the possibility of varying the D4 and D0 brane densities inside the tube. Anticipating the supergravity results, we expect three-charge, three-dipole charge tubes to be given by *seven arbitrary functions*, four coming from the shape and three from the possible brane densities inside the tube. The procedure of constructing supergravity solutions corresponding to these objects [53, 54] will be discussed in the next section, and will make this "functional freedom" very clear.

As we have already noted, the foregoing configuration also carries non-vanishing D2-brane charge associated with $\mathcal{F}_{1\theta}\mathcal{F}_{67}$ and $\mathcal{F}_{1\theta}\mathcal{F}_{89}$. It also carries dipolar D4-brane charges associated with $\mathcal{F}_{67}$ and $\mathcal{F}_{89}$. To remedy this we can introduce one more D6 brane with flipped signs of $\mathcal{F}_{67}$ and $\mathcal{F}_{89}$ [56]. This simply doubles the D4, D0, and F1 charges, while canceling the asymptotic D2 charge and the dipolar D4-brane charges. More generally, we can introduce k coincident D6-branes, with fluxes described by diagonal $k \times k$ matrices. We again take the matrix-valued field strengths $\mathcal{F}_{01}$ to be equal to the unit matrix, in order to obtain a BPS state. We also set $\mathcal{F}_{67} = \mathcal{F}_{89}$, and take $F_{1\theta}$ to have non-negative diagonal entries to preclude the appearance of $\overline{D4}$-branes. The condition of vanishing D2-brane charge is then

$$\text{Tr } \mathcal{F}_{1\theta}\ \mathcal{F}_{67} \ = \ \text{Tr } \mathcal{F}_{1\theta}\mathcal{F}_{89} \ = \ 0. \tag{18}$$

This configuration can also have D4-brane dipole charges, which we may set to zero by choosing

$$\text{Tr } \mathcal{F}_{67} \ = \ \text{Tr } \mathcal{F}_{89} \ = \ 0. \tag{19}$$

Finally, the F1 charge is described by taking Q_1 to be an arbitrary diagonal matrix with non-negative entries[16]. This results in a BPS configuration of k D6-branes wrapping curves of arbitrary shape. If the curves are circular, the radius formula is now given by (17) but with the entries replaced by the corresponding matrices. Of course, for our purposes we are interested in situations when we can use the Born-Infeld action of the D6 branes to describe the dynamics of our objects. Since the BI action does not take into account interactions between separated strands of branes, we will henceforth restrict ourselves to the situations where these curves are coincident. In analogy with the behaviour of other branes, if we take the k D6-branes to sit on top of each other we expect that they can form a marginally bound state. In the classical description we should then demand that

[16]Quantum mechanically, we should demand that Tr Q_1 be an integer to ensure that the total number of F1 strings is integral.

the radius matrix (17) be proportional to the unit matrix. Given a choice of magnetic fluxes, this determines the F1 charge matrix Q_1 up to an overall multiplicative constant that parameterizes the radius of the combined system.

Since our matrices are all diagonal, the Born-Infeld action is unchanged except for the inclusion of an overall trace. Similarly, the energy is still given by $H = \int \mathrm{Tr}\,[Q_1 + Q_4 + Q_0]$.

Consider the example in which all k D6-branes are identical modulo the sign of $\mathcal{F}_{67}$ and $\mathcal{F}_{89}$, so that both $\mathcal{F}_{1\theta}$ and $\mathcal{F}_{67}\mathcal{F}_{89}$ are proportional to the unit matrix[17]. Then, in terms of the total charges, the radius formula is

$$r^2 \;=\; \frac{1}{k^2(2\pi T_6)^2}\,\frac{Q_1^{\rm tot}(Q_4^{\rm tot})^2}{Q_0^{\rm tot}+Q_4^{\rm tot}}\,. \tag{20}$$

Observe that after fixing the conserved charges and imposing equal radii for the component tubes, there is still freedom in the values of the fluxes. These can be partially parameterized in terms of various non-conserved "charges", such as brane dipole moments. Due to the tubular configuration, our solution carries non-zero D6, D4, and D2 dipole moments, proportional to

$$\begin{aligned} Q_6^D &= T_6\, r\, k \\ Q_4^D &= T_6\, r\, \mathrm{Tr}\,\mathcal{F}_{67} \\ Q_2^D &= T_6\, r\, \mathrm{Tr}\,\mathcal{F}_{67}\,\mathcal{F}_{89} \equiv T_6\, r\, k_2. \end{aligned} \tag{21}$$

When the k D6-branes that form the tube are coincident, k_2 measures the local D2 brane dipole charge of the tube. It is also possible to see that both for a single tube, and for k tubes identical up to the sign of $\mathcal{F}_{67}$ and $\mathcal{F}_{89}$, the dipole moments are related via:

$$\frac{Q_2^D}{Q_6^D} \;=\; \frac{k_2}{k} \;=\; \frac{Q_0^{\rm tot}}{Q_4^{\rm tot}}\,. \tag{22}$$

We will henceforth drop the superscripts on the $Q_p^{\rm tot}$ and denote them by Q_p. One can also derive the microscopic relation, (22), from the supergravity solutions that we construct in Section 4.4. In the supergravity solution one has to set one of the three dipole charges to zero to obtain the solution with three asymptotic charges and two dipole charges. One then finds that (22) emerges from are careful examination of the near-horizon limit and the requirement that the solution be free of closed timelike curves [55].

If $\mathcal{F}_{67}$ and $\mathcal{F}_{89}$ are traceless, this tube has no D2 charge and no D4 dipole moment. More general tubes will not satisfy (22), and need not have vanishing D4 dipole moment when the D2 charge vanishes. We should also remark that the D2 dipole moment is

[17] One could also take $\mathrm{Tr}\mathcal{F}_{67} = \mathrm{Tr}\mathcal{F}_{89} = 0$ to cancel the D2 charge, but this does not affect the radius formula.

an essential ingredient in constructing a supersymmetric three-charge tube of finite size. When this dipole moment goes to zero, the radius of the tube also becomes zero.

In general, we can construct a tube of arbitrary shape, and this tube will generically carry angular momentum in the (x^2, x^3) and (x^4, x^5) planes. We can also consider a round tube, made of k identical D6 branes wrapping an S^1 that lies for example in the (x^2, x^3) plane. The microscopic angular momentum density of such a configuration is given by the $(0, \theta)$ component of the energy-momentum tensor:

$$J_{23} \;=\; 2\pi\, r\, T_{0\theta} \;=\; 2\pi T_6\, k\, r^2 \sqrt{(1+\mathcal{F}_{67}^2)(1+\mathcal{F}_{89}^2)}\,. \tag{23}$$

Now recall that supersymmetry requires $\mathcal{F}_{67} = \mathcal{F}_{89}$ and that $\mathrm{Tr}(\mathcal{F}_{67}\mathcal{F}_{89}) = Q_0/Q_4$ and so this may be rewritten as:

$$J_{23} \;=\; 2\pi T_6\, k\, r^2 \Big(1 \;+\; \frac{Q_0}{Q_4}\Big) \;=\; \frac{1}{2\pi T_6}\,\frac{Q_1\, Q_4}{k}\,, \tag{24}$$

where we have used (20). It is interesting to note that this microscopic angular momentum density is not necessarily equal to the angular momentum measured at infinity. As we will see in the next section from the full supergravity solution, the angular momenta of the three-charge supertube also have a piece coming from the supergravity fluxes. This is similar to the non-zero angular momentum coming from the Poynting vector, $\vec{E}\times\vec{B}$, in the static electromagnetic configuration consisting of an electron and a magnetic monopole [57].

Note also that when one adds D0 brane charge to a F1-D4 supertube, the angular momentum does not change, even if the radius becomes smaller. Hence, given charges of the same order, the angular momentum that the ring carries is of order the square of the charge (for a fixed number, k, of $D6$ branes). For more general three-charge supertubes, whose shape is an arbitrary curve inside $\mathbb{R}^4$, the angular momenta can be obtained rather straightforwardly from this shape by integrating the appropriate components of the BI energy-momentum tensor over the profile of the tube.

A T-duality along x^1 transforms our D0-D4-F1 tubes into the more familiar D1-D5-P configurations. This T-duality is implemented by the replacement $2\pi A^1 \to X^1$. The non-zero value of $\mathcal{F}_{1\theta}$ is translated by the T-duality into a non-zero value of $\partial_\theta X^1$. This means that the resulting D5-brane is in the shape of a helix whose axis is parallel to x^1. This is the same as the observation that the D2-brane supertube T-dualizes into a helical D1-brane. Since this helical shape is slightly less convenient to work with than a tube, we have chosen to emphasize the F1-D4-D0 description instead. Nevertheless, in the formulas that give the radius and angular momenta of the three-charge supertubes we will use interchangingly the D1-D5-P and the D0-D4-F1 quantities, related via U-duality $N_0 \to N_p$, $N_4 \to N_5$, and $N_1 \to N_1$, with similar replacements for the Q's.

3.3 Supertubes and black holes

The spinning three-charge black hole (also known as the BMPV black hole [58]) can only carry equal angular momenta, bounded above by[18]:

$$J_1^2 \;=\; J_2^2 \;\leq\; N_1 N_5 N_P \,. \tag{25}$$

For the three-charge supertubes, the angular momenta are not restricted to be equal. A supertube configuration can have arbitrary shape, and carry any combination of the two angular momenta. For example, we can choose a closed curve such that the supertube cross-section lies in the (x^2, x^3) plane, for which $J_{23} \neq 0$ and $J_{45} = 0$. The bound on the angular momentum can be obtained from (24):

$$|J| \;=\; \frac{1}{2\pi T_6}\,\frac{Q_1\,Q_4}{k} \;\leq\; \frac{1}{2\pi T_6}\,Q_1\,Q_4 \;=\; N_1\,N_4\,, \tag{26}$$

where we have used $k \geq 1$ since it is the number of D6 branes. The quantized charges[19] are given by $Q_1 = \frac{1}{2\pi} N_1$, $Q_4 = (2\pi)^2 T_6 N_4$. We therefore see that a single D6 brane saturates the bound and that by varying the number of D6 branes or by appropriately changing the shape and orientation of the tube cross section, we can span the entire range of angular momenta between $-N_1 N_4$ and $+N_1 N_4$. Since (26) is quadratic the charges, one can easily exceed the black hole angular momentum bound in (25) by simply making Q_1 and Q_4 sufficiently large.

One can also compare the size of the supertube with the size of the black hole. Using (26), one can rewrite (20) in terms of the angular momentum:

$$r^2 \;=\; \frac{J^2}{Q_1\,(Q_0 + Q_4)}\,, \tag{27}$$

Now recall that the tension of a D-brane varies as g_s^{-1} and that the charges, Q_0 and Q_4, appear in the Hamiltonian, (16). This means that the quantization conditions on the D-brane charges must have the form $Q_j \sim N_j/g_s$. The energy of the fundamental string is independent of g_s and so $Q_1 \sim N_1$, with no factors of g_s. If we take $N_0 \approx N_1 \approx N_4 \approx N$ then we find:

$$r^2_{\rm tube} \;\sim\; g_s\,\frac{J^2}{N^2}\,. \tag{28}$$

From the BMPV black hole metric [58, 59] one can compute the proper length of the circumference of the horizon (as measured at one of the equator circles) to be

$$r^2_{\rm hole} \;\sim\; g_s\,\frac{N^3 - J^2}{N^2}\;. \tag{29}$$

[18] In Section 4.4 we will re-derive the BMPV solution as part of a more complex solution. This bound can be seen from (1) and follows from the requirement that there are no closed time-like curves outside the horizon.

[19] These charges are related to the charges that appear in the Hamiltonian by the corresponding tensions; more details about this can be found in [27].

The most important aspect of the equations (28) and (29) is that for comparable charges and angular momenta, the black hole and the three-charge supertube have comparable sizes. Moreover, these sizes grow with g_s in the same way. This is a very counter-intuitive behavior. Most of the objects we can think about tend to become smaller when gravity is made stronger and this is consistent with our intuition and the fact that gravity is an attractive force. The only "familiar" object that becomes larger with stronger gravity is a black hole. Nevertheless, three-charge supertubes also become larger as gravity becomes stronger! The size of a tube is determined by a balance between the angular momentum of the system and the tension of the tubular brane. As the string coupling is increased, the D-brane tension decreases, and thus the size of the tube grows, at exactly the same rate as the Schwarzschild radius of the black hole[20].

This is the distinguishing feature that makes the three-charge supertubes (as well as the smooth geometries that we will obtain from their geometric transitions) unlike any other configuration that one counts in studying black hole entropy.

To be more precise, let us consider the counting of states that leads to the black hole entropy "à la Strominger and Vafa." One counts microscopic brane/string configurations at weak coupling where the system is of string scale in extent, and its Schwarzschild radius even smaller. One then imagines increasing the gravitational coupling; the Schwarzschild radius grows, becoming comparable to the size of the brane configuration at the "correspondence point" [60], and larger thereafter. When the Schwarzschild radius is much larger than the Planck scale, the system can be described as a black hole. There are thus two very different descriptions of the system: as a microscopic string theory object for small g_s, and as a black hole for large g_s. One then compares the entropy in the two regimes and finds an agreement, which is precise if supersymmetry forbids corrections during the extrapolation.

Three-charge supertubes behave differently. Their size grows at the same rate as the Schwarzschild radius, and thus they have no "correspondence point." Their description is valid in the same regime as the description of the black hole. If by counting such configurations one could reproduce the entropy of the black hole, then one should think about the supertubes as the large g_s continuation of the microstates counted at small g_s in the string/brane picture, and therefore as the microstates of the corresponding black hole.

It is interesting to note that if the supertubes did not grow with *exactly* the same power of g_s as the black hole horizon, they would not be good candidates for being black hole microstates, and Mathur's conjecture would have been in some trouble. The fact that there exists a huge number of configurations that *do* have the same growth with g_s as the black hole is a non-trivial confirmation that these configurations may well represent black-hole microstates for the three-charge system.

[20]Note that this is a feature only of three-charge supertubes; ordinary (two-charge) supertubes have a growth that is duality-frame dependent.

We therefore expect that configurations constructed from three-charge supertubes will give us a large number of three-charge BPS black hole microstates. Nevertheless, we have seen that three-charge supertubes can have angular momenta larger than the BPS black hole, and generically have $J_1 \neq J_2$. Hence one can also ask if there exists a black object whose microstates those supertubes represent. In [27] it was conjectured that such an object should be a three-charge BPS black ring, despite the belief at the time that there was theorem that such BPS black rings could not exist. After more evidence for this conjecture came from the construction of the flat limit of black rings [55], a gap in the proof of the theorem was found [61]. Subsequently the BPS black ring with equal charges and dipole charges was found in [62], followed by the rings with three arbitrary charges and three arbitrary dipole charges [53, 63, 64]. One of the morals of this story is that whenever one encounters an "established" result that contradicts intuition one should really get to the bottom of it and find out why the intuition is wrong or to expose the cracks in established wisdom.

4 Black rings and supertubes

As we have seen in the D-brane analysis of the previous section, three-charge supertubes of arbitrary shape preserve the same supersymmetries as the three-charge black hole. Moreover, as we will see, three-charge supertube solutions that have three dipole charges can also have a horizon at large effective coupling, and thus become black rings. Therefore, one expects the existence of BPS configurations with an arbitrary distribution of black holes, black rings and supertubes of arbitrary shape. Finding the complete supergravity solution for such configurations appears quite daunting. We now show that this is nevertheless possible and that the entire problem can be reduced to solving a linear system of equations in four-dimensional, Euclidean electromagnetism.

4.1 Supersymmetric configurations

We begin by considering brane configurations that preserve the same supersymmetries as the three-charge black hole. In M-theory, the latter can be constructed by compactifying on a six-torus, T^6, and wrapping three sets of M2 branes on three orthogonal two-tori (see the first three rows of Table 1). Amazingly enough, one can add a further three sets of M5 branes while preserving the same supersymmetries: Each set of M5 branes can be thought of as magnetically dual to a set of M2 branes in that the M5 branes wrap the four-torus, T^4, orthogonal to the T^2 wrapped by the M2 branes. The remaining spatial direction of the M5 branes follows a simple, closed curve, $y^\mu(\sigma)$, in the spatial section of the five-dimensional space-time. Since we wish to make a single, three-charge ring we take this curve to be the same for all three sets of M5 branes. This configuration is summarized in Table 1. In [53] it was argued that this was the most general three-charge

Brane	0	1	2	3	4	5	6	7	8	9	10
M2	$\updownarrow$	$\star$	$\star$	$\star$	$\star$	$\updownarrow$	$\updownarrow$	$\leftrightarrow$	$\leftrightarrow$	$\leftrightarrow$	$\leftrightarrow$
M2	$\updownarrow$	$\star$	$\star$	$\star$	$\star$	$\leftrightarrow$	$\leftrightarrow$	$\updownarrow$	$\updownarrow$	$\leftrightarrow$	$\leftrightarrow$
M2	$\updownarrow$	$\star$	$\star$	$\star$	$\star$	$\leftrightarrow$	$\leftrightarrow$	$\leftrightarrow$	$\leftrightarrow$	$\updownarrow$	$\updownarrow$
M5	$\updownarrow$		$y^\mu(\sigma)$			$\leftrightarrow$	$\leftrightarrow$	$\updownarrow$	$\updownarrow$	$\updownarrow$	$\updownarrow$
M5	$\updownarrow$		$y^\mu(\sigma)$			$\updownarrow$	$\updownarrow$	$\leftrightarrow$	$\leftrightarrow$	$\updownarrow$	$\updownarrow$
M5	$\updownarrow$		$y^\mu(\sigma)$			$\updownarrow$	$\updownarrow$	$\updownarrow$	$\updownarrow$	$\leftrightarrow$	$\leftrightarrow$

Table 1: Layout of the branes that give the supertubes and black rings in an M-theory duality frame. Vertical arrows $\updownarrow$, indicate the directions along which the branes are extended, and horizontal arrows, $\leftrightarrow$, indicate the smearing directions. The functions, $y^\mu(\sigma)$, indicate that the brane wraps a simple closed curve in $\mathbb{R}^4$ that defines the black-ring or supertube profile. A star, $\star$, indicates that a brane is smeared along the supertube profile, and pointlike on the other three directions.

brane configuration[21] consistent with the supersymmetries of the three-charge black-hole.

The metric corresponding to this brane configuration can be written as

$$\begin{aligned} ds_{11}^2 = ds_5^2 \;&+\; \left(Z_2 Z_3 Z_1^{-2}\right)^{\frac{1}{3}} (dx_5^2 + dx_6^2) \\ &+\; \left(Z_1 Z_3 Z_2^{-2}\right)^{\frac{1}{3}} (dx_7^2 + dx_8^2) + \left(Z_1 Z_2 Z_3^{-2}\right)^{\frac{1}{3}} (dx_9^2 + dx_{10}^2)\,, \end{aligned} \tag{30}$$

where the five-dimensional space-time metric has the form:

$$ds_5^2 \;\equiv\; -\left(Z_1 Z_2 Z_3\right)^{-\frac{2}{3}} (dt + k)^2 + \left(Z_1 Z_2 Z_3\right)^{\frac{1}{3}}\, h_{\mu\nu} dy^\mu dy^\nu\,, \tag{31}$$

for some one-form field, k, defined upon the spatial section of this metric. Since we want the metric to be asymptotic to flat $\mathbb{R}^{4,1} \times T^6$, we require

$$ds_4^2 \;\equiv\; h_{\mu\nu} dy^\mu dy^\nu\,, \tag{32}$$

to limit to the flat, Euclidean metric on $\mathbb{R}^4$ at spatial infinity and we require the warp factors, Z_I, to limit to constants at infinity. To fix the normalization of the corresponding Kaluza-Klein $U(1)$ gauge fields, we will take $Z_I \to 1$ at infinity.

The supersymmetry, ϵ, consistent with the brane configurations in Table 1 must satisfy:

$$(\mathbb{1} \;-\; \Gamma^{056})\,\epsilon \;=\; (\mathbb{1} \;-\; \Gamma^{078})\,\epsilon \;=\; (\mathbb{1} \;-\; \Gamma^{09\,10})\,\epsilon \;=\; 0\,. \tag{33}$$

Since the product of all the gamma-matrices is the identity matrix, this implies

$$(\mathbb{1} \;-\; \Gamma^{1234})\,\epsilon \;=\; 0\,, \tag{34}$$

[21] Obviously one can choose add multiple curves and black hole sources.

which means that one of the four-dimensional helicity components of the four dimensional supersymmetry must vanish identically. The holonomy of the metric, (32), acting on the spinors is determined by

$$[\,\nabla_\mu\,,\,\nabla_\nu\,]\,\epsilon \;=\; \tfrac{1}{4}\,R^{(4)}_{\mu\nu cd}\,\Gamma^{cd}\,\epsilon\,, \tag{35}$$

where $R^{(4)}_{\mu\nu cd}$ is the Riemann tensor of (32). Observe that (35) vanishes identically as a consequence of (34) if the Riemann tensor is self-dual:

$$R^{(4)}_{abcd} \;=\; \tfrac{1}{2}\,\varepsilon_{cd}{}^{ef}\,R^{(4)}_{abef}\,. \tag{36}$$

Such four-metrics are called "half-flat." Equivalently, note that the holonomy of a general Euclidean four-metric is $SU(2)\times SU(2)$ and that (36) implies that the holonomy lies only in one of these $SU(2)$ factors and that the metric is flat in the other factor. The condition (34) means that all the components of the supersymmetry upon which the non-trivial holonomy would act actually vanish. The other helicity components feel no holonomy and so the supersymmetry can be defined globally. One should also note that $SU(2)$ holonomy in four-dimensions is equivalent to requiring that the metric be hyper-Kähler.

Thus we can preserve the supersymmetry if and only if we take the four-metric to be hyper-Kähler. However, there is a theorem that states that any metric that is (i) Riemannian (signature +4) and regular, (ii) hyper-Kähler and (iii) asymptotic to the flat metric on $\mathbb{R}^4$, *must be globally* the flat metric on $\mathbb{R}^4$. The obvious conclusion, which we will follow in this section, is that we simply take (32) to be the flat metric on $\mathbb{R}^4$. However, there are very important exceptions. First, we require the four-metric to be asymptotic to flat $\mathbb{R}^4$ because we want to interpret the object in asymptotically flat, five-dimensional space-time. If we want something that can be interpreted in terms of asymptotically flat, *four*-dimensional space-time then we want the four-metric to be asymptotic to the flat metric on $\mathbb{R}^3\times S^1$. This allows for a lot more possibilities, and includes the multi-Taub-NUT metrics [65]. Using such Taub-NUT metrics provides a straightforward technique for reducing the five-dimensional solutions to four dimensions [35, 66, 67, 68, 69].

The other exception will be the subject of subsequent sections of this thesis: The requirement that the four-metric be globally Riemannian is too stringent. As we will see, the metric can be allowed to change the overall sign since this can be compensated by a sign change in the warp factors of (31). In this section, however, we will suppose that the four-metric is simply that of flat $\mathbb{R}^4$.

4.2 The BPS equations

The Maxwell three-form potential is given by

$$C^{(3)} = A^{(1)}\wedge dx_5\wedge dx_6 \;+\; A^{(2)}\wedge dx_7\wedge dx_8 \;+\; A^{(3)}\wedge dx_9\wedge dx_{10}\,, \tag{37}$$

where the six coordinates, x_A, parameterize the compactification torus, T^6, and $A^{(I)}$, $I=1,2,3$, are one-form Maxwell potentials in the five-dimensional space-time and de-

pend only upon the coordinates, y^μ, that parameterize the spatial directions. It is convenient to introduce the Maxwell "dipole field strengths," $\Theta^{(I)}$, obtained by removing the contributions of the electrostatic potentials

$$\Theta^{(I)} \equiv dA^{(I)} + d(Z_I^{-1}(dt + k)), \tag{38}$$

The most general supersymmetric configuration is then obtained by solving the *BPS equations*:

$$\Theta^{(I)} = \star_4 \Theta^{(I)}, \tag{39}$$

$$\nabla^2 Z_I = \frac{1}{2} C_{IJK} \star_4 (\Theta^{(J)} \wedge \Theta^{(K)}), \tag{40}$$

$$dk + \star_4 dk = Z_I \Theta^{(I)}, \tag{41}$$

where $\star_4$ is the Hodge dual taken with respect to the four-dimensional metric $h_{\mu\nu}$, and structure constants[22] are given by $C_{IJK} \equiv |\epsilon_{IJK}|$. It is important to note that if these equations are solved in the order presented above, then one is solving a linear system.

At each step in the solution-generating process one has the freedom to add homogeneous solutions of the equations. Since we are requiring that the fields fall off at infinity, this means that these homogeneous solutions must have sources in the base space and since there is no topology in the $\mathbb{R}^4$ base, these sources must be singular. One begins by choosing the profiles, in $\mathbb{R}^4$, of the three types of M5 brane that source the $\Theta^{(I)}$. These fluxes then give rise to the explicit sources on the right-hand side of (40), but one also has the freedom to choose singular sources for (40) corresponding to the densities, $\rho_I(\sigma)$, of the three types of M2 branes. The M2 branes can be distributed at the same location as the M5 profile, and can also be distributed away from this profile. (See Fig. 4.) The functions, Z_I, then appear in the final solution as warp factors and as the electrostatic potentials. There are thus two contributions to the total electric charge of the solution: The localized M2 brane sources described by $\rho_I(\sigma)$ and the induced charge from the fields, $\Theta^{(I)}$, generated by the M5 branes. It is in this sense that the solution contains electric charges that are dissolved in the fluxes generated by M5 branes, much like in the Klebanov-Strassler or Klebanov-Tseytlin solutions [70, 71].

The final step is to solve the last BPS equation, (41), which is sourced by a cross term between the magnetic and electric fields. Again there are homogeneous solutions that may need to be added and this time; however they need to be adjusted so as to ensure that (31) has no closed time-like curves (CTC's). Roughly one must make sure that the angular momentum at each point does not exceed what can be supported by local energy density.

[22] If the T^6 compactification manifold is replaced by a more general Calabi-Yau manifold, the C_{IJK} change accordingly.

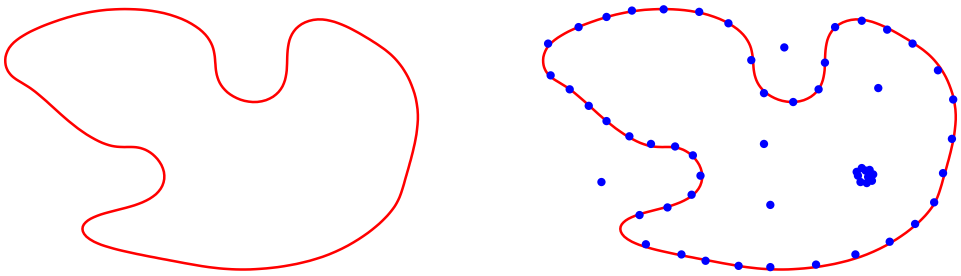

Figure 4: The first two steps of the procedure to construct solutions. One first chooses an arbitrary M5 brane profile, and then sprinkles the various types of M2 branes, either on the M5 brane profile, or away from it. This gives a solution for an arbitrary superposition of black rings, supertubes and black holes.

4.3 Asymptotic charges

Even though a generic black ring is made from six sets of branes, there are only three conserved electric charges that can be measured from infinity. These are obtained from the three vector potentials, $A^{(I)}$, defined in (37), by integrating $\star_5 dA^{(I)}$ over the three-sphere at spatial infinity. Since the M5 branes run in a closed loop, they do not directly contribute to the electric charges. The electric charges are determined by electric fields at infinity, and hence by the functions Z_I (38). Indeed, one has:

$$Z_I \;\sim\; 1 \;+\; c_1 \frac{Q_I}{\rho^2} \;+\; \ldots\,, \qquad \rho \to \infty\,, \tag{42}$$

where c_1 is a normalization constant (discussed below), ρ is the standard, Euclidean radial coordinate in $\mathbb{R}^4$ and the Q_I are the electric charges. Note that while the M5 branes do not *directly* contribute to the electric charges, they do contribute indirectly via "charges dissolved in fluxes," that is, through the source terms on the right-hand side of (40).

To compute the angular momentum it is convenient to write the spatial $\mathbb{R}^4$ as $\mathbb{R}^2 \times \mathbb{R}^2$ and pass to two sets of polar coordinates, (u, θ_1) and (v, θ_2) in which the flat metric on $\mathbb{R}^4$ is:

$$ds_4^2 \;=\; (du^2 \;+\; u^2\, d\theta_1^2) \;+\; (dv^2 \;+\; v^2\, d\theta_2^2)\,. \tag{43}$$

There are two commuting angular momenta, J_1 and J_2, corresponding to the components of rotation in these two planes. One can then read off the angular momentum by making an expansion at infinity of the angular momentum vector, k, in (31):

$$k \;\sim\; c_2 \left(J_1 \frac{u^2}{(u^2+v^2)^2} \;+\; J_2 \frac{v^2}{(u^2+v^2)^2} \right) \;+\; \ldots\;, \qquad u, v \to \infty\,, \tag{44}$$

where c_2 is a normalization constant. The charges, Q_I, and the angular momenta, J_1, J_2, need to be correctly normalized in order to express them in terms of the quantized charges.

The normalization depends upon the eleven-dimensional Planck length, ℓ_p, and the volume of the compactifying torus, T^6. The correct normalization can be found [53], and has been computed in many references. (For a good review, see [72].) Here we simply state that if L denotes the radius of the circles that make up the T^6 (so that the compactification volume is $V_6 = (2\pi L)^6$), then one obtains the canonically normalized quantities by using

$$c_1 \;=\; \frac{\ell_p^6}{L^4}\,, \qquad c_2 \;=\; \frac{\ell_p^9}{L^6}\,. \tag{45}$$

For simplicity, in most of the rest of this thesis we will take as system of units in which $\ell_p = 1$ and we will fix the torus volume so that $L = 1$. Thus one has $c_1 = c_2 = 1$.

4.4 An example: A three-charge black ring with a black hole in the middle

By solving the BPS equations, (39)–(41), one can, in principle, find the supergravity solution for an arbitrary distribution of black rings and black holes. The metric for a general distribution of these objects will be extremely complicated, and so to illustrate the technique we will concentrate on a simpler system: A BMPV black hole at the center of a three-charge BPS black ring. An extensive review of black rings, both BPS and non-BPS can be found in [73]. Other interesting papers related to non-BPS black rings include [74].

Since the ring sits in an $\mathbb{R}^2$ inside $\mathbb{R}^4$, it is it is natural to pass to the two sets of polar coordinates, (u, θ_1) and (v, θ_2) in which the base-space metric takes the form (43) We then locate the ring at $u = R$ and $v = 0$ and the black hole at $u = v = 0$.

The best coordinate system for actually solving the black ring equations is the one that has become relatively standard in the black-ring literature (see, for example, [62]). The change of variables is:

$$x \;=\; -\frac{u^2 + v^2 - R^2}{\sqrt{((u-R)^2 + v^2)((u+R)^2 + v^2)}}\,, \tag{46}$$

$$y \;=\; -\frac{u^2 + v^2 + R^2}{\sqrt{((u-R)^2 + v^2)((u+R)^2 + v^2)}}\,, \tag{47}$$

where $-1 \leq x \leq 1$, $-\infty < y \leq -1$, and the ring is located at $y = -\infty$. This system has several advantages: it makes the electric and magnetic two-form field strengths sourced by the ring have a very simple form (see (49)), and it makes the ring look like a single point while maintaining separability of the Laplace equation. In these coordinates the flat $\mathbb{R}^4$ metric has the form:

$$ds_4^2 \;=\; \frac{R^2}{(x-y)^2}\left(\frac{dy^2}{y^2-1} + (y^2-1)d\theta_1^2 + \frac{dx^2}{1-x^2} + (1-x^2)d\theta_2^2\right). \tag{48}$$

The self-dual[23] field strengths that are sourced by the ring are then:

$$\Theta^{(I)} \;=\; 2\,q_i\,(dx\wedge d\theta_2 \;-\; dy\wedge d\theta_1)\,. \tag{49}$$

The warp factors then have the form

$$Z_I \;=\; 1 \;+\; \frac{\overline{Q}_I}{R}(x-y) \;-\; \frac{2\,C_{IJK}\,q^J q^K}{R^2}\,(x^2-y^2) \;-\; \frac{Y_I}{R^2}\,\frac{x-y}{x+y}\,, \tag{50}$$

and the angular momentum components are given by:

$$k_\psi \;=\; (y^2-1)\,g(x,y) - \,A\,(y+1)\,, \qquad k_\phi = (x^2-1)\,g(x,y)\,; \tag{51}$$

$$g(x,y) \;\equiv\; \left(\frac{C}{3}\,(x+y) \;+\; \frac{B}{2} - \frac{D}{R^2(x+y)} + \frac{K}{R^2(x+y)^2}\right) \tag{52}$$

where K represents the angular momentum of the BMPV black hole and

$$A \;\equiv\; 2(\textstyle\sum q^I)\,, \qquad B \;\equiv\; \dfrac{2}{R}\,(Q_I q^I)\,, \tag{53}$$

$$C \;\equiv\; -\frac{8\,C_{IJK}\,q^I q^J q^K}{R^2}\,, \qquad D \;\equiv\; 2\,Y_I q^I\,. \tag{54}$$

The homogeneous solutions of (41) have already been chosen so as to remove any closed timelike curves (CTC).

The relation between the quantized ring and black-hole charges and the parameters appearing in the solution are:

$$\overline{Q}_I = \frac{\overline{N}_I\,\ell_p^6}{2L^4R}\,, \qquad q^I = \frac{n^I\,\ell_p^3}{4L^2}\,, \qquad Y_I = \frac{N_I^{\rm BH}\,\ell_p^6}{L^4}\,, \qquad K = \frac{J^{\rm BMPV}\,\ell_p^9}{L^6}\,, \tag{55}$$

where L is the radius of the circles that make up the T^6 (so that $V_6 = (2\pi L)^6$) and ℓ_p is the eleven-dimensional Planck length.

As we indicated earlier, the asymptotic charges, N_I, of the solution are the sum of the microscopic charges on the black ring, $\overline{N}_I$, the charges of the black hole, $N_I^{\rm BH}$, and the charges dissolved in fluxes:

$$N_I \;=\; \overline{N}_I \;+\; N_I^{\rm BH} \;+\; \tfrac{1}{2}\,C_{IJK}\,n^J n^K\,. \tag{56}$$

The angular momenta of this solution are:

$$J_1 \;=\; J_\Delta \;+\; \left(\tfrac{1}{6}\,C_{IJK}\,n^I n^J n^K \;+\; \tfrac{1}{2}\,\overline{N}_I n^I \;+\; N_I^{\rm BH} n^I \;+\; J^{\rm BMPV}\right), \tag{57}$$

$$J_2 \;=\; -\left(\tfrac{1}{6}\,C_{IJK}\,n^I n^J n^K \;+\; \tfrac{1}{2}\,\overline{N}_I n^I \;+\; N_I^{\rm BH} n^I \;+\; J^{\rm BMPV}\right), \tag{58}$$

[23] Our orientation is $\epsilon^{yx\theta_1\theta_2} = +1$.

where

$$J_\Delta \;\equiv\; \frac{R^2L^4}{l_p^6}\left(\sum n^I\right). \tag{59}$$

The entropy of the ring is:

$$S \;=\; \frac{2\pi A}{\kappa_{11}^2} \;=\; \pi\sqrt{\mathcal{M}} \tag{60}$$

where

$$\begin{aligned}\mathcal{M} \;\equiv\;& 2\,n^1n^2\overline{N}_1\overline{N}_2 + 2\,n^1n^3\overline{N}_1\overline{N}_3 + 2\,n^2n^3\overline{N}_2\overline{N}_3 - (n^1\overline{N}_1)^2 \\ & -(n^2\overline{N}_2)^2 - (n^3\overline{N}_3)^2 - 4\,n^1n^2n^3\,J_T\,.\end{aligned} \tag{61}$$

and

$$J_T \;\equiv\; J_\Delta + n^I N_I^{\rm BH} \;=\; \frac{R^2L^4}{l_p^6}\left(\sum n^I\right) \;+\; n^I N_I^{\rm BH}\,. \tag{62}$$

As we will explain in more detail in section 6.6, black rings can be related to four-dimensional black holes, and (61) is the square root of the $E_{7(7)}$ quartic invariant of the microscopic charges of the ring [45]; these microscopic charges are the n^I, the $\overline{N}_I$ and the angular momentum J_T. More generally, in configurations with multiple black rings and black holes, the quantity multiplying $n^1n^2n^3$ in $\mathcal{M}$ should be identified with the microscopic angular momentum of the ring. There are several ways to confirm that this identification is correct. First, one should note that J_T is the quantity that appears in the near-horizon limit of the metric and, in particular, determines the horizon area and hence entropy of the ring as in (60). This means that J_T is an intrinsic property of the ring. In the next section we will discuss the process of lowering a black hole into the center of a ring and we will see, once again, that it is J_T that represents the intrinsic angular momentum of the ring.

The angular momenta of the solution may be re-written in terms of fundamental charges as:

$$\begin{aligned} J_1 \;&=\; J_T \;+\; \left(\tfrac{1}{6}\,C_{IJK}\,n^In^Jn^K \;+\; \tfrac{1}{2}\,\overline{N}_In^I \;+\; J^{\rm BMPV}\right) \\ J_2 \;&=\; -\left(\tfrac{1}{6}\,C_{IJK}\,n^In^Jn^K \;+\; \tfrac{1}{2}\,\overline{N}_In^I \;+\; N_I^{\rm BH}n^I \;+\; J^{\rm BMPV}\right). \end{aligned} \tag{63}$$

Notice that in this form, J_1 contains no contribution coming from the combined effect of the electric field of the black hole and the magnetic field of the black ring. Such a contribution only appears in J_2.

4.5 Merging black holes and black rings

One can also use the methods above to study processes in which black holes and black rings are brought together and ultimately merge. Such processes are interesting in their

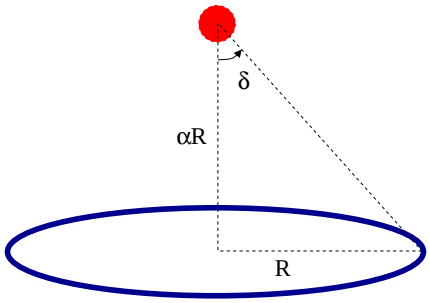

Figure 5: The configuration black ring with an off-set black hole on its axis. The parameter, α, is related to the angle of approach, δ, by $\alpha \equiv \cot\delta$.

own right, but we will also see later that they can be very useful in the study of microstate geometries.

It is fairly straightforward to generalize the solution of Section 4.4 to one that describes a black ring with a black hole on the axis of the ring, but offset above the ring by a distance, $a = \alpha R$, where R is radius of the ring. (Both a and R are measured in the $\mathbb{R}^4$ base.) This is depicted in Fig. 5. The details of the exact solution may be found in [75] and we will only summarize the main results here.

The total charge of the combined system is independent of α and is given by (56). Similarly, the entropy of the black ring is still given by (60) and (61), but now with J_T defined by:

$$J_T \;=\; J_\Delta \;+\; \frac{n^I N_I^{\rm BH}}{1+\alpha^2} \;\equiv\; \frac{R^2 L^4}{l_p^6}\Big(\sum n^I\Big) \;+\; \frac{n^I N_I^{\rm BH}}{1+\alpha^2}\,. \tag{64}$$

The horizon area of the black hole is unmodified by the presence of the black ring and, in particular, its dependence on α only comes via J_T. Thus, for an adiabatic process, the quantity, $\mathcal{M}$, in (61) must remain fixed, and therefore J_T must remain fixed. This is consistent with identifying J_T as the intrinsic angular momentum of the ring.

The two angular momenta of the system are:

$$J_1 \;=\; J_T \;+\; \Big(\tfrac{1}{6}\,C_{IJK}n^I n^J n^K \;+\; \tfrac{1}{2}\,\overline{N}_I n^I \;+\; J^{\rm BMPV}\Big)\,, \tag{65}$$

$$J_2 \;=\; -\Big(\tfrac{1}{6}\,C_{IJK}n^I n^J n^K \;+\; \tfrac{1}{2}\,\overline{N}_I n^I \;+\; \frac{N_I^{\rm BH} n^I}{1+\alpha^2} \;+\; J^{\rm BMPV}\Big)\,. \tag{66}$$

If we change the separation of the black hole and black ring while preserving the axial symmetry, that is, if we vary α, then the symmetry requires J_1 to be conserved. Once again we see that this means that J_T must remain fixed.

The constancy of J_T along with (64) imply that as the black hole is brought near the black ring, the embedding radius of the latter, R, must change according to:

$$R^2 \;=\; \frac{l_p^6}{L^4}\,\big(\sum n^I\big)^{-1}\Big(J_T - \frac{n^I N_I^{\rm BH}}{1+\alpha^2}\Big)\,. \tag{67}$$

For fixed microscopic charges this formula gives the radius of the ring as a function of the parameter α. The black hole will merge with the black ring if and only if R vanishes for some value of α. That is, if and only if

$$J_T \;\leq\; n^I N_I^{\rm BH}\,. \tag{68}$$

The vanishing of R suggests that the ring is pinching off, however, in the physical metric, (31), the ring generically has finite size as it settles onto the horizon of the black hole. Indeed, the value of $\alpha = \tan\zeta$ at the merger determines the latitude, ζ, at which the ring settles on the black hole. If it occurs at $\alpha = 0$ then the ring merges by grazing the black hole at the equator.

At merger ($R = 0$) one can see that $J_1 = J_2$ and so the resulting object will have $J_1 = J_2$ given by (65). This will be a BMPV black hole and its electric charges are simply given by (56). We can therefore use (1) to determine the final entropy after the merger. Note that the process we are considering is adiabatic up to the point where the ring touches the horizon of the black hole. The process of swallowing the ring is not necessarily adiabatic, but we assume that the black hole does indeed swallow the black ring and we can then compute the entropy from the charges and angular momentum of the resulting BMPV black hole.

In general, the merger of a black hole and a black ring is irreversible, that is, the total horizon area increases in the process. However, there is precisely one situation in which the merger is reversible, and that requires *all* of the following to be true:

1. The ring must have zero horizon area (with a slight abuse of terminology we will also refer to such rings as *supertubes*).

2. The black hole that one begins with must have zero horizon area, *i.e.* it must be *maximally spinning.*

3. The ring must meet the black hole by grazing it at the equator.

4. There are two integers, $\bar{P}$ and P^{BH} such that

$$\overline{N}_I \;=\; \frac{\overline{P}}{n^I} \qquad \text{and} \qquad N_I^{BH} \;=\; \frac{P^{BH}}{n^I}\,, \qquad I = 1,2,3\,. \tag{69}$$

If all of these conditions are met then the end result is also a maximally spinning BMPV black hole and hence also has zero horizon area.

Note that the last condition implies that

$$N_I \;\equiv\; \overline{N}_I + \tfrac{1}{2}\,C_{IJK}\,n^J\,n^K \;=\; \frac{(\overline{P} + n^1\,n^2\,n^3)}{n^I}\,, \tag{70}$$

and therefore the electric charges of black ring *and* its charges dissolved in fluxes ($\frac{1}{2}\,C_{IJK}\,n^J\,n^K$) must both be aligned exactly parallel to the electric charges of the black

hole. Conversely, if conditions 1–3 are satisfied, but the charge vectors of the black hole and black ring are *not parallel* then the merger will be irreversible. This observation will be important in Section 9.

5 Geometric interlude: Four-dimensional black holes and five-dimensional foam

In Section 4.1 we observed that supersymmetry allows us to take the base-space metric to be any hyper-Kähler metric. There are certainly quite a number of interesting four-dimensional hyper-Kähler metrics and in particular, there are the multi-centered Gibbons-Hawking metrics. These provide examples of asymptotically locally Euclidean (ALE) and asymptotically locally flat (ALF) spaces, which are asymptotic to $\mathbb{R}^4/\mathbb{Z}_n$ and $\mathbb{R}^3 \times S^1$ respectively. Using ALF metrics provides a smooth way to transition between a five-dimensional and a four-dimensional interpretation of a certain configurations. Indeed, the size of the S^1 is usually a modulus of a solution, and thus is freely adjustable. When this size is large compared to the size of the source configuration, this configuration is essentially five-dimensional; if the S^1 is small, then the configuration has a four-dimensional description.

We noted earlier that a regular, Riemannian, hyper-Kähler metric that is asymptotic to flat $\mathbb{R}^4$ is necessarily flat $\mathbb{R}^4$ *globally*. The non-trivial ALE metrics get around this by having a discrete identification at infinity but, as a result, do not have an asymptotic structure that lends itself to a space-time interpretation. However, there is an unwarranted assumption here: One should remember that the goal is for the five-metric (31) to be regular and Lorentzian and this might be achievable if singularities of the four-dimensional base space were canceled by the warp factors. More specifically, we are going to consider base-space metrics (32) whose overall sign is allowed to change in interior regions. That is, we are going to allow the signature to flip from $+4$ to -4. We will call such metrics *ambipolar*.

The potentially singular regions could actually be regular if the warp factors, Z_I, all flip sign whenever the four-metric signature flips. Indeed, we suspect that the desired property may follow quite generally from the BPS equations through the four-dimensional dualization on the right-hand side of (40). Obviously, there are quite a number of details to be checked before complete regularity is proven, but we will see below that this can be done for ambipolar Gibbons-Hawking metrics.

Because of these two important applications, we now give a review of Gibbons-Hawking geometries [65, 76] and their elementary ambipolar generalization. These metrics have the virtue of being simple enough for very explicit computation and yet capture some extremely interesting physics.

5.1 Gibbons-Hawking metrics

Gibbons-Hawking metrics have the form of a $U(1)$ fibration over a flat $\mathbb{R}^3$ base:

$$h_{\mu\nu}dx^\mu dx^\nu \;=\; V^{-1}\,(d\psi + \vec{A}\cdot d\vec{y})^2 \;+\; V\,(dx^2+dy^2+dz^2)\,, \tag{71}$$

where we write $\vec{y} = (x, y, z)$. The function, V, is harmonic on the flat $\mathbb{R}^3$ while the connection, $A = \vec{A}\cdot d\vec{y}$, is related to V via

$$\vec{\nabla}\times\vec{A} \;=\; \vec{\nabla}V\,. \tag{72}$$

This family of metrics is the unique set of hyper-Kähler metrics with a tri-holomorphic $U(1)$ isometry[24]. Moreover, four-dimensional hyper-Kähler manifolds with $U(1)\times U(1)$ symmetry must, at least locally, be Gibbons-Hawking metrics with an extra $U(1)$ symmetry around an axis in the $\mathbb{R}^3$ [77].

In the standard form of the Gibbons-Hawking metrics one takes V to have a finite set of isolated sources. That is, let $\vec{y}^{(j)}$ be the positions of the source points in the $\mathbb{R}^3$ and let $r_j \equiv |\vec{y}-\vec{y}^{(j)}|$. Then one takes:

$$V = \varepsilon_0 \;+\; \sum_{j=1}^{N}\frac{q_j}{r_j}\,, \tag{73}$$

where one usually takes $q_j \geq 0$ to ensure that the metric is Riemannian (positive definite). We will later relax this restriction. There appear to be singularities in the metric at $r_j = 0$, however, if one changes to polar coordinates centered at $r_j = 0$ with radial coordinate to $\rho = 2\sqrt{|\vec{y}-\vec{y}^{(j)}|}$, then the metric is locally of the form:

$$ds_4^2 \;\sim\; d\rho^2 \;+\; \rho^2\,d\Omega_3^2\,, \tag{74}$$

where $d\Omega_3^2$ is the standard metric on $S^3/\mathbb{Z}_{|q_j|}$. In particular, this means that one must have $q_j \in \mathbb{Z}$ and if $|q_j| = 1$ then the space looks locally like $\mathbb{R}^4$. If $|q_j| \neq 1$ then there is an orbifold singularity, but since this is benign in string theory, we will view such backgrounds as regular.

If $\varepsilon_0 \neq 0$, then $V \to \varepsilon_0$ at infinity and so the metric (71) is asymptotic to flat $\mathbb{R}^3\times S^1$, that is, the base is asymptotically locally flat (ALF). The five-dimensional space-time is thus asymptotically compactified to a four-dimensional space-time. This a standard Kaluza-Klein reduction and the gauge field, $\vec{A}$, yields a non-trivial, four-dimensional Maxwell field whose sources, from the ten-dimensional perspective, are simply D6 branes. In Subsection 6.6 we will make extensive use of of the fact that introducing a constant term

[24]Tri-holomorphic means that the $U(1)$ preserves all three complex structures of the hyper-Kähler metric.

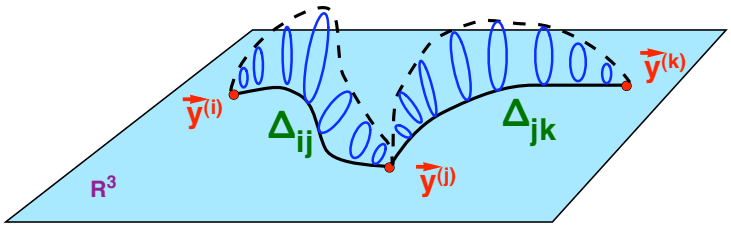

Figure 6: This figure depicts some non-trivial cycles of the Gibbons-Hawking geometry. The behaviour of the $U(1)$ fiber is shown along curves between the sources of the potential, V. Here the fibers sweep out a pair of intersecting homology spheres.

into V yields a further compactification and through this we can relate five-dimensional physics to four-dimensional physics.

Now suppose that one has $\varepsilon_0 = 0$. At infinity in $\mathbb{R}^3$ one has $V \sim q_0/r$, where $r \equiv |\vec{y}|$ and

$$q_0 \equiv \sum_{j=1}^{N} q_j \,. \tag{75}$$

Hence spatial infinity in the Gibbons-Hawking metric also has the form (74), where

$$r = \tfrac{1}{4}\rho^2 \,, \tag{76}$$

and $d\Omega_3^2$ is the standard metric on $S^3/\mathbb{Z}_{|q_0|}$. For the Gibbons-Hawking metric to be asymptotic to the positive definite, flat metric on $\mathbb{R}^4$ one must have $q_0 = 1$. Note that for the Gibbons-Hawking metrics to be globally positive definite one would also have to take $q_j \geq 0$ and thus the only such metric would have to have $V \equiv \frac{1}{r}$. The metric (71) is then the flat metric on $\mathbb{R}^4$ globally, as can be seen by using the change of variables (76). The only way to get non-trivial metrics that are asymptotic to flat $\mathbb{R}^4$ is by taking some of the $q_j \in \mathbb{Z}$ to be negative.

5.2 Homology and cohomology

The multi-center Gibbons-Hawking (GH) metrics also contain $\frac{1}{2}N(N-1)$ topologically non-trivial two-cycles, Δ_{ij}, that run between the GH centers. These two-cycles can be defined by taking any curve, γ_{ij}, between $\vec{y}^{(i)}$ and $\vec{y}^{(j)}$ and considering the $U(1)$ fiber of (71) along the curve. This fiber collapses to zero at the GH centers, and so the curve and the fiber sweep out a 2-sphere (up to $\mathbb{Z}_{|q_j|}$ orbifolds). See Fig. 6. These spheres intersect one another at the common points $\vec{y}^{(j)}$. There are $(N-1)$ linearly independent homology two-spheres, and the set $\Delta_{i\,(i+1)}$ represents a basis[25].

[25]The integer homology corresponds to the root lattice of $SU(N)$ with an intersection matrix given by the inner product of the roots.

It is also convenient to introduce a set of frames

$$\hat{e}^1 \;=\; V^{-\frac{1}{2}}\,(d\psi \;+\; A)\,, \qquad \hat{e}^{a+1} \;=\; V^{\frac{1}{2}}\,dy^a\,, \quad a=1,2,3\,. \tag{77}$$

and two associated sets of two-forms:

$$\Omega^{(a)}_{\pm} \;\equiv\; \hat{e}^1\wedge\hat{e}^{a+1} \;\pm\; \tfrac{1}{2}\,\epsilon_{abc}\,\hat{e}^{b+1}\wedge\hat{e}^{c+1}\,, \qquad a=1,2,3\,. \tag{78}$$

The two-forms, $\Omega^{(a)}_{-}$, are anti-self-dual, harmonic and non-normalizable and they define the hyper-Kähler structure on the base. The forms, $\Omega^{(a)}_{+}$, are self-dual and can be used to construct harmonic fluxes that are dual to the two-cycles. Consider the self-dual two-form:

$$\Theta \;\equiv\; \sum_{a=1}^{3}\,(\partial_a(V^{-1}\,H))\,\Omega^{(a)}_{+}\,. \tag{79}$$

Then Θ is closed (and hence co-closed and harmonic) if and only if H is harmonic in $\mathbb{R}^3$, *i.e.* $\nabla^2 H=0$. We now have the choice of how to distribute sources of H throughout the $\mathbb{R}^3$ base of the GH space; such a distribution may correspond to having multiple black rings and black holes in this space. Nevertheless, if we want to obtain a geometry that has no singularities and no horizons, Θ has to be regular, and this happens if and only if H/V is regular; this occurs if and only if H has the form:

$$H \;=\; h_0 \;+\; \sum_{j=1}^{N}\,\frac{h_j}{r_j}\,. \tag{80}$$

Also note that the "gauge transformation:"

$$H \;\rightarrow\; H \;+\; c\,V\,, \tag{81}$$

for some constant, c, leaves Θ unchanged, and so there are only N independent parameters in H. In addition, if $\varepsilon=0$ then one must take $h_0=0$ for Θ to remain finite at infinity. The remaining $(N-1)$ parameters then describe harmonic forms that are dual to the non-trivial two-cycles. If $\varepsilon\neq 0$ then the extra parameter is that of a Maxwell field whose gauge potential gives the Wilson line around the S^1 at infinity.

It is straightforward to find a *local* potential such that $\Theta=dB$:

$$B \;\equiv\; V^{-1}\,H\,(d\psi \;+\; A) \;+\; \vec{\xi}\cdot d\vec{y}\,, \tag{82}$$

where

$$\vec{\nabla}\times\vec{\xi} \;=\; -\,\vec{\nabla}H\,. \tag{83}$$

Hence, $\vec{\xi}$ is a vector potential for magnetic monopoles located at the singular points of H.

To determine how these fluxes thread the two-cycles we need the explicit forms for the vector potential, B, and to find these we first need the vector fields, $\vec{v}_i$, that satisfy:

$$\vec{\nabla} \times \vec{v}_i \;=\; \vec{\nabla}\Big(\frac{1}{r_i}\Big)\,. \tag{84}$$

One then has:

$$\vec{A} \;=\; \sum_{j=1}^{N} q_j\,\vec{v}_j\,, \qquad \vec{\xi} \;=\; \sum_{j=1}^{N} h_j\,\vec{v}_j\,. \tag{85}$$

If we choose coordinates so that $\vec{y}^{(i)} \;=\; (0,0,a)$ and let ϕ denote the polar angle in the (x,y)-plane, then:

$$\vec{v}_i \cdot d\vec{y} \;=\; \Big(\frac{(z-a)}{r_i} \;+\; c_i\Big)\,d\phi\,, \tag{86}$$

where c_i is a constant. The vector field, $\vec{v}_i$, is regular away from the z-axis, but has a Dirac string along the z-axis. By choosing c_i we can cancel the string along the positive or negative z-axis, and by moving the axis we can arrange these strings to run in any direction we choose, but they must start or finish at some $\vec{y}^{(i)}$, or run out to infinity.

Now consider what happens to B in the neighborhood of $\vec{y}^{(i)}$. Since the circles swept out by ψ and ϕ are shrinking to zero size, the string singularities near $\vec{y}^{(i)}$ are of the form:

$$B \;\sim\; \frac{h_i}{q_i}\Big(d\psi + q_i\,\Big(\frac{(z-a)}{r_i} + c_i\Big)\,d\phi\Big) \;-\; h_i\,\Big(\frac{(z-a)}{r_i} + c_i\Big)\,d\phi \;\sim\; \frac{h_i}{q_i}\,d\psi\,. \tag{87}$$

This shows that the vector, $\vec{\xi}$, in (82) cancels the string singularities in the $\mathbb{R}^3$. The singular components of B thus point along the $U(1)$ fiber of the GH metric.

Choose any curve, γ_{ij}, between $\vec{y}^{(i)}$ and $\vec{y}^{(j)}$ and define the two-cycle, Δ_{ij}, as in Fig. 6. If one has $V > 0$ then the vector field, B, is regular over the whole of Δ_{ij} except at the end-points, $\vec{y}^{(i)}$ and $\vec{y}^{(j)}$. Let $\widehat{\Delta}_{ij}$ be the cycle Δ_{ij} with the poles excised. Since Θ is regular at the poles, then the expression for the flux, Π_{ij}, through Δ_{ij} can be obtained as follows:

$$\begin{aligned}\Pi_{ij} \quad &\equiv \quad \frac{1}{4\,\pi}\int_{\Delta_{ij}}\Theta \;=\; \frac{1}{4\,\pi}\int_{\widehat{\Delta}_{ij}}\Theta \;=\; \frac{1}{4\,\pi}\int_{\partial\widehat{\Delta}_{ij}} B \\ &= \quad \frac{1}{4\,\pi}\int_0^{4\pi} d\psi\,(B|_{y^{(j)}} \;-\; B|_{y^{(i)}}) \;=\; \Big(\frac{h_j}{q_j} \;-\; \frac{h_i}{q_i}\Big)\,.\end{aligned} \tag{88}$$

We have normalized these periods for later convenience.

On an ambipolar GH space where the cycle runs between positive and negative GH points, the flux, Θ, and the potential B are both singular when $V = 0$ and so this integral is a rather formal object. However, we will see in Subsection 7.3 that when we extend to the five-dimensional metric, the physical flux of the complete Maxwell field combines Θ with another term so that the result is completely regular. Moreover, the physical flux through the cycle is still given by (88). We will therefore refer to (88) as the magnetic flux even in ambipolar metrics and we will see that such fluxes are directly responsible for holding up the cycles

6 Solutions on a Gibbons-Hawking base

6.1 Solving the BPS equations

Our task now is to solve the BPS equations (39)–(41) but now with a Gibbons-Hawking base metric. Such solutions have been derived before for positive-definite Gibbons-Hawking metrics [78, 64], and it is trivial to generalize to the ambipolar form. For the present we will not impose any conditions on the sources of the BPS equations.

In Subsection 5.2 we saw that there was a simple way to obtain self-dual two-forms, $\Theta^{(I)}$, that satisfy (39). That is, we introduce three harmonic functions, K^I, on $\mathbb{R}^3$ that satisfy $\nabla^2 K^I = 0$, and define $\Theta^{(I)}$ as in (79) by replacing H with K^I. We will not, as yet, assume any specific form for K^I.

If we substitute these two-forms into (40), one can show that the resulting equation has the solution:

$$Z_I \;=\; \tfrac{1}{2}\, C_{IJK}\, V^{-1}\, K^J K^K \;+\; L_I\,, \tag{89}$$

where the L_I are three more independent harmonic functions.

We now write the one-form, k, as:

$$k \;=\; \mu\,(d\psi + A) \;+\; \omega \tag{90}$$

and then (41) becomes:

$$\vec{\nabla}\times\vec{\omega} \;=\; (V\vec{\nabla}\mu \;-\; \mu\vec{\nabla}V) \;-\; V\sum_{I=1}^{3} Z_I\,\vec{\nabla}\Big(\frac{K^I}{V}\Big)\,. \tag{91}$$

Taking the divergence yields the following equation for μ:

$$\nabla^2\mu \;=\; V^{-1}\,\vec{\nabla}\cdot\Big(V\sum_{I=1}^{3} Z_I\;\vec{\nabla}\frac{K^I}{V}\Big)\,, \tag{92}$$

which is solved by:

$$\mu \;=\; \tfrac{1}{6}\, C_{IJK}\,\frac{K^I K^J K^K}{V^2} \;+\; \frac{1}{2\,V}\,K^I L_I \;+\; M\,, \tag{93}$$

where M is yet another harmonic function on $\mathbb{R}^3$. Indeed, M determines the anti-self-dual part of dk that cancels out of (41). Substituting this result for μ into (91) we find that ω satisfies:

$$\vec{\nabla}\times\vec{\omega} \;=\; V\vec{\nabla}M \;-\; M\vec{\nabla}V \;+\; \tfrac{1}{2}\,(K^I\vec{\nabla}L_I - L_I\vec{\nabla}K^I)\,. \tag{94}$$

The integrability condition for this equation is simply the fact that the divergence of both sides vanish, which is true because K^I, L_I, M and V are harmonic.

6.2 Some properties of the solution

The solution is thus characterized by the harmonic functions K^I, L_I, V and M. The gauge invariance, (81), extends in a straightforward manner to the complete solution:

$$\begin{aligned} K^I &\rightarrow K^I + c^I V\,, \\ L_I &\rightarrow L_I - C_{IJK}\, c^J\, K^K - \tfrac{1}{2}\, C_{IJK}\, c^J\, c^K\, V\,, \\ M &\rightarrow M - \tfrac{1}{2}\, c^I\, L_I + \frac{1}{12}\, C_{IJK} \left(V\, c^I\, c^J\, c^K + 3\, c^I\, c^J\, K^K \right)\,, \end{aligned} \tag{95}$$

where the c^I are three arbitrary constants[26].

The eight functions that give the solution may also be identified with the eight independent parameters in the **56** of the $E_{7(7)}$ duality group in four dimensions:

$$\begin{aligned} x_{12} &= L_1\,, \quad x_{34} = L_2\,, \quad x_{56} = L_3\,, \quad x_{78} = -V\,, \\ y_{12} &= K^1\,, \quad y_{34} = K^2\,, \quad y_{56} = K^3\,, \quad y_{78} = 2\,M\,. \end{aligned} \tag{96}$$

With these identifications, the right-hand side of (94) is the symplectic invariant of the **56** of $E_{7(7)}$:

$$\vec{\nabla} \times \vec{\omega} = \tfrac{1}{4} \sum_{A,B=1}^{8} (y_{AB} \vec{\nabla} x_{AB} - x_{AB} \vec{\nabla} y_{AB})\,. \tag{97}$$

We also note that the quartic invariant of the **56** of $E_{7(7)}$ is determined by:

$$\begin{aligned} J_4 = & -\frac{1}{4}(x_{12}y^{12} + x_{34}y^{34} + x_{56}y^{56} + x_{78}y^{78})^2 - x_{12}x_{34}x_{56}x_{78} \\ & -y^{12}y^{34}y^{56}y^{78} + x_{12}x_{34}y^{12}y^{34} + x_{12}x_{56}y^{12}y^{56} + x_{34}x_{56}y^{34}y^{56} \\ & +x_{12}x_{78}y^{12}y^{78} + x_{34}x_{78}y^{34}y^{78} + x_{56}x_{78}y^{56}y^{78}\,, \end{aligned} \tag{98}$$

and we will see that this plays a direct role in the expression for the scale of the $U(1)$ fibration. It also plays a central role in the expression for the horizon area of a four-dimensional black hole [79].

In principle we can choose the harmonic functions K^I, L_I and M to have sources that are localized anywhere on the base. These solutions then have localized brane sources, and include, for example, supertubes and black rings in Taub-NUT [35, 67, 68, 69], which we will review in Subsection 6.5. Such solutions also include more general multi-center black hole configurations in four dimensions, of the type considered by Denef and collaborators [80].

Nevertheless, our focus for the moment is on obtaining smooth horizonless solutions, which correspond to microstates of black holes and black rings and we choose the harmonic functions so that there are no brane charges anywhere, and all the charges come from the smooth cohomological fluxes that thread the non-trivial cycles.

[26] Note that this gauge invariance exists for any C_{IJK}, not only for those coming from reducing M-theory on T^6.

6.3 Closed time-like curves

To look for the presence of closed time-like curves in the metric one considers the space-space components of the metric given by (30), (31) and (71). That is, one goes to the space-like slices obtained by taking t to be a constant. The T^6 directions immediately yield the requirement that $Z_I Z_J > 0$ while the metric on the four-dimensional base reduces to:

$$\begin{aligned} ds_4^2 &= -W^{-4}\,(\mu(d\psi + A) + \omega)^2 \\ &\quad + W^2 V^{-1}(d\psi + A)^2 + W^2 V(dr^2 + r^2 d\theta^2 + r^2 \sin^2\theta\, d\phi^2)\,, \end{aligned} \tag{99}$$

where we have chosen to write the metric on $\mathbb{R}^3$ in terms of a generic set of spherical polar coordinates, (r, θ, ϕ) and where we have defined the warp-factor, W, by:

$$W \equiv (Z_1\, Z_2\, Z_3)^{1/6}\,. \tag{100}$$

There is some potentially singular behavior arising from the fact that the Z_I, and hence W, diverge on the locus, $V = 0$ (see (89)). However, one can show that if one expands the metric (99) and uses the expression, (93), then all the dangerous divergent terms cancel and the metric is regular. We will discuss this further below and in Subsection 6.4.

Expanding (99) leads to:

$$\begin{aligned} ds_4^2 &= W^{-4}\,(W^6 V^{-1} - \mu^2)\Big(d\psi + A - \frac{\mu\,\omega}{W^6 V^{-1} - \mu^2}\Big)^2 - \frac{W^2\,V^{-1}}{W^6 V^{-1} - \mu^2}\,\omega^2 \\ &\quad + W^2 V(dr^2 + r^2 d\theta^2 + r^2 \sin^2\theta\, d\phi^2) \\ &= \frac{\mathcal{Q}}{W^4 V^2}\Big(d\psi + A - \frac{\mu\, V^2}{\mathcal{Q}}\,\omega\Big)^2 + W^2 V\Big(r^2 \sin^2\theta\, d\phi^2 - \frac{\omega^2}{\mathcal{Q}}\Big) \\ &\quad + W^2 V(dr^2 + r^2 d\theta^2)\,, \end{aligned} \tag{101}$$

where we have introduced the quantity:

$$\mathcal{Q} \equiv W^6\, V - \mu^2\, V^2 = Z_1 Z_2 Z_3 V - \mu^2\, V^2\,. \tag{102}$$

Upon evaluating $\mathcal{Q}$ as a function of the harmonic functions that determine the solution one obtains a beautiful result:

$$\begin{aligned} \mathcal{Q} &= -M^2\, V^2 - \tfrac{1}{3}\, M\, C_{IJK} K^I\, K^J\, K^k - M\, V\, K^I\, L_I - \tfrac{1}{4}\,(K^I L_I)^2 \\ &\quad + \tfrac{1}{6}\, V C^{IJK} L_I L_J L_K + \tfrac{1}{4}\, C^{IJK} C_{IMN} L_J L_K K^M K^N \end{aligned} \tag{103}$$

with $C^{IJK} \equiv C_{IJK}$. We can straightforwardly see that when we consider M-theory compactified on T^6, then $C^{IJK} = |\epsilon^{IJK}|$, and $\mathcal{Q}$ is nothing other than the $E_{7(7)}$ quartic invariant (98) where the x's and y's are identified as in (96). This is expected from the fact that the solutions on a GH base have an extra $U(1)$ invariance, and hence can be

thought of as four-dimensional. The four-dimensional supergravity obtained by compactifying M-theory on T^7 is $N = 8$ supergravity, which has an $E_{7(7)}$ symmetry group. Of course, the analysis above and in particular equation (103) are valid for solutions of arbitrary five-dimensional $U(1)^N$ ungauged supergravities on a GH base. More details on the explicit relation for general theories can be found in [81].

Observe that (101) only involves V in the combinations W^2V and $\mathcal{Q}$ and both of these are regular as $V \to 0$. Thus, at least the spatial metric is regular at $V = 0$. In Section 6.4 we will show that the complete solution is regular as one passes across the surface $V = 0$.

From (101) and (30) we see that to avoid CTC's, the following inequalities must be true everywhere:

$$\mathcal{Q} \;\geq\; 0\,, \quad W^2\,V \;\geq\; 0\,, \quad (Z_J\,Z_K\,Z_I^{-2})^{\frac{1}{3}} \;=\; W^2 Z_I^{-1} \;\geq\; 0\,, \quad I = 1,2,3\,. \tag{104}$$

The last two conditions can be subsumed into:

$$V\,Z_I \;=\; \tfrac{1}{2}\,C_{IJK}\,K^J\,K^K \;+\; L_I\,V \;\geq\; 0\,, \qquad I = 1,2,3\,. \tag{105}$$

The obvious danger arises when V is negative. We will show in the next sub-section that all these quantities remain finite and positive in a neighborhood of $V = 0$, despite the fact that W blows up. Nevertheless, these quantities could possibly be negative away from the $V = 0$ surface. While we will, by no means, make a complete analysis of the positivity of these quantities, we will discuss it further in Section 7.5, and show that (105) does not present a significant problem in a simple example. One should also note that $\mathcal{Q} \geq 0$ requires $\prod_I (V Z_I) \geq \mu^2 V^4$, and so, given (105), the constraint $\mathcal{Q} \geq 0$ is still somewhat stronger.

Also note that there is a danger of CTC's arising from Dirac-Misner strings in ω. That is, near $\theta = 0, \pi$ the $-\omega^2$ term could be dominant unless ω vanishes on the polar axis. We will analyze this issue completely when we consider bubbled geometries in Section 7.

Finally, one can also try to argue [37] that the complete metric is stably causal and that the t coordinate provides a global time function [82]. In particular, t will then be monotonic increasing on future-directed non-space-like curves and hence there can be no CTC's. The coordinate t is a time function if and only if

$$-g^{\mu\nu}\partial_\mu t\,\partial_\nu t = -g^{tt} = (W^2V)^{-1}(\mathcal{Q} - \omega^2) > 0\,, \tag{106}$$

where ω is squared using the $\mathbb{R}^3$ metric. This is obviously a slightly stronger condition than $\mathcal{Q} \geq 0$ in (104).

6.4 Regularity of the solution and critical surfaces

As we have seen, the general solutions we will consider have functions, V, that change sign on the $\mathbb{R}^3$ base of the GH metric. Our purpose here is to show that such solutions are

completely regular, with positive definite metrics, in the regions where V changes sign. As we will see the "critical surfaces," where V vanishes are simply a set of completely harmless, regular hypersurfaces in the full five-dimensional geometry.

The most obvious issue is that if V changes sign, then the overall sign of the metric (71) changes and there might be whole regions of closed time-like curves when $V < 0$. However, we remarked above that the warp factors, in the form of W, prevent this from happening. Specifically, the expanded form of the complete, eleven-dimensional metric when projected onto the GH base yields (101). Moreover

$$W^2\, V \;=\; (Z_1\, Z_2\, Z_3\, V^3)^{\frac{1}{3}} \;\sim\; ((K_1\, K_2\, K_3)^2)^{\frac{1}{3}} \tag{107}$$

on the surface $V = 0$. Hence W^2V is regular and positive on this surface, and therefore the space-space part (101) of the full eleven-dimensional metric is regular.

There is still the danger of singularities at $V = 0$ for the other background fields. We first note that there is no danger of such singularities being hidden implicitly in the $\vec{\omega}$ terms. Even though (91) suggests that the source of $\vec{\omega}$ is singular at $V = 0$, we see from (94) that the source is regular at $V = 0$ and thus there is nothing hidden in $\vec{\omega}$. We therefore need to focus on the explicit inverse powers of V in the solution.

The factors of V cancel in the torus warp factors, which are of the form $(Z_I Z_J Z_K^{-2})^{\frac{1}{3}}$. The coefficient of $(dt + k)^2$ is W^{-4}, which vanishes as V^2. The singular part of the cross term, $dt\, k$, is $\mu\, dt\, (d\psi + A)$, which, from (93), diverges as V^{-2}, and so the overall cross term, $W^{-4} dt\, k$, remains finite at $V = 0$.

So the metric is regular at critical surfaces. The inverse metric is also regular at $V = 0$ because the $dt\, d\psi$ part of the metric remains finite and so the determinant is non-vanishing.

This surface is therefore not an event horizon even though the time-like Killing vector defined by translations in t becomes null when $V = 0$. Indeed, when a metric is stationary but not static, the fact that g_{tt} vanishes on a surface does not make it an event horizon (the best known example of this is the boundary of the ergosphere of the Kerr metric). The necessary condition for a surface to be a horizon is rather to have $g^{rr} = 0$, where r is the coordinate transverse to this surface. This is clearly not the case here.

Hence, the surface given by $V = 0$ is like a boundary of an ergosphere, except that the solution has no ergosphere[27] because this Killing vector is time-like on both sides and does not change character across the critical surface. In the Kerr metric the time-like Killing vector becomes space-like and this enables energy extraction by the Penrose process. Here there is no ergosphere and so energy extraction is not possible, as is to be expected from a BPS geometry.

At first sight, it does appear that the Maxwell fields are singular on the surface $V = 0$. Certainly the "magnetic components," $\Theta^{(I)}$, (see (79)) are singular when $V = 0$. However,

[27] The non-supersymmetric smooth three-charge solutions found in [83] do nevertheless have ergospheres [83, 84].

one knows that the metric is non-singular and so one should expect that the singularity in the $\Theta^{(I)}$ to be unphysical. This intuition is correct: One must remember that the complete Maxwell fields are the $A^{(I)}$, and these are indeed non-singular at $V = 0$. One finds that the singularities in the "magnetic terms" of $A^{(I)}$ are canceled by singularities in the "electric terms" of $A^{(I)}$, and this is possible at $V = 0$ precisely because g_{tt} goes to zero, and so the magnetic and electric terms can communicate. Specifically, one has, from (38) and (82):

$$dA^{(I)} \;=\; d\Big(B^{(I)} \;-\; \frac{(dt+k)}{Z_I}\Big)\,. \tag{108}$$

Near $V = 0$ the singular parts of this behave as:

$$\begin{aligned} dA^{(I)} \quad &\sim \quad d\Big(\frac{K^I}{V} \;-\; \frac{\mu}{Z_I}\Big)\,(d\psi + A) \\ &\sim \quad d\Big(\frac{K^I}{V} \;-\; \frac{K^1\,K^2\,K^3}{\frac{1}{2}\,V\,C_{IJK}\,K^J\,K^K}\Big)\,(d\psi + A) \;\sim\; 0\,. \end{aligned} \tag{109}$$

The cancellations of the V^{-1} terms here occur for much the same reason that they do in the metric (101).

Therefore, even if V vanishes and changes sign and the base metric becomes negative definite, the complete eleven-dimensional solution is regular and well-behaved around the $V = 0$ surfaces. It is this fact that gets us around the uniqueness theorems for asymptotically Euclidean self-dual (hyper-Kähler) metrics in four dimensions, and as we will see, there are now a vast number of candidates for the base metric.

6.5 Black rings in Taub-NUT

Having analyzed the general form of solutions with a GH base, it is interesting to re-examine the black ring solution of Section 4.4 and rewrite it in the form discussed in Section 6.1 with a trivial GH base (with $V = \frac{1}{r}$). We do this because it is then elementary to generalize the solution to more complicated base spaces and most particularly to a Taub-NUT base. This will then illustrate a very important technique that makes it elementary to further compactify solutions to four-dimensional space-times and establish the relationship between four-dimensional and five-dimensional quantities. For pedagogical reasons, we will focus on the metric; details on the field strengths and the moduli can be found in [69].

One cans also show that the black ring warp factors and rotation vector, when written in usual $\mathbb{R}^4$ coordinates

$$ds^2 = d\tilde{r}^2 + \tilde{r}^2(d\tilde{\theta}^2 + \sin^2\tilde{\theta}d\tilde{\psi}^2 + \cos^2\tilde{\theta}d\tilde{\phi}^2) \tag{110}$$

are given by:

$$Z_I \;=\; 1 + \frac{\overline{Q}_I}{\tilde{\Sigma}} + \frac{1}{2}C_{IJK}q^J q^K\frac{\tilde{r}^2}{\tilde{\Sigma}^2}$$

$$
\begin{aligned}
k &= -\frac{\tilde{r}^2}{2\tilde{\Sigma}^2}\left(q^I\overline{Q}_I + \frac{2q^1q^2q^3\tilde{r}^2}{\tilde{\Sigma}}\right)(\cos^2\tilde{\theta}\,d\tilde{\phi} + \sin^2\tilde{\theta}\,d\tilde{\psi}) \\
&- J_T\,\frac{2\tilde{r}^2\sin^2\tilde{\theta}}{\tilde{\Sigma}(\tilde{r}^2+\widetilde{R}^2+\tilde{\Sigma})}\,d\tilde{\psi}\,,
\end{aligned}
\tag{111}
$$

where $C_{IJK} = 1$ for $(IJK) = (123)$ and permutations thereof,

$$
\tilde{\Sigma} \equiv \sqrt{(\tilde{r}^2 - \widetilde{R}^2)^2 + 4\widetilde{R}^2\tilde{r}^2\cos^2\tilde{\theta}}\,,
\tag{112}
$$

and $J_T \equiv J_{\tilde{\psi}} - J_{\tilde{\phi}}$.

In the foregoing, we have written the solution in terms of the ring charges, $\overline{Q}_I$ and, as we have already noted, for the five-dimensional black ring these charges differ from the charges measured at infinity because of the charge "dissolved" in the M5-brane fluxes. The charges measured at infinity are $Q_I = \overline{Q}_I + \frac{1}{2}C_{IJK}q^Jq^K$. We will also make a convenient choice of units in which $G_5 = \frac{\pi}{4}$, and choose the three T^2's of the M-theory metric to have equal size.

From (67), the radius of the ring, $\widetilde{R}$, and is related to J_T by

$$
J_T = (q^1 + q^2 + q^3)\widetilde{R}^2.
\tag{113}
$$

We now perform a change of coordinates, to bring the black ring to a form that can easily be generalized to Taub-NUT. Define

$$
\phi = \tilde{\phi} - \tilde{\psi}, \quad \psi = 2\tilde{\psi}, \quad \theta = 2\tilde{\theta}, \quad \rho = \frac{\tilde{r}^2}{4}\,,
\tag{114}
$$

where the ranges of these coordinates are given by

$$
\theta \in (0,\pi), \quad (\psi,\phi) \cong (\psi+4\pi,\phi) \cong (\psi,\phi+2\pi)\ .
\tag{115}
$$

One can easily verify that when $V = \frac{1}{\rho}$, the coordinate change (114) transforms the metric in the first line of (117) to that of flat $\mathbb{R}^4$. In the new coordinates the black-ring metric is

$$
\begin{aligned}
ds^2 &= -(Z_1Z_2Z_3)^{-2/3}(dt+k)^2 + (Z_1Z_2Z_3)^{1/3}h_{mn}dx^m dx^n\,, \\
Z_I &= 1 + \frac{\overline{Q}_I}{4\Sigma} + \frac{1}{2}C_{IJK}q^Jq^K\frac{\rho}{4\Sigma^2}\,, \\
k &= \mu\,(d\psi + (1+\cos\theta)d\phi) + \omega\,, \\
\mu &= -\frac{1}{16}\frac{\rho}{\Sigma^2}\left(q^I\overline{Q}_I + \frac{2q^1q^2q^3\rho}{\Sigma}\right) + \frac{J_T}{16R}\left(1 - \frac{\rho}{\Sigma} - \frac{R}{\Sigma}\right)\,, \\
\omega &= -\frac{J_T\rho}{4\Sigma(\rho+R+\Sigma)}\sin^2\theta d\phi\,,
\end{aligned}
\tag{116}
$$

with

$$\begin{aligned} h_{mn}dx^m dx^n &= V^{-1}\left(d\psi + (1+\cos\theta)d\phi\right)^2 + V(d\rho^2 + \rho^2(d\theta^2 + \sin^2\theta d\phi^2))\,, \\ V &= \frac{1}{\rho}\,, \quad \Sigma = \sqrt{\rho^2 + R^2 + 2R\rho\cos\theta}\,, \quad R = \frac{\widetilde{R}^2}{4}\,. \end{aligned} \tag{117}$$

The solution (116) has the form described in Section 6.1 with the eight harmonic functions:

$$\begin{aligned} K^I &= -\frac{q^I}{2\Sigma}\,, \qquad L_I = 1 + \frac{\overline{Q}_I}{4\Sigma}\,, \\ M &= \frac{J_T}{16}\left(\frac{1}{R} - \frac{1}{\Sigma}\right)\,, \qquad V = \frac{1}{\rho}\,. \end{aligned} \tag{118}$$

We should also note for completeness that the conventions we use here for these harmonic functions are those of [69], and differ from those of [64] by various factors of two. When $\mathbb{R}^4$ is written in Gibbons-Hawking form, the ring is sitting at a distance R along the negative z-axis of the three-dimensional base. Adding more sources on the z axis corresponds to making concentric black rings [85, 64][28].

To change the four-dimensional base metric into Taub-NUT one simply needs to add a constant, h, to the harmonic function V:

$$V = h + \frac{1}{\rho}\,. \tag{119}$$

Since the functions in the metric are harmonic, equations (89), (90), (93), (94) and (118), still imply that we have a supersymmetric solution. Actually, in order to avoid both Dirac string singularities and closed time-like curves, the relation (113) between J_T and the dipole charges must be modified to:

$$J_T\left(h + \frac{1}{R}\right) = 4(q^1 + q^2 + q^3)\,. \tag{120}$$

This is discussed in detail in [69, 68, 67] and in later sections here, but it follows because the absence of singularities in ω puts constraints on the sources on the right hand side of (94).

For small ring radius (or for small h), $R \ll h^{-1}$, this reduces to the five-dimensional black ring described earlier. We now wish to consider the opposite limit, $R \gg h^{-1}$. However, to keep "the same ring" we must to keep all its quantized charges fixed, and so (120) means $h + \frac{1}{R}$ must remain constant. We can think of this as keeping the physical radius of the ring fixed while changing its position in Taub-NUT: The ring slides to a point

[28] In particular adding sources on the same side of the origin in the $\mathbb{R}^3$ base of (117), correspond to rings that sit in the same $\mathbb{R}^2$ inside $\mathbb{R}^4$. Rings that sit in orthogonal $\mathbb{R}^2$'s inside $\mathbb{R}^4$ correspond to sources sitting on opposite sides of the origin of the $\mathbb{R}^3$ base of (117).

where the physical ring radius is the same as the physical size of the compactification circle. In the limit where R is large, the black ring is far from the Taub-NUT center and it is effectively wrapped around an infinite cylinder. In other words, it has become a straight black string wrapped on a circle and, from the four-dimensional perspective, it is point-like and is nothing but a four-dimensional black hole.

To see this in more detail, we consider the geometry in the region far from the tip, that is, for $\rho \gg 1$, where we can take $V = h$. We also want to center the three-dimensional spherical coordinates on the ring, and so we change to coordinates such that Σ is the radius away from the ring. We then have:

$$d\rho^2 + \rho^2(d\theta^2 + \sin^2\theta d\phi^2) = d\Sigma^2 + \Sigma^2(d\hat{\theta}^2 + \sin^2\hat{\theta} d\phi^2) \,, \tag{121}$$

and

$$\rho = \sqrt{\Sigma^2 + R^2 - 2R\Sigma\cos\hat{\theta}}, \quad \cos\theta = \frac{\Sigma\cos\hat{\theta} - R}{\rho} \,. \tag{122}$$

Taking $R \to \infty$, at fixed $(\Sigma, \hat{\theta}, \hat{\phi})$ and $h + \frac{1}{R}$, we find that the metric is:

$$\begin{aligned} ds^2 &= -(\tilde{Z}_1\tilde{Z}_2\tilde{Z}_3)^{-2/3}(d\tilde{t} + \tilde{\mu} d\psi)^2 \\ &\quad + (\tilde{Z}_1\tilde{Z}_2\tilde{Z}_3)^{1/3}\left(dr^2 + r^2(d\hat{\theta}^2 + \sin^2\hat{\theta} d\hat{\phi}^2) + d\psi^2\right) \,, \end{aligned} \tag{123}$$

where

$$\tilde{Z}_I \equiv \frac{Z_I}{h} \,, \qquad \tilde{\mu} \equiv \frac{\mu}{h} \,, \qquad r \equiv h\Sigma \,, \qquad \tilde{t} \equiv \frac{t}{h} \,. \tag{124}$$

Note that the spatial section of (123) is precisely $\mathbb{R}^3 \times S^1$. When written in terms of the coordinate r the metric functions become:

$$\tilde{Z}_I = \frac{1}{h} + \frac{\overline{Q}_I}{4r} + \frac{C_{IJK}q^J q^K}{8r^2} \,, \qquad \tilde{\mu} = -\frac{J_T}{16r} - \frac{q^I\overline{Q}_I}{16r^2} - \frac{q^1q^2q^3}{8r^3} \,, \qquad \omega = 0 \,. \tag{125}$$

This is precisely the four-dimensional black hole found by wrapping the black string solution of [55] on a circle.

As noted in [45], the entropy of the five-dimensional black ring takes a simple form in terms of the quartic invariant of $E_{7(7)}$:

$$S = 2\pi\sqrt{J_4} \,, \tag{126}$$

where J_4 is given by (98) with

$$\begin{aligned} x_{12} &= \overline{Q}_1, \quad x_{34} = \overline{Q}_2, \quad x_{56} = \overline{Q}_3, \quad x_{78} = 0, \\ y^{12} &= q^1, \quad y^{34} = q^2, \quad y^{56} = q^3, \quad y^{78} = J_T = J_{\tilde{\psi}} - J_{\tilde{\phi}} \,. \end{aligned} \tag{127}$$

Hence, the "tube angular momentum," J_T, plays the role of another charge in the four-dimensional black hole picture. From the five-dimensional perspective, J_T is the difference

of the two independent angular momenta and is given by (113). Upon compactification on the Taub-NUT circle, J_T represents the momentum around that circle and, as is very familiar in Kaluza-Klein (KK) reduction, a KK momentum becomes a conserved charge in the lower dimension.

It has long been known that maximal supergravity in four dimensions has $E_{7(7)}$ duality group and that the general entropy for the corresponding class of four-dimensional black holes can be expressed in terms of the quartic invariant [79]. The observation in [45] thus provided the first clue as to the relationship between five-dimensional black rings and four-dimensional black holes. We now examine this relationship in more detail.

6.6 Parameters, charges and the "4D-5D" connection

As we have seen, the ability to introduce a constant, h, into V as in (119) enables us to interpolate between configurations in five-dimensional space-time and configurations in four-dimensional space-time. For small h, the Taub-NUT circle is very large and the configuration behaves as if it were in a five-dimensional space-time while, for large h, the Taub-NUT circle is small and the configuration is effectively compactified. The first connection between a five-dimensional configuration and such a four-dimensional solution was made in [35], where the simple two-charge supertube [22] was put in Taub-NUT, and was related to a two-centered, four-dimensional configuration of the type previously analyzed in [80]. One can also consider a four-dimensional black hole that has a non-trivial KKM charge, and that sits at the center of Taub-NUT. When the KKM charge is one, this black hole also has two interpretations, both as a four-dimensional and as a five-dimensional black hole [66]. Since one can interpolate between the five-dimensional and the four-dimensional regimes by changing the moduli of the solution, one can give microscopic descriptions of black rings and black holes both from a four-dimensional perspective and from a five-dimensional perspective. This is called the "4D-5D" connection. This connection enables us to relate the parameters and charges appearing in the five-dimensional description of a system to those appearing in the four-dimensional description. We now examine this more closely and we will encounter some important subtleties. To appreciate these, we need to recall some of the background behind the BPS black ring solutions.

One of the reasons that makes the BPS black ring solution so interesting is that it shows the failure of black-hole uniqueness in five dimensions. To be more specific, for the round ($U(1) \times U(1)$ invariant) BPS black ring solution there are only five conserved quantities: The two angular momenta, J_1, J_2, and the three electric charges, Q_I, *as measured from infinity.* However, these rings are determined by seven parameters: $\overline{Q}_I$, q^I and J_T. We have seen how these parameters are related to details of the constituent branes and we have stressed, in particular, that the q^I are dipole charges that, *a priori*, are not conserved charges and so cannot be measured from infinity in five dimensions. As discussed in Section 4.4 the true conserved charges in five dimensions are non-trivial combinations of the fundamental "brane parameters," $\overline{Q}_I$, q^I and J_T.

- **5D dipole charges and 4D charges**.

In discussing the conserved charges of a system there is a very significant assumption about the structure of infinity. To determine the charges one integrates various field strengths and their duals on certain Gaussian surfaces. If one changes the structure of infinity, one can promote dipoles to conserved charges or lose conserved charges. One sees this very explicitly in the case of Taub-NUT space (117): by turning one a constant piece in harmonic function V, one replaces the S^3 at infinity of $\mathbb{R}^4$ by an $S^2 \times S^1$. In particular, the "dipole" charges, q^I, of the five-dimensional black-ring become conserved magnetic charges in the Taub-NUT space. This is evident from the identification in (127) in which the x^{AB} and y^{AB} respectively represent conserved electric and magnetic charges measured on the Gaussian two-spheres at infinity in $\mathbb{R}^3$. More generally, from (96) we see that the leading behaviour of each of the eight harmonic functions, K^I, L_I, M, and V yields a conserved charge in the Taub-NUT compactification.

In terms of the thermodynamics of black holes and black rings, the conserved charges measured at infinity are thermodynamic state functions of the system and the set of state functions depends upon the asymptotic geometry of the "box" in which we place the system. If a solution has free parameters that cannot be measured by the thermodynamic state functions then these parameters should be thought of as special properties of a particular microstate, or set of microstates, of the system. Thus, in a space-time that is asymptotic to flat $\mathbb{R}^{4,1}$, one cannot identify the microstates of a particular round black-ring solution by simply looking at the charges and angular momenta at infinity. Moreover, given a generic microstate with certain charges it is not possible to straightforwardly identify the black ring (or rings) to which this microstate corresponds. The only situation in which one can do this is when there exists a box in which one can place both the ring and the microstate, and one uses the box to define extra state functions that the two objects must share. Putting these objects in Taub-NUT and changing the moduli such that both the ring and the microstate have a four-dimensional interpretation, allows one to define a box that can be used to measure the "specialized microstate structure" (i.e. the dipoles), as charges at infinity in four dimensions.

A good analogy is the thermodynamics and the kinetic theory of gases. The conserved charges correspond to the state functions while the internal, constituent brane parameters correspond to details of the motions of molecules in particular microstates. The state functions are non-trivial combinations of parameters of microstate, but do not capture all the individual microstate parameters. If the box is a simple cube then there is no state function to capture vorticity, but there is such a state function for a toroidal box.

Thus solutions come with two classes of parameters: Those that are conserved and can be measured from infinity and those that represent particular, internal configurations of the thermodynamic system. There are two ways in which one can hope to give a microscopic interpretation of black rings. One is to take a near-horizon limit in which the black ring solution becomes asymptotically $AdS_3 \times S^3 \times T^4$ [63, 45], and to describe the ring in the D1-D5-P CFT dual to this system. The other is to focus on the near-ring

geometry (or to put the ring in Taub-NUT) and describe it as a four-dimensional BPS black hole [45, 86, 67, 69], using the microscopic description of 4D black holes constructed in given in [87, 88].

If one wants to describe black rings in the D1-D5-P CFT, it is, *a priori*, unclear how the dipole charges, which are not conserved charges (state functions) appear in this CFT. A phenomenological proposal for this has been put forth in [45], but clearly more work remains to be done. Moreover, the obvious partition functions that one can define and compute in this CFT [89], which only depend on the charges and angular momenta, cannot be compared to the bulk entropy of a particular black ring. One rather needs to find the ring (or rings) with the largest entropy for a given set of charges, and match their entropy to that computed in the CFT.

Moreover, if one wants to describe the ring using a CFT corresponding to a four-dimensional black hole, it is essential to identify the correct M2 charges of the ring. The beauty of the brane description (or any other stringy description) of supertubes and black rings is that it naturally points out what these charges are.

- **5D electric charges and their 4D interpretation.**

There has been some discussion in the literature about the correct identification of the charges of the black-ring system. In particular, there was the issue of whether the Q_I or the $\overline{Q}_I$ are the "correct" charges of the black-ring. There is no dispute about the charge measured at infinity, the only issue was the physical meaning, if any, to the $\overline{Q}_I$. In [90] it was argued that the only meaningful charge was the "Page charge" that measures Q_I and not $\overline{Q}_I$ even when the Gaussian surface is small surface surrounding the black ring. This is an interesting, mathematically self-consistent view but it neglects a lot of the important underlying physics. It also generates some confusion as to the proper identification of the microscopic charges of the underlying system. The competing view [53] is the one we have presented here: The $\overline{Q}_I$ represent the number of constituent M2 branes and the Q_I get two contributions, one from the $\overline{Q}_I$ and another from the "charges dissolved in fluxes" arising from the M5 branes. It is certainly true that the $\overline{Q}_I$ and the q^I are not conserved individually, but they do represent critically important physical parameters.

This is easily understood in analogy with a heavy nucleus. The energy of the nucleus has two contributions, one coming from the rest mass of the neutrons and protons, and the other coming from the interactions between them. In trying to find the "microscopic" features of the nucleus, like the number of nucleons, one obtains an incorrect result if one simply divides the total energy by the mass of a nucleon. To find the correct answer one should first subtract the energy coming from interactions, and then divide the remainder by the mass of the nucleon.

One of the nice features of Taub-NUT compactification and the "4D-5D" connection is that it provides a very simple resolution of the foregoing issue in the identification of constituent microscopic charges. If one simply compactifies M-theory on $T^6 \times S^1$ from the outset, wrapping q^I M5 branes on the S^1 and each of the tori as shown in Table 1, then the q^I simply emerge as magnetic charges in four dimensions as in (127). Similarly, the

$\overline{Q}_I$ are, unambiguously, the conserved electric charges of the system. This is also true of the Taub-NUT compactification of the black ring and the fact that we can adiabatically vary h in (119) means we can bring the ring from a region that looks like M-theory on $T^6 \times S^1 \times \mathbb{R}^{3,1}$ into a region that looks like M-theory on $T^6 \times \mathbb{R}^{4,1}$, and still have confidence that the identification is correct because M2 and M5 brane charges are quantized and cannot jump in an adiabatic process. This establishes that the microscopic charges of the black ring are not the same as the charges measured at infinity in the five-dimensional black ring solution.

There are, of course, many situations where the rings cannot be put in Taub-NUT, and one cannot obtain the microscopic charges using the 4D-5D connection. The simplest example is the black ring with a black hole offset from is center [75] that we reviewed in Section 4.5. However, based upon our experience with the single black ring, we expect that the values of $\overline{Q}_I$ in the near-ring geometry will yield the number of M2 brane constituents of each individual ring.

There has also been a proposal to understand the entropy of BPS black rings in terms of microscopic charges, in which Q_I are interpreted as the M2 brane charges. This is based on a four-dimensional black hole CFT with charges Q_I rather than $\overline{Q}_I$, and with momentum J_ψ rather than J_T [86]. In order to recover the entropy formula (60,61) an important role in that description was played by a non-extensive zero point energy shift of L_0. In light of our analysis, it is rather mysterious why this gives the right entropy, since we have shown explicitly that the relevant four-dimensional black hole CFT is the one with charges $\overline{Q}_I$, momentum J_T, and no zero point shift of L_0. We should also note that the approach of [86] seems to run into problems when describing concentric black rings because the total charge Q_A is not simply a sum of the individual $Q_{A,i}$, but gets contributions from cross terms of the form $C_{ABC}\, q_i^B\, q_j^C$. The approach of [86] also appears not to correctly incorporate some of the higher order corrections to the black ring entropy [91, 92].

One of the other benefits of the 4D-5D connection is that it also unites what have been two parallel threads in research. Prior to this there had been extensive, and largely independent bodies of research on four-dimensional objects and upon on five-dimensional objects. It is now evident that the four-dimensional two-center solution corresponding to black rings and supertubes in Taub-NUT [35, 67, 68, 69] is part of the family of multi-center solutions that have been explored by Denef and collaborators [80]. In fact, one can also imagine putting in Taub-NUT multiple concentric black rings of the type studied by Gauntlett and Gutowski in [85, 64]. These descend in four dimensions to a multi-black hole configuration, in which the center of the rings becomes a center of KKM charge one, the black rings in one plane become black holes on the right of the KKM center, and the black rings in the other plane becomes black holes on the left of this center.

More generally, we expect that the 4D-5D connection will lead to a valuable symbiosis. For example, the work on attractor flows in Calabi-Yau manifolds and the branching of these flows could have important consequences for the bubbled geometries that we will

discuss in the next section.

7 Bubbled geometries

7.1 The geometric transition

The main purpose of our investigation thus far has been to construct smooth horizonless geometries starting from three-charge supertubes. We have seen that if one considers a process in which one takes a three-charge, three-dipole charge supertube to a regime where the gravitational back-reaction becomes important, the resulting supergravity solution is generically that of a BPS black ring. Although black rings are very interesting in their own right, they do have event horizons and therefore do not correspond to microstates of the boundary theory.

Hence it is natural to try to obtain microstates by starting with brane configurations that do not develop a horizon at large effective coupling, or alternatively to consider a black ring solution in the limit where its entropy decreases and becomes zero. However, the geometry of a zero-entropy black ring is singular. This singularity is not a curvature singularity, since the curvature is bounded above by the inverse of the dipole charges. Rather, the singularity is caused by the fact that the size of the S^1 of the horizon shrinks to zero size and the result is a "null orbifold." One can also think about this singularity as caused by the gravitational back-reaction of the branes that form the three-charge supertube, which causes the S^1 wrapped by these branes to shrink to zero size.

Fortunately, string theory is very good at solving this kind of singularities, and the mechanism by which it does is that of "geometric transition." To understand what a geometric transition is, consider a collection of branes wrapped on a certain cycle. At weak effective coupling one can describe these branes by studying the open strings that live on them. One can also find the number of branes by integrating the corresponding flux over a "Gaussian" cycle dual to that wrapped by the branes. However, when one increases the coupling, the branes back-react on the geometry, and shrink the cycle they wrap to zero size. At the same time, the "Gaussian cycle" becomes large and topologically non-trivial. (See Fig. 7.) The resulting geometry has a different topology, and *no brane sources*; the only information about the branes is now in the integral of the flux over the blown-up dual "Gaussian cycle." Hence, even if in the open-string (weakly coupled) description we had a configuration of branes, in the closed-string (large effective coupling) description these branes have disappeared and have been replaced by a non-trivial topology with flux.

Geometric transitions appear in many systems [93, 71, 94, 95]. A classic example of such system are the brane models that break an $\mathcal{N} = 2$ superconformal field theory down to an $\mathcal{N} = 1$ supersymmetric field theory [71, 96]. Typically, the $\mathcal{N} = 2$ superconformal field theory is realized on a stack of D3 branes in some Calabi-Yau compactification. One can then break the supersymmetry to $\mathcal{N} = 1$ by introducing extra D5 branes that

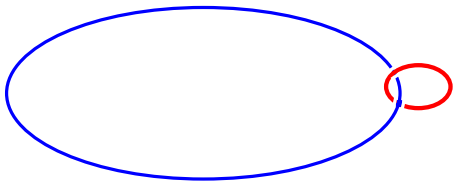

Figure 7: *Geometric transitions*: The branes wrap the large (blue) cycle; the flux through the Gaussian (small, red) cycle measures the brane charge. In the open-string picture the small (red) cycle has non-zero size, and the large (blue) cycle is contractible. After the geometric transition the size of the large (blue) cycle becomes zero, while the small (red) cycle becomes topologically non-trivial.

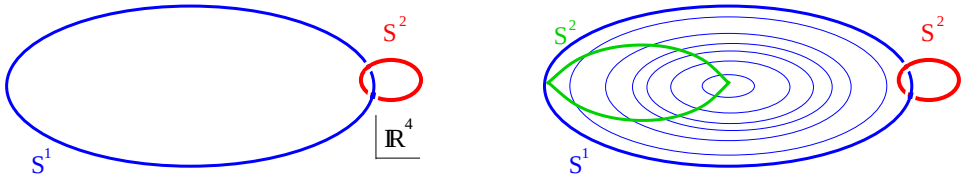

Figure 8: *The geometric transition of the black ring:* Before the transition the branes wrap the large (blue) S^1; the flux through the Gaussian S^2 (small, red) cycle measures the brane charge. After the transition the Gaussian S^2 (small, red) cycle is topologically non-trivial and of finite size and a new (green) S^2 appears, coming from the fact that the blue S^1 shrinks to zero so that the disk spanning the S^1 becomes an S^2. The resulting geometry has two non-trivial S^2's and no brane sources.

wrap a two-cycle. When one investigates the closed-string picture, the two cycle collapses and the dual three-cycle blows up (this is also known as a conifold transition). The D5 branes disappear and are replaced by non-trivial fluxes on the three-cycle. The resulting geometry has no more brane sources, and has a different topology than the one we started with.

Our purpose here is to see precisely how geometric transitions resolve the singularity of the zero-entropy black ring (*supertube*) of Section 4. Here the ring wraps a curve $y^\mu(\sigma)$, that is topologically an S^1 inside $\mathbb{R}^4$. (In Fig. 8 this S^1 is depicted as a large, blue cycle.) The Gaussian cycle for this S^1 is a two-sphere around the ring (illustrated by the red small cycle in Fig. 8). If one integrates the field strengths $\Theta^{(I)}$ on the red Gaussian two-cycle one obtains the M5 brane dipole charges of the ring, n^I.

After the geometric transition the large (blue) S^1 becomes of zero length, and the red S^2 becomes topologically non-trivial. Moreover, because the original topology is trivial, the curve $y^\mu(\sigma)$ was the boundary of a disk. When after the transition this boundary curve collapses, the disk becomes a (topologically non-trivial) two-sphere. Alternatively, one can think about this two-sphere (shown in Fig. 8 in green) as coming from having an S^1 that has zero size both at the origin of the space $r = 0$ and at the location of the ring.

Hence, before the transition we had a ring wrapping a curve of arbitrary shape inside $\mathbb{R}^4$, and after the transition we have a manifold that is asymptotically $\mathbb{R}^4$, and has two non-trivial two-spheres, and no brane sources.

Can we determine the geometry of such a manifold? If the curve has an arbitrary shape the only information about this manifold is that it is asymptotically $\mathbb{R}^4$ and that it is hyper-Kähler, as required by supersymmetry[29]. If the curve wrapped by the supertube has arbitrary shape, this is not enough to determine the space that will come out after the geometric transition. However, if one considers a circular supertube, the solution before the transition has a $U(1) \times U(1)$ invariance, and so one naturally expects the solution resulting from the transition should also have this invariance.

With such a high level of symmetry we do have enough information to determine what the result of the geometric transition is:
• By a theorem of Gibbons and Ruback [77], a hyper-Kähler manifold that has a $U(1) \times U(1)$ invariance must have a translational $U(1)$ invariance and hence, must be Gibbons-Hawking.
• We also know that this manifold should have two non-trivial two-cycles, and hence, as we have discussed in Section 5.1 it should have three centers.
• Each of these centers must have integer GH charge.
• The sum of the three charges must be 1, in order for the manifold to be asymptotically $\mathbb{R}^4$.
• Moreover, we expect the geometric transition to be something that happens locally near the ring, and so we expect the region near the center of the ring (which is also the origin of our coordinate system) to remain the same. Hence, the GH center at the origin of the space must have charge + 1.

The conclusion of this argument is that the space that results from the geometric transition of a $U(1) \times U(1)$ invariant supertube must be a GH space with three centers, that have charges 1, $+Q$, $-Q$, where Q is any integer. As we have seen in Section 6.5, equation (118), if we think about $\mathbb{R}^4$ as a trivial Gibbons-Hawking metric with $V = \frac{1}{r}$, the black ring solution of Section 4.4 has a GH center at the origin, and the ring at a certain point on the $\mathbb{R}^3$ base of the GH space. In the "transitioned" solution, the singularity of the zero-entropy black ring is resolved by the nucleation, or "pair creation," of two equal and oppositely charged GH points.

This process is depicted in Fig. 9. The nucleation of a GH pair of oppositely-charged centers blows up a pair of two-cycles. In the resolved geometry there are no more brane sources, only fluxes through the two-cycles. The charge of the solution does not come from any brane sources, but from having non-trivial fluxes over intersecting two-cycles (or "bubbles").

[29]This might cause the faint-hearted to give up hope because of the theorem that the only such manifold is flat $\mathbb{R}^4$. This is the second instance when such theorems appear to preclude further progress in this research programme (the first is discussed at the end of Section 3). As in the previous example, we will proceed guided by the string-theory intuition, and will find a way to avoid the theorem.

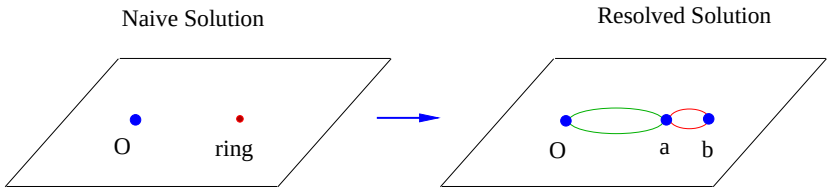

Figure 9: *Geometric transition of supertube*: The first diagram shows the geometry before the transition. The second shows the resolved geometry, where a pair of GH charges has nucleated at positions a and b.

Similarly, if one considers the geometric transition of multiple concentric black rings, one will nucleate one pair of GH points for each ring, resulting in a geometry with no brane sources, and with a very large number of positive and negative GH centers. As we will see, these centers are not restricted to be on a line, but can have arbitrary positions in the $\mathbb{R}^3$ base of the GH space, as long as certain algebraic equations (discussed in Section 7.3) are satisfied.

There is one further piece of physical intuition that is extremely useful in understanding these bubbled geometries. As we have already remarked, GH points can be interpreted, from a ten-dimensional perspective, as D6 branes. Since these branes are mutually BPS, there should be no force between them. On the other hand, D6 branes of opposite charge attract one another, both gravitationally and electromagnetically. If one simply compactifies M-theory on an ambipolar GH space, one can only hold in equilibrium GH points of opposite charge at the cost of having large regions where the metric has the wrong signature and CTC's. To eliminate these singular regions, one must hold the GH points apart by some other mechanism. In the geometries we seek, this is done by having fluxes threading the bubbles: Collapsing a bubble concentrates the energy density of the flux and increases the energy in the flux sector. Thus a flux tends to blow up a cycle. The regular, ambipolar BPS configurations that we construct come about when these two competing effects - the tendency of oppositely charged GH points to attract each other and the tendency of the fluxes to make the bubbles large - are in balance. We will see precisely how this happens in Section 7.3.

Before proceeding to construct these solutions, we should note that there are two other completely different ways of arriving at the conclusion that three-charge black hole microstates can have a base given by a GH space with negative centers.

One direction, mostly followed by Mathur, Giusto and Saxena [31, 32, 33] is to construct microstates by taking a novel extremal limit of the non-extremal five-dimensional black hole [97]. This limit produces a smooth horizonless geometries that have a GH base with two centers, of charges $N+1$ and $-N$. These geometries have a known CFT interpretation, and form a subset of the class described above. A solution that is locally identical (but differs by a global identification of charges) was also found in [34] by do-

ing a spectral flow on a two-charge solution and extending the resulting solution to an asymptotically flat one.

The second direction, followed by Kraus and one of the present authors is to consider the four-dimensional black hole with D1-D5-KKM-P charges, when the momentum is taken to zero. The resulting naive solution for the zero-entropy four-dimensional black hole is singular, and is resolved by an intriguing mechanism: The branes that form the black hole split into two stacks, giving a non-singular solution [35]. One can then relate the black ring to a four-dimensional black hole by putting it in a Taub-NUT background, as discussed in Section 6.6 and in [67, 68, 69], and then the nucleation of a pair of oppositely-charged GH centers corresponds, from a four-dimensional point of view, to the splitting of the zero-entropy four-dimensional black hole into two stacks of branes, giving a smooth resulting solution.

Hence, we have three completely independent routes for obtaining three-charge microstates and resolving the singularity of the zero-entropy black ring, and all three routes support the same conclusion: *The singularity of the zero-entropy black ring is resolved by the nucleation of GH centers of opposite charge. The solutions that result, as well as other three-charge microstate solutions, are topologically non-trivial, have no brane sources, and are smooth despite the fact that they are constructed using an ambipolar GH metric (with regions where the metric is negative-definite).*

7.2 The bubbled solutions

We now proceed to construct the general form of bubbling solutions constructed using an ambipolar Gibbons-Hawking base [36, 37, 38]. In Section 5.2 we saw that the two-forms, $\Theta^{(I)}$, will be *regular*, self-dual, harmonic two-forms, and thus representatives of the cohomology dual to the two-cycles, provided that the K^I have the form:

$$K^I \;=\; k^I_0 \;+\; \sum_{j=1}^{N} \frac{k^I_j}{r_j}\,. \tag{128}$$

Moreover, from (88), the flux of the two-form, $\Theta^{(I)}$, through the two-cycle Δ_{ij} is given by

$$\Pi^{(I)}_{ij} \;=\; \Big(\frac{k^I_j}{q_j} \;-\; \frac{k^I_i}{q_i}\Big)\,, \qquad 1 \le i, j \le N\,. \tag{129}$$

The functions, L_I and M, must similarly be chosen to ensure that the warp factors, Z_I, and the function, μ, are regular as $r_j \to 0$. This means that we must take:

$$L^I \;=\; \ell^I_0 \;+\; \sum_{j=1}^{N} \frac{\ell^I_j}{r_j}\,, \quad M \;=\; m_0 \;+\; \sum_{j=1}^{N} \frac{m_j}{r_j}\,, \tag{130}$$

with

$$\ell^I_j \;=\; -\tfrac{1}{2}\, C_{IJK}\, \frac{k^J_j\, k^K_j}{q_j}\,, \qquad j = 1, \ldots, N\,; \tag{131}$$

$$m_j \;=\; \tfrac{1}{12}\, C_{IJK} \frac{k^I_j\, k^J_j\, k^K_j}{q^2_j} \;=\; \tfrac{1}{2}\, \frac{k^1_j\, k^2_j\, k^3_j}{q^2_j}\,, \qquad j = 1, \ldots, N\,. \tag{132}$$

Since we have now fixed the eight harmonic functions, all that remains is to solve for ω in equation (94). The right-hand side of (94) has two kinds of terms:

$$\frac{1}{r_i}\,\vec{\nabla}\,\frac{1}{r_j} \;-\; \frac{1}{r_j}\,\vec{\nabla}\,\frac{1}{r_i} \qquad \text{and} \qquad \vec{\nabla}\,\frac{1}{r_i}\,. \tag{133}$$

Hence ω will be built from the vectors $\vec{v}_i$ of (84) and some new vectors, $\vec{w}_{ij}$, defined by:

$$\vec{\nabla} \times \vec{w}_{ij} \;=\; \frac{1}{r_i}\,\vec{\nabla}\,\frac{1}{r_j} \;-\; \frac{1}{r_j}\,\vec{\nabla}\,\frac{1}{r_i}\,. \tag{134}$$

To find a simple expression for $\vec{w}_{ij}$ it is convenient to use the coordinates outlined earlier with the z-axis running through $\vec{y}^{(i)}$ and $\vec{y}^{(j)}$. Indeed, choose coordinates so that $\vec{y}^{(i)} \;=\; (0,0,a)$ and $\vec{y}^{(j)} \;=\; (0,0,b)$ and one may take $a > b$. Then the explicit solutions may be written very simply:

$$w_{ij} \;=\; -\,\frac{(x^2 + y^2 + (z-a)(z-b))}{(a-b)\, r_i\, r_j}\, d\phi\,. \tag{135}$$

This is then easy to convert to a more general system of coordinates. One can then add up all the contributions to ω from all the pairs of points.

There is, however, a more convenient basis of vector fields that may be used instead of the w_{ij}. Define:

$$\omega_{ij} \;\equiv\; w_{ij} + \tfrac{1}{(a-b)}\,(v_i - v_j + d\phi) \;=\; -\,\frac{(x^2 + y^2 + (z-a+r_i)(z-b-r_j))}{(a-b)\, r_i\, r_j}\, d\phi\,, \tag{136}$$

These vector fields then satisfy:

$$\vec{\nabla} \times \vec{\omega}_{ij} \;=\; \frac{1}{r_i}\,\vec{\nabla}\,\frac{1}{r_j} \;-\; \frac{1}{r_j}\,\vec{\nabla}\,\frac{1}{r_i} \;+\; \frac{1}{r_{ij}}\left(\vec{\nabla}\,\frac{1}{r_i} \;-\; \vec{\nabla}\,\frac{1}{r_j}\right), \tag{137}$$

where

$$r_{ij} \;\equiv\; |\vec{y}^{(i)} \;-\; \vec{y}^{(j)}| \tag{138}$$

is the distance between the i^{th} and j^{th} center in the Gibbons-Hawking metric.

We then see that the general solution for $\vec{\omega}$ may be written as:

$$\vec{\omega} \;=\; \sum_{i,j}^{N} a_{ij}\,\vec{\omega}_{ij} \;+\; \sum_{i}^{N} b_i\,\vec{v}_i\,, \tag{139}$$

for some constants a_{ij}, b_i.

The important point about the ω_{ij} is that they have *no string singularities whatsoever.* They can be used to solve (94) with the first set of source terms in (133), without introducing Dirac-Misner strings, but at the cost of adding new source terms of the form of the second term in (133). If there are N source points, $\vec{y}^{(j)}$, then using the w_{ij} suggests that there are $\frac{1}{2}N(N-1)$ possible string singularities associated with the axes between every pair of points $\vec{y}^{(i)}$ and $\vec{y}^{(j)}$. However, using the ω_{ij} makes it far more transparent that all the string singularities can be reduced to those associated with the second set of terms in (133) and so there are at most N possible string singularities and these can be arranged to run in any direction from each of the points $\vec{y}^{(j)}$.

Finally, we note that the constant terms in (73), (128) and (130) determine the behavior of the solution at infinity. If the asymptotic geometry is Taub-NUT, all these term can be non-zero, and they correspond to combinations of the moduli. However, in order to obtain solutions that are asymptotic to five-dimensional Minkowski space, $\mathbb{R}^{4,1}$, one must take $\varepsilon_0 = 0$ in (73), and $k_0^I = 0$ in (128). Moreover, μ must vanish at infinity, and this fixes m_0. For simplicity we also fix the asymptotic values of the moduli that give the size of the three T^2's, and take $Z_I \to 1$ as $r \to \infty$. Hence, the solutions that are asymptotic to five-dimensional Minkowski space have:

$$\varepsilon_0 = 0\,, \qquad k_0^I = 0\,, \qquad l_0^I = 1\,, \qquad m_0 = -\tfrac{1}{2}\,q_0^{-1}\sum_{j=1}^{N}\sum_{I=1}^{3} k_j^I\,. \tag{140}$$

It is straightforward to generalize these results to solutions with different asymptotics, and in particular to Taub-NUT.

7.3 The bubble equations

In Section 6.3 we examined the conditions for the absence of CTC's and in general the following must be true globally:

$$\mathcal{Q} \;\geq\; 0\,, \qquad V\,Z_I \;=\; \tfrac{1}{2}\,C_{IJK}\,K^J\,K^K \;+\; L_I\,V \;\geq\; 0\,, \qquad I = 1,2,3\,. \tag{141}$$

As yet, we do not know how to verify these conditions in general, but one can learn a great deal by studying the limits in which one approaches a Gibbons-Hawking point, *i.e.* $r_j \to 0$. From this one can derive some simple, physical conditions (the *Bubble Equations*) that in some examples ensure that (141) are satisfied globally.

To study the limit in which $r_j \to 0$, it is simpler to use (99) than (101). In particular, as $r_j \to 0$, the functions, Z_I, μ and W limit to finite values while V^{-1} vanishes. This means that the circle defined by ψ will be a CTC unless we impose the additional condition:

$$\mu(\vec{y} = \vec{y}^{(j)}) \;=\; 0\,, \quad j = 1, \ldots, N\,. \tag{142}$$

There is also potentially another problem: The small circles in ϕ near $\theta = 0$ or $\theta = \pi$ will be CTC's if ω has a finite $d\phi$ component near $\theta = 0$ or $\theta = \pi$. Such a finite $d\phi$ component corresponds precisely to a Dirac-Misner string in the solution and so we must make sure that ω has no such string singularities.

It turns out that these two sets of constraints are exactly the same. One can check this explicitly, but it is also rather easy to see from (91). The string singularities in $\vec{\omega}$ potentially arise from the $\vec{\nabla}(r_j^{-1})$ terms on the right-hand side of (91). We have already arranged that the Z_I and μ go to finite limits at $r_j = 0$, and the same is automatically true of $K^I V^{-1}$. This means that the only term on the right hand side of (91) that could, and indeed will, source a string is the $\mu\vec{\nabla}V$ term. Thus removing the string singularities is equivalent to (142).

One should note that by arranging that μ, ω and Z_I are regular one has also guaranteed that the physical Maxwell fields, $dA^{(I)}$, in (108) are regular. Furthermore, by removing the Dirac strings in ω and by requiring μ to vanish at GH points one has guaranteed that the physical flux of $dA^{(I)}$ through the cycle Δ_{ij} is still given by (88) (and (129)). This is because the extra terms, $d(Z_I^{-1}k)$, in (108), while canceling the singular behaviour when $V = 0$, as in (109), give no further contribution in (88). Thus the fluxes, $\Pi_{ij}^{(I)}$, are well-defined and represent the true physical, magnetic flux in the five-dimensional extension of the ambipolar GH metrics.

Performing the expansion of μ using (93), (128), (130) and (132) around each Gibbons-Hawking point one finds that (142) becomes the *Bubble Equations*:

$$\sum_{\substack{j=1\\ j\neq i}}^{N} \Pi_{ij}^{(1)}\,\Pi_{ij}^{(2)}\,\Pi_{ij}^{(3)}\,\frac{q_i\,q_j}{r_{ij}} \;=\; -\,2\left(m_0\,q_i \;+\; \tfrac{1}{2}\sum_{I=1}^{3} k_i^I\right), \tag{143}$$

where $r_{ij} \equiv |\vec{y}^{(i)} - \vec{y}^{(j)}|$. One obtains the same set of equations if one collects all the Dirac string contributions to ω and sets them to zero by imposing $b_i = 0$ in (139). If one adds together all of the bubble equations, then the left-hand side vanishes identically, and one obtains the condition on m_0 in (140). This is simply the condition $\mu \to 0$ as $r \to \infty$ and means that there is no Dirac-Misner string running out to infinity. Thus there are only $(N-1)$ independent bubble equations.

We refer to (143) as the bubble equations because they relate the flux through each bubble to the physical size of the bubble, represented by r_{ij}. Note that for a generic configuration, a bubble size can only be non-zero if and only if *all three* of the fluxes are non-zero. Thus the bubbling transition will only be generically possible for the three-charge system.

We should also note that from a four-dimensional perspective these equations describe a collection of BPS stacks of branes, and are thus particular case of a collection of BPS black holes. Such configurations have been constructed in [80], and the equations that must be satisfied by the positions of the black holes are called "integrability equations" and reduce to the equations (143) when the charges are such that the five-dimensional solution is smooth.

7.4 The asymptotic charges

As in Section 4.3, one can obtain the electric charges and angular momenta of bubbled geometries by expanding Z_I and k at infinity. It is, however, more convenient to translate the asymptotics into the standard coordinates of the Gibbons-Hawking spaces. Thus, remembering that $r = \frac{1}{4}\rho^2$, one has

$$Z_I \;\sim\; 1 \;+\; \frac{Q_I}{4\,r} \;+\; \ldots\,, \qquad \rho \to \infty\,, \tag{144}$$

and from (89) one easily obtains

$$Q_I \;=\; -\,2\,C_{IJK}\,\sum_{j=1}^{N} q_j^{-1}\,\tilde{k}_j^J\,\tilde{k}_j^K\,, \tag{145}$$

where

$$\tilde{k}_j^I \;\equiv\; k_j^I \;-\; q_j\,N\,k_0^I\,, \qquad \text{and} \qquad k_0^I \;\equiv\; \frac{1}{N}\sum_{j=1}^{N} k_j^I\,. \tag{146}$$

Note that $\tilde{k}_j^I$ is gauge invariant under (81).

One can read off the angular momenta using an expansion like that of (44). However, it is easiest to re-cast this in terms of the Gibbons-Hawking coordinates. The flat GH metric (near infinity) has $V = \frac{1}{r}$ and making the change of variable $r = \frac{1}{4}\rho^2$, one obtains the metric in spherical polar coordinates:

$$ds_4^2 \;=\; d\rho^2 \;+\; \tfrac{1}{4}\,\rho^2\,(d\theta^2 + \sin^2\theta\,d\phi^2 \;+\; (d\psi + \cos\theta\,d\phi)^2)\,. \tag{147}$$

This can be mapped to the form of (43) via the change of variable:

$$u\,e^{i\theta_1} \;=\; \rho\cos(\tfrac{1}{2}\theta)\,e^{\frac{i}{2}(\psi+\phi)}\,, \qquad v\,e^{i\theta_2} \;=\; \rho\sin(\tfrac{1}{2}\theta)\,e^{\frac{i}{2}(\psi-\phi)}\,. \tag{148}$$

Using this in (44) one finds that

$$k \;\sim\; \frac{1}{4\,\rho^2}\,((J_1 + J_2) \;+\; (J_1 - J_2)\,\cos\theta)\,d\psi \;+\; \ldots\,. \tag{149}$$

Thus, one can get the angular momenta from the asymptotic expansion of $g_{t\psi}$, which is given by the coefficient of $d\psi$ in the expansion of k, which is proportional to μ. There

are two types of such terms, the simple $\frac{1}{r}$ terms and the dipole terms arising from the expansion of $V^{-1}K^I$. Following [37], define the dipoles

$$\vec{D}_j \;\equiv\; \sum_I \tilde{k}^I_j\, \vec{y}^{(j)}\,, \qquad \vec{D} \;\equiv\; \sum_{j=1}^{N} \vec{D}_j\,. \tag{150}$$

and then the expansion of k takes the form (149) if one takes $\vec{D}$ to define the polar axis from which θ is measured. One then arrives at

$$J_R \;\equiv\; J_1 + J_2 \;=\; \tfrac{4}{3}\, C_{IJK} \sum_{j=1}^{N} q_j^{-2}\, \tilde{k}^I_j\, \tilde{k}^J_j\, \tilde{k}^K_j\,, \tag{151}$$

$$J_L \;\equiv\; J_1 - J_2 \;=\; 8\,|\vec{D}|\,. \tag{152}$$

While we have put modulus signs around $\vec{D}$ in (152), one should note that it does have a meaningful orientation, and so we will sometimes consider $\vec{J}_L = 8\vec{D}$.

One can use the bubble equations to obtain another, rather more intuitive expression for $J_1 - J_2$. One should first note that the right-hand side of the bubble equation, (143), may be written as $-\sum_I \tilde{k}^I_i$. Multiplying this by $\vec{y}^{(i)}$ and summing over i yields:

$$\begin{aligned}
\vec{J}_L \quad &\equiv \quad 8\,\vec{D} \;=\; -\tfrac{4}{3}\, C_{IJK} \sum_{\substack{i,j=1\\ j\neq i}}^{N} \Pi^{(I)}_{ij}\, \Pi^{(J)}_{ij}\, \Pi^{(K)}_{ij}\, \frac{q_i\, q_j\, \vec{y}^{(i)}}{r_{ij}} \\
&= \quad -\tfrac{2}{3}\, C_{IJK} \sum_{\substack{i,j=1\\ j\neq i}}^{N} q_i\, q_j\, \Pi^{(I)}_{ij}\, \Pi^{(J)}_{ij}\, \Pi^{(K)}_{ij}\, \frac{(\vec{y}^{(i)} - \vec{y}^{(j)})}{|\vec{y}^{(i)} - \vec{y}^{(j)}|}\,,
\end{aligned} \tag{153}$$

where we have used the skew symmetry $\Pi_{ij} = -\Pi_{ji}$ to obtain the second identity. This result suggests that one should define an angular momentum flux vector associated with the ij^{th} bubble:

$$\vec{J}_{L\,ij} \;\equiv\; -\tfrac{4}{3}\, q_i\, q_j\, C_{IJK}\, \Pi^{(I)}_{ij}\, \Pi^{(J)}_{ij}\, \Pi^{(K)}_{ij}\, \hat{y}_{ij}\,, \tag{154}$$

where $\hat{y}_{ij}$ are *unit* vectors,

$$\hat{y}_{ij} \;\equiv\; \frac{(\vec{y}^{(i)} - \vec{y}^{(j)})}{|\vec{y}^{(i)} - \vec{y}^{(j)}|}\,. \tag{155}$$

This means that the flux terms on the left-hand side of the bubble equation actually have a natural spatial direction, and once this is incorporated, it yields the contribution of the bubble to J_L.

7.5 Comments on closed time-like curves and the bubble equations

While the bubble equations are necessary to avoid CTC's near the Gibbons-Hawking points, they are not sufficient to guarantee the absence of CTC's globally. Indeed, there are non-trivial examples that satisfy the bubble equations and still have CTC's. On the other hand, there are quite a number of important physical examples in which the bubble equations *do* guarantee the absence of CTC's globally. For example, the simplest bubbled supertube will be discussed in Section 8.1 and it has been shown numerically in some examples that the bubble equations do indeed ensure the global absence of CTC's. Some more complex examples that are free of CTC's are described in Section 9.4. It is an open question as to how and when a bubbled configuration that satisfies (143) is globally free of CTC's. In this section we will make some simple observations that suggest approaches to solving this problem.

First we need to dispel a "myth" or, more precisely, give a correct statement of an often mis-stated theorem that in a BPS solution of extremal black holes, all the black holes must have electric charges of the same sign. The physical intuition is simple: If two BPS black holes have opposite charges, then they necessarily attract both gravitationally and electromagnetically and cannot be stationary and this time dependence breaks the supersymmetry of the original BPS solutions. While this is physically correct, there is an implicit assumption that we are not going to allow physical solutions to have CTC's, changes in metric signature, or regions with complex metrics. A simple example is to make a solution with BMPV black holes given by the harmonic function:

$$Z_I \;=\; Z \;\equiv\; 1 \;+\; \frac{Q}{r_1} \;-\; \frac{Q}{r_2}\,. \tag{156}$$

We are not advocating that solutions like this, or ones with CTC's in general, should be taken as physically sensible. Nevertheless, this solution does satisfy all the equations of motion. The point we wish to make is that if one takes a completely standard, multi-centered BPS solution one can get lots of CTC's or imaginary metric coefficients if one is sloppy about the relative signs of the distributed charges. For this reason, one cannot expect to take a bubbled geometry and randomly assign some flux parameters and expect to avoid CTC's even if one has satisfied the bubble equations. Indeed, a bubbled analogue of the BMPV configuration (156) could easily satisfy the bubble equations thereby avoiding CTC's near the Gibbons-Hawking points, only to have all sorts of pathology in between the two bubbled black holes.

There must therefore be some kind of positivity condition on the flux parameters. One suggestion might be to look at every subset, $\mathcal{S}$, of the Gibbons-Hawking points. To such a subset one can associate a contribution, $Q_I^{(\mathcal{S})}$, to the electric charges by summing (145) only over the subset, $\mathcal{S}$. One could then require that the $Q_I^{(\mathcal{S})}$ have the same sign for all choices of $\mathcal{S}$. This would exclude bubbled analogs of (156), but it might also

be too stringent. It may be that one can tolerate a "mild failure" of the conditions on relative signs of electric charges if the Gibbons-Hawking points are all clustered; the danger might only occur in "classical limits" when some fluxes are very large so that the solution decomposes into two widely separated "blobs" of opposite charge.

Another natural, and possibly related condition is to remember that given N Gibbons-Hawking centers, the cycles are related to the root lattice of $SU(N)$ and the dual fluxes can be labeled by the weight lattice. In this language, the obvious positivity condition is to insist that the fluxes all lie in the positive Weyl chamber of the lattice. Moreover, when there are N_1 positive and N_2 negative GH points, it may be more appropriate to think in terms of the weight lattice of a super Lie algebra, $SU(N_1|N_2)$. In this context, one can rewrite $Z_I V$ in a rather more suggestive manner:

$$Z_I\, V \;=\; V \;-\; \tfrac{1}{4}\, C_{IJK} \sum_{i,j=1}^{N} \Pi_{ij}^{(J)}\, \Pi_{ij}^{(K)}\, \frac{q_i\, q_j}{r_i\, r_j}\,. \tag{157}$$

With suitable positivity conditions on the fluxes one can arrange all the terms with $q_i q_j < 0$ to be positive. It is not clear why, in general, these terms dominate the terms with $q_i q_j > 0$, but one can certainly verify it in examples like the one below.

Consider the situation where all the flux parameters corresponding to a given $U(1)$ are equal and positive:

$$k_j^1 \;=\; a\,, \qquad k_j^2 \;=\; b\,, \qquad k_j^3 \;=\; c\,, \qquad a,b,c>0\,, \quad j=1,\ldots,N\,. \tag{158}$$

Also suppose that $q_j = \pm 1$ and let $P_\pm$ be the subsets of integers, j, for which $\pm q_j > 0$. Define

$$V_\pm \;\equiv\; \sum_{j\in P_\pm} \frac{1}{r_j}\,. \tag{159}$$

Then one has

$$Z_I\, V \;=\; V \;+\; 4\, h_I\, V_+\, V_-\,, \tag{160}$$

where $h_1 \equiv bc$, $h_2 \equiv ac$, $h_3 \equiv ab$.

For this flux distribution the bubble equations reduce to:

$$8\, abc\, V_-(\vec{y}=\vec{y}^{(i)}) \;=\; (N-1)\,(a+b+c) \qquad \text{for all } i\in P_+\,, \tag{161}$$

$$8\, abc\, V_+(\vec{y}=\vec{y}^{(j)}) \;=\; (N+1)\,(a+b+c) \qquad \text{for all } j\in P_-\,. \tag{162}$$

Multiply the first of these equations by r_i^{-1} and sum, and multiply the second equation by r_j^{-1} and sum, and one obtains:

$$V_+ \;=\; \frac{8\, abc}{(N-1)\,(a+b+c)} \sum_{i\in P_+} \sum_{j\in P_-} \frac{1}{r_{ij}}\, \frac{1}{r_i}\,, \tag{163}$$

$$V_- \;=\; \frac{8\, abc}{(N+1)\,(a+b+c)} \sum_{i\in P_+} \sum_{j\in P_-} \frac{1}{r_{ij}}\, \frac{1}{r_j}\,. \tag{164}$$

Now note that $V = V_+ - V_-$ and use the foregoing expressions in (160) to obtain:

$$Z_I\, V \;=\; \sum_{i\in P_+}\sum_{j\in P_-} \frac{1}{r_i\, r_j\, r_{ij}} \Big[\frac{8\, abc}{(a+b+c)} \Big(\frac{r_j}{(N-1)} \;-\; \frac{r_i}{(N+1)} \Big) \\ +\; 4\, h_I\, r_{ij} \Big] \,. \tag{165}$$

Since $a, b, c > 0$ and $N > 1$, one has

$$\frac{8\, abc}{(N+1)\,(a+b+c)} \;<\; 4\, h_I \,, \qquad I = 1, 2, 3 \,, \tag{166}$$

and thus the positivity of $Z_I V$ follows trivially from the triangle inequality:

$$r_j \;+\; r_{ij} \;\geq\; r_i \,. \tag{167}$$

Note that it was relatively easy to prove positivity under the forgoing assumptions and that there was a lot of "wiggle room" in establishing the inequality. More formally, one can show that (165) is uniformly bounded below in a large compact region and so one can allow some variation of the flux parameters with j and still preserve positivity. It would, of course, be very nice to know what the possible ranges of flux parameters are.

8 Microstates for black holes and black rings

Having explored the general way to construct smooth three-charge bubbling solutions that have charges and angular momenta of the same type as three-charge black holes and black rings, we now turn to exploring such solutions in greater generality. We will begin by describing several simple examples, like the simplest bubbled black ring, or a bubbled black hole made of several bubbles. We will find that when the number of bubbles is large, and the fluxes on them are generic, these solutions have the same relation between charges and angular momenta as the maximally-spinning (zero-entropy) three-charge BPS black hole ($J^2 = N_1 N_5 N_p$). Moreover, when all the GH centers except one are in the same blob, and one GH center sits away from the blob, the solutions have the same charges, dipole charges and angular momenta as a zero-entropy, three-charge BPS black ring. Thus, to any zero-entropy black hole or any round three-charge supertube there corresponds a very large number of bubbled counterparts.

It is interesting to recall how the upper bound on the angular momentum is obtained for the BMPV black hole: One takes a solution with $J^2 < N_1 N_2 N_3$, and imagines spinning it faster. As this happens, the closed timelike curves (CTC's) inside the horizon get closer and closer to the horizon. When J^2 becomes larger than $N_1 N_2 N_3$, these CTC's sit outside of the horizon and the solution has to be discarded as unphysical. A similar story happens with the black ring. What is remarkable is that this relation between the charges and

angular momentum, which came from studying the solution near the horizon of the black hole and black ring, also comes out from investigating horizonless solutions with a large number of bubbles and generic fluxes. The fact that this coincidence happens both for black holes, and for black rings (as well as for BPS black holes and rings in any $U(1)^N$ $\mathcal{N} = 2$, five-dimensional, ungauged supergravity), is indicative of a stronger connection between black holes and their bubbling counterparts.

Nevertheless, the fact that generic bubbling solutions correspond to zero-entropy black holes or to zero-entropy black rings means that we have only found a special corner of the microstate geometries. One might suspect, for example, that this feature comes from using a GH base space, and that obtaining microstates of positive-entropy black holes might be impossible unless one considers a more general base space. As we will see, this is not the case: We will be able to obtain microstates of black holes with $J^2 < N_1 N_2 N_3$ by merging together zero-entropy black hole microstates and zero-entropy black ring microstates[30].

As we have seen in Section 4.5, unlike the merger of two BPS black holes, which is always irreversible, the merger of a BPS black hole and a BPS black ring can be reversible or irreversible, depending on the charges of the two objects. We therefore expect the merger of microstates to result in an zero-entropy microstate or a positive-entropy black-hole microstate, depending on the charges of the merging microstates. Moreover, since the merger can be achieved in a Gibbons-Hawking base, we will obtain positive-entropy black-hole microstates that have a Gibbons-Hawking base. However, as we will see in the following sections, the merger process will be full of surprises.

We will find there is a huge qualitative difference between the behaviour of the internal structure of microstates in "reversible" and "irreversible" mergers[31]. A "reversible" merger of an zero-entropy black-hole microstate and an zero-entropy black-ring microstate produces another zero-entropy black-hole microstate. For reversible mergers we find the bubbles corresponding to the ring simply join the bubbles corresponding to the black hole, and form a bigger bubbled structure.

In an "irreversible" merger, as the ring bubbles and the black hole bubbles get closer and closer, we find that the distances between the GH points that form the black hole foam and the black ring foam also decrease. As one approaches the merger point, all the sizes in the GH base scale down to zero while preserving their relative proportions. In the limit in which the merger occurs, the solutions have $J_1 = J_2 < \sqrt{Q_1 Q_2 Q_3}$, and all the points have scaled down to zero size on the base. Therefore, it naively looks like the configuration is singular; however, the full physical size of the bubbles also depends on the warp factors, and taking these into account one can show that the physical size of

[30] Obviously, the term "zero-entropy" applies to the black hole and black ring whose microstate geometries we discuss, and *not* to the horizonless microstate geometries themselves. Such horizonless microstate geometries trivially have zero entropy.

[31] With an obvious abuse of terminology, we will refer to such solutions as "reversible" and "irreversible" mergers of microstates with the understanding that the notion of reversibility refers to the classical black-hole and black-ring solutions to which the microstates correspond.

all the bubbles that form the black hole and the black ring remains the same. The fact that the GH points get closer and closer together implies that the throat of the solution becomes deeper and deeper, and more and more similar to the throat of a BPS black hole (which is infinite).

8.1 The simplest bubbled supertube

As we have discussed in Section 7.1, we expect the solution resulting from the geometric transition of a zero-entropy black ring to contain three GH centers, of charges $q_1 = 1$, $q_2 = -Q$ and $q_3 = +Q$. The integral of the flux on the Gaussian two-cycle bubbled at the position of the ring gives the dipole charges of the latter, d^I. It is useful to define another physical variables f^I, measuring the fluxes through the other two-cycle:

$$d^I \;\equiv\; 2\,(k_2^I \;+\; k_3^I)\,, \qquad f_I \;\equiv\; 2\,k_1^I \;+\; (1+\tfrac{1}{Q})\,k_2^I \;+\; (1-\tfrac{1}{Q})\,k_3^I\,. \tag{168}$$

Note that d^I and f^I are invariant under (95).

The electric charges of the bubbled tube are:

$$Q_I \;=\; C_{IJK}\,d^J\,f^K\,, \tag{169}$$

and the angular momenta are:

$$J_1 \;=\; -\,\frac{(Q-1)}{12\,Q}\,C_{IJK}\,d^I\,d^J\,d^K \;+\; \frac{1}{2}\,C_{IJK}\,d^I\,d^J\,f^K\,, \tag{170}$$

$$J_2 \;=\; \frac{(Q-1)^2}{24\,Q^2}\,C_{IJK}\,d^I\,d^J\,d^K \;+\; \frac{1}{2}\,C_{IJK}\,f^I\,f^J\,d^K\,. \tag{171}$$

In particular, the angular momentum of the tube is:

$$\begin{aligned} J_T \;=\; J_2 - J_1 \;=\; & \frac{1}{2}\,C_{IJK}\,(f^I\,f^J\,d^K - d^I\,d^J\,f^K) \\ & +\; \Big(\frac{3\,Q^2-4\,Q+1}{24\,Q^2}\Big)\,C_{IJK}\,d^I\,d^J\,d^K\,. \end{aligned} \tag{172}$$

When the size of the 2-3 bubble (between GH charges q_2 and q_3) is small, this configuration can be thought of as the resolution of the singularity of the zero-entropy supertube, and has the same charges, angular momenta and size as the naive zero-entropy black ring solution. In the bubble equations, the size of the 2-3 bubble comes from a balance between the attraction of oppositely charged GH points, and the fluxes that have a lot of energy when the cycle they wrap becomes very small. Hence, both when Q is large and when d is much smaller than f the solution approaches the naive zero-entropy black ring solution

It is not hard to verify that in the limit of large Q, as well as in the limit $d/f \to 0$ equations (170) and (171) match exactly the charges and angular momenta of a three-charge black ring of zero entropy.

One can also estimate, in this limit, the distance from the small 2-3 bubble to the origin of space, and find that this distance asymptotes to the radius, R_T, of the unbubbled black ring solution (as measured in the $\mathbb{R}^3$ metric of the GH base), given by

$$J_T \;=\; 4\,R_T\,(d^1 + d^2 + d^3)\,. \tag{173}$$

8.2 Microstates of many bubbles

We now consider bubbled solutions that have a large number of localized centers, and show that these solutions correspond to maximally-spinning (zero-entropy) BMPV black holes, or to maximally spinning BPS black rings [40]. The ring microstates have a blob of GH centers of zero total charge with a single GH center away from the blob while the black hole microstates have all the centers in one blob of net GH charge one. We will see that this apparently small difference can very significantly influence the solution of the bubble equations.

8.2.1 A black-hole blob

We first consider a configuration of N GH centers that lie is a single "blob" and take all these centers to have roughly the same flux parameters, to leading order in N. To argue that such a blob corresponds to a BMPV black hole, we first need to show that $J_1 = J_2$. If the overall configuration has three independent $\mathbb{Z}_2$ reflection symmetries then this is trivial because the $\vec{D}_j$ in (152) will then come in equal and opposite pairs, and so one has $J_L = 0$. More generally, for a "random" distribution[32] the vectors $\hat{y}_{ij}$ (defined in (155)) will point in "random" directions and so the $\vec{J}_{L\,ij}$ will generically cancel one another at leading order in N. The only way to generate a non-zero value of J_L is to bias the distribution such that there are more positive centers in one region and more negative ones in another. This is essentially what happens in the microstate solutions constructed and analyzed by [31, 32]. However, a single generic blob will have $J_1 - J_2$ small compared to $|J_1|$ and $|J_2|$.

To compute the other properties of such a blob, we will simplify things by taking $N = 2M + 1$ to be odd, and assume that $q_j = (-1)^{j+1}$. Using the gauge invariance, we can take all of k_i^I to be positive numbers, and we will assume that they have small variations about their mean value:

$$k_j^I \;=\; k_0^I\,(1 \;+\; \mathcal{O}(1))\,, \tag{174}$$

where k_0^I is defined in (146). The charges are given by:

$$Q_I \;=\; -2\,C_{IJK}\sum_j q_j^{-1}\,(k_j^J - q_j N k_0^J)\,(k_j^K - q_j N k_0^K)$$

[32]Such a distribution must, of course, satisfy the bubble equations, (143), but this will still allow a sufficiently random distribution of GH points.

$$
\begin{aligned}
&= -2\,C_{IJK}\Big(\sum_j q_j^{-1}k_j^J k_j^K - Nk_0^J\sum_j k_j^K - Nk_0^K\sum_j k_j^J + N^2k_0^Jk_0^K\sum_j q_j\Big)\\
&= 2\,C_{IJK}\Big(N^2k^Jk^K - \sum_j k_j^Jk_j^Kq_j^{-1}\Big)\\
&\approx 2\,C_{IJK}(N^2+\mathcal{O}(1))\,k_0^Jk_0^K
\end{aligned}
\tag{175}
$$

where we used (174) and the fact that $|q_i| = 1$ only in the last step. In the large N limit, for M theory on T^6 we have

$$
Q_1 \approx 4N^2k_0^2k_0^3 + \mathcal{O}(1)\,,\quad Q_2 \approx 4N^2k_0^1k_0^3 + \mathcal{O}(1)\,,\quad Q_3 \approx 4N_0^2k^1k_0^3 + \mathcal{O}(1)\,. \tag{176}
$$

We can make a similar computation for the angular momenta:

$$
\begin{aligned}
J_R \quad &= \quad \tfrac{4}{3}\,C_{IJK}\sum_j q_j^{-2}\,(k_j^I - q_jNk_0^I)\,(k_j^J - q_jNk_0^J)\,(k_j^K - q_jNk_0^K)\\
&= \quad \tfrac{4}{3}\,C_{IJK}\Big(\sum_j q_j^{-2}\,k_j^Ik_j^Jk_j^K - 3Nk_0^I\sum_j q_j^{-1}\,k_j^Jk_j^K\\
&\qquad\qquad +3N^2k_0^Ik_0^J\sum_j k_j^K - N^3k_0^Ik_0^Jk_0^K\sum_j q_j\Big)\\
&\approx \quad \tfrac{4}{3}\,C_{IJK}(N - 3N + 3N^3 - N^3 + \mathcal{O}(N))\,k_0^Ik_0^Jk_0^K\,,
\end{aligned}
\tag{177}
$$

where we used the fact that, for a "well behaved" distribution of positive k_i^I with $|q_j| = 1$, one has:

$$
\sum_i q_i^{-1}k_i^Jk_i^K \;=\; \sum_i q_ik_i^Jk_i^K \;\approx\; k_0^Jk_0^K\,,\qquad \sum_i k_i^Ik_i^Jk_i^K \;\approx\; Nk_0^Ik_0^Jk_0^K\,. \tag{178}
$$

Therefore we simply have:

$$
J_R \;\approx\; 16N^3k_0^1k_0^2k_0^3 + O(N)\;. \tag{179}
$$

Since $J_L \approx 0$ for a generic blob at large N we therefore have, at leading order:

$$
J_1^2 \;\approx\; J_2^2 \;\approx\; \tfrac{1}{4}\,J_R^2 \;\approx Q_1Q_2Q_3\,, \tag{180}
$$

and so, in the large-N limit, these microstates always correspond to a maximally spinning BMPV black hole. At sub-leading order in N:

$$
\frac{J_R^2}{4Q_1Q_2Q_3} \;-\; 1 \sim O\left(\frac{1}{N^2}\right)\,. \tag{181}
$$

Interestingly enough, the value of J_R is slightly bigger than $\sqrt{4Q_1Q_2Q_3}$. However, this is not a problem because in the classical limit this correction vanishes. Moreover, it is possible to argue that a classical black hole with zero horizon area will receive higher-order curvature corrections, that usually increase the horizon area; hence a zero-entropy configuration will have J_R slightly larger then the maximal classically allowed value, by an amount that vanishes in the large N (classical) limit.

8.2.2 A supertube blob

The next simplest configuration to consider is one in which one starts with the blob considered above and then moves a single GH point of charge +1 out to a very large distance from the blob. That is, one considers a blob of total GH charge zero with a single very distant point of GH-charge +1. Since one now has a strongly "biased" distribution of GH charges one should now expect $J_1 - J_2 \neq 0$.

Again we will assume N to be odd, and take the a GH charge distribution to be $q_j = (-1)^{j+1}$, with the distant charge being the N^{th} GH charge. The blob therefore has $\frac{1}{2}(N-1)$ points of GH charge +1 and $\frac{1}{2}(N-1)$ points of GH charge -1. When seen from far away one might expect this blob to resemble the three-point solution described above with $Q = \frac{1}{2}(N-1)$. We will show that this is exactly what happens in the large-N limit.

To have the N^{th} GH charge far from the blob means that all the two-cycles, $\Delta_{j\,N}$ must support a very large flux compared to the fluxes on the Δ_{ij} for $i, j < N$. To achieve this we therefore take:

$$k^I_j \;=\; a^I_0\,(1 \;+\; \mathcal{O}(1))\,, \quad j = 1, \ldots, N-1\,, \qquad k^I_N \;=\; -\,b^I_0\,N\,. \tag{182}$$

where

$$a^I_0 \;\equiv\; \frac{1}{(N-1)}\,\sum_{j=1}^{N-1} k^I_j\,. \tag{183}$$

We also assume that a^I_0 and b^I_0 are of the same order. The fluxes of this configuration are then:

$$\begin{aligned}
\Pi^{(I)}_{ij} \quad &= \quad \Big(\frac{k^I_j}{q_j} \;-\; \frac{k^I_i}{q_i}\Big)\,, &(184)\\
\Pi^{(I)}_{i\,N} \quad &= \quad -\Pi^{(I)}_{N\,i} \;=\; -\,\Big(\frac{k^I_i}{q_i} \;+\; N\,b^I_0\Big)\,, \quad i, j = 1, \ldots, N-1\,.
\end{aligned}$$

For this configuration one has:

$$\begin{aligned}
k^I_0 \quad &= \quad \frac{(N-1)}{N}\,a^I_0 \;-\; b^I_0\,, \qquad \tilde{k}^I_N \;=\; -\,(N-1)\,a^I_0\,, &(185)\\
\tilde{k}^I_j \quad &= \quad k^I_j \;+\; q_j\,(N\,b^I_0 - (N-1)\,a^I_0)\,, \quad j = 1, \ldots, N-1\,. &(186)
\end{aligned}$$

Motivated by the bubbling black ring of [40] and Section 8.1, define the physical parameters:

$$d^I \;\equiv\; 2\,(N-1)\,a^I_0\,, \qquad f^I \;\equiv\; (N-1)\,a^I_0 - 2\,N\,b^I_0\,. \tag{187}$$

Keeping only the terms of leading order in N in (145) and (151), one finds:

$$\begin{aligned}
Q_I \quad &= \quad C_{IJK} d^J f^K\,, &(188)\\
J_1 + J_2 \quad &= \quad \tfrac{1}{2}\,C_{IJK}(d^I d^J f^K + f^I f^J d^K) \;-\; \tfrac{1}{24}\,C_{IJK} d^I d^J d^K\,. &(189)
\end{aligned}$$

Since the $N^{\rm th}$ point is far from the blob, we can take $r_{iN} \approx r_0$ and then the $N^{\rm th}$ bubble equation reduces to:

$$\tfrac{1}{6}\, C_{IJK} \sum_{j=1}^{N-1} \left(\frac{k_j^I}{q_j} + N\, b_0^I\right)\left(\frac{k_j^J}{q_j} + N\, b_0^J\right)\left(\frac{k_j^K}{q_j} + N\, b_0^K\right)\frac{q_j}{r_0} = (N-1)\sum_I a_0^I\,. \tag{190}$$

To leading order in N this means that the distance from the blob to the $N^{\rm th}$ point, r_0, in the GH space is given by:

$$\begin{aligned} r_0 \quad &\approx \quad \tfrac{1}{2}\, N^2 \left[\sum_I a^I\right]^{-1} C_{IJK}\, a_0^I\, b_0^J\, b_0^K \\ &= \quad \tfrac{1}{32}\left[\sum_I d^I\right]^{-1} C_{IJK}\, d^I\, (2f^J - d^J)\,(2f^K - d^K)\,. \end{aligned} \tag{191}$$

Finally, considering the dipoles (150), it is evident that, to leading order in N, $\vec{D}$ is dominated by the contribution coming from the $N^{\rm th}$ point and that:

$$J_1 - J_2 \quad = \quad 8\,|\vec{D}| \;=\; 8\,N\left(\sum_I a_0^I\right) r_0 \;=\; 4\,N^3\, C_{IJK}\, a_0^I\, b_0^J\, b_0^K \tag{192}$$

$$= \quad \tfrac{1}{8}\, C_{IJK}\, d^I\, (2f^J - d^J)\,(2f^K - d^K)\,. \tag{193}$$

Thus, the bubbling supertube of many centers also has *exactly* the same size, angular momenta, charges and dipole charges as a zero-entropy black ring, and should be thought of a microstate of the later.

9 Mergers and deep microstates

As we have seen in Section 4.5, a merger of a zero-entropy black ring and a zero-entropy black hole can produce both a zero-entropy black hole (reversible merger) or a non-zero-entropy one (irreversible merger). We expect that in a similar fashion, the merger of the microstates of zero-entropy black holes and zero-entropy black rings should produce microstates of both zero-entropy and positive-entropy black holes. Since we have already constructed zero-entropy black-hole microstates, we will mainly focus on irreversible mergers and their physics. One can learn more about reversible mergers of microstates in Section 6 of [42].

Even though the original black-ring plus black-hole solution that describes the merger in Section 4.5 and [75] does not have a tri-holomorphic $U(1)$ symmetry (and thus the merger of the corresponding microstates cannot be done using a GH base), one can also study the merger of black rings and black holes by considering a $U(1)\times U(1)$ invariant solution describing a black ring with a black hole in the center. As the ring is made smaller and smaller by, for example, decreasing its angular momentum, it eventually merges into

the black hole. At the point of merger, this solution is identical to the merger described in Section 4.5 with the black ring grazing the black-hole horizon. Hence this $U(1) \times U(1)$ invariant solution can be used to study mergers where the black ring grazes the black hole horizon at the point of merger. As we have seen in Section 4.5, all the reversible mergers and some of the irreversible mergers belong to this class.

In the previous section we have seen how to create bubbled solutions corresponding to a zero-entropy black ring and maximally-spinning black holes. The generic bubbled solutions with GH base have a $U(1)$ symmetry corresponding to $J_R \equiv J_1 + J_2$ and if the GH points all lie on an axis then the solution is $U(1) \times U(1)$ invariant. We can therefore study the merger of bubbled microstates by constructing $U(1) \times U(1)$ invariant bubbling solutions describing a black ring with a black hole in the center. By changing some of the flux parameters of the solution, one can decrease the radius of the bubbling black ring and merge it into the bubbling black hole to create a larger bubbling black hole.

In this section we consider a bubbling black hole with a very large number of GH centers, sitting at the center of the simplest bubbled supertube, generated by a pair of GH points[33]. We expect two different classes of merger solution depending upon whether the flux parameters on the bubbled black hole and bubbled black ring are parallel or not. These correspond to reversible and irreversible mergers respectively. The reversible mergers involve the GH points approaching and joining the black-hole blob to make a similar, slightly larger black-hole blob [42]. The irreversible merger is qualitatively very different and we will examine it in detail. First, however, we will establish some general results about the charges and angular momenta of the bubbled solutions that describe a bubbled black ring of two GH centers with a bubbling black-hole at the center.

9.1 Some exact results

We begin by seeing what may be deduced with no approximations whatsoever. Our purpose here is to separate all the algebraic formulae for charges and angular momenta into those associated with the black hole foam and those associated with the bubbled supertube. We will consider a system of N GH points in which the first $N-2$ points will be considered to be a blob and the last two points will have $q_{N-1} = -Q$ and $q_N = Q$. The latter two points can then be used to define a bubbled black ring.

Let $\hat{k}_0^I$ denote the average of the flux parameters over the first $(N-2)$ points:

$$\hat{k}_0^I \equiv \frac{1}{(N-2)} \sum_{j=1}^{N-2} k_j^I \,, \tag{194}$$

[33]Of course it is straightforward to generalize our analysis to the situation where both the supertube and the black hole have a large number of GH centers. However, the analysis is simpler and the numerical stability is better for mergers in which the supertube is composed of only two points, and we have therefore focussed on this.

and introduce k-charges that have a vanishing average over the first $(N-2)$ points:

$$\hat{k}^I_j \;\equiv\; k^I_j \;-\; (N-2)\, q_j\, \hat{k}^I_0\,, \qquad j = 1, \ldots, N-2\,. \tag{195}$$

We also parameterize the last two k^I-charges in exactly the same manner as for the bubbled supertube (see equation (168)):

$$\begin{aligned} d^I \;&\equiv\; 2\,(k^I_{N-1} + k^I_N)\,, \\ f^I \;&\equiv\; 2\,(N-2)\,\hat{k}^I_0 + (1+\tfrac{1}{Q})\,k^I_{N-1} + (1-\tfrac{1}{Q})\,k^I_N\,. \end{aligned} \tag{196}$$

One can easily show that the charge (145) decomposes into

$$Q_I \;=\; \widehat{Q}_I \;+\; C_{IJK}\, d^J\, f^K\,, \tag{197}$$

where

$$\widehat{Q}_I \;\equiv\; -\,2\,C_{IJK} \sum_{j=1}^{N-2} q_j^{-1}\, \hat{k}^J_j\, \hat{k}^K_j\,. \tag{198}$$

The $\widehat{Q}_I$ are simply the charges of the black-hole blob, made of the first $(N-2)$ points. The second term in (197) is exactly the expression, (169), for the charges of a bubbled supertube with GH centers of charges $+1$, $-Q$ and Q and k-charges $(N-2)\hat{k}^I_0$, k^I_{N-1} and k^I_N, respectively. Thus the charge of this configuration decomposes exactly as if it were a black-hole blob of $(N-2)$ centers and a bubbled supertube.

There is a similar result for the angular momentum, J_R. One can easily show that:

$$J_R \;=\; \widehat{J}_R \;+\; d^I\, \widehat{Q}_I \;+\; j_R\,, \tag{199}$$

where

$$\hat{J}_R \;\equiv\; \frac{4}{3}\, C_{IJK} \sum_{j=1}^{N-2} q_j^{-2}\, \hat{k}^I_j\, \hat{k}^J_j\, \hat{k}^K_j\,, \tag{200}$$

and

$$j_R \;\equiv\; \tfrac{1}{2}\, C_{IJK}\, (f^I f^J d^K \;+\; f^I d^J d^K) \;-\; \tfrac{1}{24}\,(1-Q^{-2})\, C_{IJK}\, d^I d^J d^K\,. \tag{201}$$

The term, $\hat{J}_R$, is simply the right-handed angular momentum of the black-hole blob made from $N-2$ points. The "ring" contribution to the angular momentum, j_R, agrees precisely with $J_1 + J_2$ given by (170) and (171) for an isolated bubbled supertube. The cross term, $d^I \widehat{Q}_I$ is represents the interaction of the flux of the bubbled ring and the charge of the black-hole blob. This interaction term is exactly the same as that found in Section 4.5 and in [53, 64, 75] for a concentric black hole and black ring.

Thus, as far as the charges and J_R are concerned, the complete system is behaving as though it were a black-hole blob of $(N-2)$ points interacting with a bubbled black ring defined by the points with GH charges $\pm Q$ and a single point with GH charge $+1$

replacing the black-hole blob. Note that no approximations were made in the foregoing computations, and the results are true independent of the locations of the GH centers.

To make further progress we need to make some assumptions about the configuration of the points. Suppose, for the moment, that all the GH charges lie on the z-axis at points z_i with $z_i < z_{i+1}$. In particular, the GH charges, $-Q$ and $+Q$, are located at z_{N-1} and z_N respectively.

With this ordering of the GH points, the expression for $\vec{J}_L$ collapses to:

$$J_L \;=\; \tfrac{4}{3}\, C_{IJK} \sum_{1\le i<j\le N} q_i\, q_j\, \Pi^{(I)}_{ij}\, \Pi^{(J)}_{ij}\, \Pi^{(K)}_{ij}\,. \tag{202}$$

This expression can then be separated, just as we did for J_R, into a black-hole blob component, a ring component, and interaction cross-terms. To that end, define the left-handed angular momentum of the blob to be:

$$\widehat{J}_L \;=\; \tfrac{4}{3}\, C_{IJK} \sum_{1\le i<j\le N-2} q_i\, q_j\, \Pi^{(I)}_{ij}\, \Pi^{(J)}_{ij}\, \Pi^{(K)}_{ij}\,. \tag{203}$$

Note that

$$\Pi^{(I)}_{ij} \;\equiv\; \Big(\frac{k^I_j}{q_j} \;-\; \frac{k^I_i}{q_i}\Big) \;=\; \Big(\frac{\hat{k}^I_j}{q_j} \;-\; \frac{\hat{k}^I_i}{q_i}\Big)\,, \qquad 1\le i,j\le N-2\,, \tag{204}$$

and so this only depends upon the fluxes in the blob.

The remaining terms in (202) may then be written in terms of $\hat{k}^I_j$, d^I and f^I defined in (195) and (196). In particular, there are terms that depend only upon d^I and f^I, and then there are terms that are linear, quadratic and cubic in $\hat{k}^I_j$ (and depend upon d^I and f^I). The linear terms vanish because $\sum_{j=1}^{N-2} \hat{k}^I_j \equiv 0$, the quadratic terms assemble into $\widehat{Q}_I$ of (198) and the cubic terms assemble into $\hat{J}_R$ of (200). The terms proportional to (200) cancel between the terms with $j = N-1$ and $j = N$, and one is left with:

$$J_L \;=\; \widehat{J}_L \;-\; d^I\, \widehat{Q}_I \;+\; j_L\,, \tag{205}$$

where j_L is precisely the angular momentum, J_T, of the tube:

$$j_L \;\equiv\; \tfrac{1}{2}\, C_{IJK}\, (d^I f^J f^K \;-\; f^I d^J d^K) \;+\; \Big(\frac{3\,Q^2 - 4\,Q + 1}{24\,Q^2}\Big)\, C_{IJK}\, d^I d^J d^K\,. \tag{206}$$

Observe that (201) and (206) are exactly the angular momenta of a simple bubbled ring, (170) and (171). Again we see the cross-term from the interaction of the ring dipoles and the electric charge of the blob. Indeed, combining (199) and (205), we obtain:

$$J_1 \;=\; \widehat{J}_1 \;+\; j_1\,, \qquad J_2 \;=\; \widehat{J}_2 \;+\; j_2 \;-\; d^I\, \widehat{Q}_I\,, \tag{207}$$

which is exactly how the angular momenta of the classical ring-hole solution in Section 4.5 decomposed. In particular, the term coming from the interaction of the ring dipole moment with the black hole charge only contributes to J_2.

The results obtained above are independent of whether the blob of $N-2$ points is a BMPV black-hole blob, or a more generic configuration. However, to study mergers we now take the blob to be a black-hole microstate, with $\widehat{J}_L = 0$. The end result of the merger process is also a BMPV black hole microstate, and so $J_L = 0$. Therefore, the *exact* merger condition is simply:

$$\begin{aligned}\Omega &\equiv \tfrac{1}{2}\, C_{IJK}\,(d^I f^J f^K - f^I d^J d^K) + \Big(\frac{3\,Q^2 - 4\,Q + 1}{24\,Q^2}\Big)\, C_{IJK}\, d^I d^J d^K - d^I\, \widehat{Q}_I \\ &= 0\,. \end{aligned} \tag{208}$$

Using (172), this may be written:

$$J_T \;-\; d^I\, \widehat{Q}_I \;=\; 0\,, \tag{209}$$

which is precisely the condition obtained in Section 4.5 and [75] for a classical black ring to merge with a black hole at its equator.

One should note that the argument that led to the expressions (205) and (206) for J_L, and to the exact merger condition, (208), apply far more generally. In particular we only needed the fact that the unit vectors, $\hat{y}_{ij}$, defined in (155), are all parallel for $j = N-1$ and $j = N$. This is approximately true in many contexts, and most particularly if the line between the $(N-1)^{\text{th}}$ and N^{th} points runs through the blob and the width of the blob is small compared to the distance to the two exceptional points.

One should also not be surprised by the generality of the result in equation (206). The angular momentum, J_T, is an intrinsic property of a black ring, and hence for a zero-entropy black ring, J_T can only depend on the d's and f's, and cannot depend on the black hole charges (that is, the $\hat{k}^I_j$). Therefore, we could have obtained (206) by simply setting the black hole charge to zero, and then reading off J_T from the bubbling black ring solution of Section 8.1. Hence, one should think about the expression of J_T in (172) as a universal relation between intrinsic properties of the bubbled ring: J_T, d^I and f^I.

9.2 Some simple approximations

We now return to a general distribution of GH points, but we will assume that the two "black ring points" (the $(N-1)^{\text{th}}$ and N^{th} points) are close together but very far from the black-hole blob of the remaining $(N-2)$ points. Set up coordinates in the geometric center of the black-hole blob, *i.e.* choose the origin so that

$$\sum_{i=1}^{N-2} \vec{r}_i \;=\; 0\,. \tag{210}$$

Let $r_0 \equiv |\vec{r}_{N-1}|$ be the distance from the geometric center of the blob to the first exceptional point, and let $\hat{r}_0$ be the the unit vector in that direction. The vector, $\vec{\Delta} \equiv \vec{r}_N - \vec{r}_{N-1}$, defines the width of the ring. We will assume that the magnitudes $\Delta \equiv |\vec{\Delta}|$ and $r_j \equiv |\vec{r}_j|$ are small compared to r_0. We will also need the first terms of the multipole expansions:

$$\frac{1}{|\vec{r}_{N-1} - \vec{r}_j|} \;=\; \frac{1}{r_0} \;+\; \frac{\vec{r}_j \cdot \hat{r}_0}{r_0^2} \;+\; \ldots \tag{211}$$

$$\frac{1}{|\vec{r}_N - \vec{r}_j|} \;=\; \frac{1}{r_0} \;+\; \frac{(\vec{r}_j - \vec{\Delta}) \cdot \hat{r}_0}{r_0^2} \;+\; \ldots . \tag{212}$$

For simplicity, we will also assume that the two black-ring points (we will also call these points "exceptional points") are co-linear with the origin so that

$$r_N \;\equiv\; |\vec{r}_N| \;=\; r_0 + \Delta \,. \tag{213}$$

The last two bubble equations are then:

$$\frac{\gamma}{\Delta} \;-\; \sum_{j=1}^{N-2} \frac{q_j\,\alpha_j}{|\vec{r}_N - \vec{r}_j|} \;=\; \sum_I \left(N\,Q\,k_0^I - k_N^I\right), \tag{214}$$

$$-\frac{\gamma}{\Delta} \;+\; \sum_{j=1}^{N-2} \frac{q_j\,\beta_j}{|\vec{r}_{N-1} - \vec{r}_j|} \;=\; -\sum_I \left(N\,Q\,k_0^I + k_{N-1}^I\right) \tag{215}$$

where k_0^I is given in (146) and

$$\alpha_j \;\equiv\; \tfrac{1}{6}\,Q\,C_{IJK}\,\Pi^{(I)}_{j\,N}\,\Pi^{(J)}_{j\,N}\,\Pi^{(K)}_{j\,N} \tag{216}$$

$$\;=\; \tfrac{1}{6}\,Q\,C_{IJK}\left(\frac{k_N^I}{Q} - \frac{k_j^I}{q_j}\right)\left(\frac{k_N^J}{Q} - \frac{k_j^J}{q_j}\right)\left(\frac{k_N^K}{Q} - \frac{k_j^K}{q_j}\right), \tag{217}$$

$$\beta_j \;\equiv\; \tfrac{1}{6}\,Q\,C_{IJK}\,\Pi^{(I)}_{j\,(N-1)}\,\Pi^{(J)}_{j\,(N-1)}\,\Pi^{(K)}_{j\,(N-1)} \tag{218}$$

$$\;=\; -\tfrac{1}{6}\,Q\,C_{IJK}\left(\frac{k_{N-1}^I}{Q} + \frac{k_j^I}{q_j}\right)\left(\frac{k_{N-1}^J}{Q} + \frac{k_j^J}{q_j}\right)\left(\frac{k_{N-1}^K}{Q} + \frac{k_j^K}{q_j}\right), \tag{219}$$

$$\gamma \;\equiv\; \tfrac{1}{6}\,Q^2\,C_{IJK}\,\Pi^{(I)}_{(N-1)\,N}\,\Pi^{(J)}_{(N-1)\,N}\,\Pi^{(K)}_{(N-1)\,N} \;=\; \tfrac{1}{48}\,Q^{-1}\,C_{IJK}\,d^I\,d^J\,d^K \,. \tag{220}$$

It is also convenient to introduce

$$\alpha_0 \;\equiv\; \sum_{j=1}^{N-2} q_j\,\alpha_j \,, \qquad \beta_0 \;\equiv\; \sum_{j=1}^{N-2} q_j\,\beta_j \,. \tag{221}$$

If one adds (214) and (215) then the terms involving γ cancel and using (212) one then obtains:

$$\sum_{j=1}^{N-2} q_j \left[\alpha_j \left(\frac{1}{r_0} + \frac{(\vec{r}_j - \vec{\Delta}) \cdot \hat{r}_0}{r_0^2} \right) \; - \; \beta_j \left(\frac{1}{r_0} + \frac{\vec{r}_j \cdot \hat{r}_0}{r_0^2} \right) \right] \; = \; \tfrac{1}{2} \sum_I d^I \,. \tag{222}$$

One now needs to perform the expansions with some care. Introduce the flux vector:

$$X^I \; \equiv \; 2\, f^I - d^I - 4\,(N-2)\, \hat{k}_0^I \,, \tag{223}$$

and note that the fluxes between the blob and ring points are given by:

$$\Pi^{(I)}_{j\,(N-1)} \;\; = \;\; -\tfrac{1}{4}\,[\, X^I + Q^{-1}\, d^I + 4\, q_j^{-1}\, k_j^I \,] \,, \tag{224}$$

$$\Pi^{(I)}_{j\,N} \;\; = \;\; -\tfrac{1}{4}\,[\, X^I - Q^{-1}\, d^I + 4\, q_j^{-1}\, k_j^I \,] \,. \tag{225}$$

In particular, the difference of these fluxes is simply the flux through the two-cycle running between the two ring points:

$$\Pi^{(I)}_{j\,N} \; - \; \Pi^{(I)}_{j\,(N-1)} \; = \; \frac{d^I}{2\,Q} \; = \; \Pi^{(I)}_{(N-1)\,N} \,. \tag{226}$$

For the ring to be far from the black hole, the fluxes $\Pi^{(I)}_{j\,(N-1)}$ and $\Pi^{(I)}_{j\,N}$ must be large. For the ring to be thin ($\Delta \ll r_0$), these fluxes must be of similar order, or $\Pi^{(I)}_{(N-1)\,N}$ should be small. Hence we are assuming that $\frac{d^I}{2Q}$ is small compared to X^I. We are also going to want the black hole and the black ring to have similar charges and angular momenta, J_R, and one of the ways of achieving this is to make f^I, d^I and $N\hat{k}_0^I$ of roughly the same order.

Given this, the leading order terms in (222) become:

$$\sum_{j=1}^{N-2} q_j \left[\frac{(\alpha_j - \beta_j)}{r_0} \; - \; \alpha_j \, \frac{\Delta}{r_0^2} \right] \; = \; \tfrac{1}{2} \sum_I d^I \,. \tag{227}$$

One can then determine the ring width, Δ, using (214) or (215). In particular, when the ring width is small while the ring radius is large, the left-hand side of each of these equations is the difference of two very large numbers of similar magnitude. To leading order we may therefore neglect the right-hand sides and use the leading monopole term to obtain:

$$\beta_0 \, \frac{\Delta}{r_0} \; \approx \; \alpha_0 \, \frac{\Delta}{r_0} \; = \; \left[\sum_{j=1}^{N-2} q_j \, \alpha_j \right] \frac{\Delta}{r_0} \; \approx \; \gamma \,, \tag{228}$$

and hence (222) becomes:

$$-\gamma \; + \; \sum_{j=1}^{N-2} q_j \, (\alpha_j - \beta_j) \; \approx \; \left[\tfrac{1}{2} \sum_I d^I \right] r_0 \,. \tag{229}$$

Using the explicit expressions for α_j, β_j and γ, one then finds:

$$\begin{aligned} r_0 \;\approx\; & \Big[4\sum_I d^I\Big]^{-1}\Big[\tfrac{1}{2}\,C_{IJK}\,(d^I f^J f^K - f^I d^J d^K) \\ & + \Big(\frac{3\,Q^2-4\,Q+1}{24\,Q^2}\Big)\,C_{IJK}\,d^I d^J d^K \;-\; d^I\widehat{Q}_I\Big]\,. \end{aligned} \tag{230}$$

This is exactly the same as the formula for the tube radius that one obtains from (173) and (172). Note also that we have:

$$r_0 \;\approx\; \Big[4\sum_I d^I\Big]^{-1}[\,j_L \;-\; d^I\widehat{Q}_I\,]\,, \tag{231}$$

where j_L the angular momentum of the supertube (205). In making the comparison to the results of Section 4.5 recall that for a black ring with a black hole exactly in the center, the embedding radius in the standard, flat $\mathbb{R}^4$ metric is given by:

$$R^2 \;=\; \frac{l_p^6}{L^4}\,\Big[\sum d^I\Big]^{-1}\Big(J_T \;-\; d^I\widehat{Q}_I\Big)\,. \tag{232}$$

The transformation between a flat $\mathbb{R}^4$ and the GH metric with $V = \frac{1}{r}$ involves setting $r = \frac{1}{4}\rho^2$, and this leads to the relation $R^2 = 4R_T$. We therefore have complete consistency with the classical merger result.

Note that the classical merger condition is simply $r_0 \to 0$, which is, of course, very natural. This might, at first, seem to fall outside the validity of our approximation, however we will see in the next section that for irreversible mergers one does indeed maintain $\Delta, r_j \ll r_0$ in the limit $r_0 \to 0$. Reversible mergers cannot however be described in this approximation, and have to be analyzed numerically.

9.3 Irreversible mergers and scaling solutions

All the results we have obtained in Sections 9.1 and 9.2 apply equally to reversible and irreversible mergers. However, since our main purpose is to obtain microstates of a BPS back hole with classically large horizon area, we now focus on irreversible mergers.

We will show that an irreversible merger occurs in such a manner that the ring radius, r_0, the ring width, Δ, and a typical separation of points within the black-hole blob all limit to zero while their ratios all limit to finite values. We will call these scaling solutions, or scaling mergers. As the merger progresses, the throat of the solution becomes deeper and deeper, and corresponding redshift becomes larger and larger. The resulting microstates have a very deep throat, and will be called "deep microstates."

Using the solution constructed in the previous sections, we begin decreasing the radius of the bubbled ring, r_0, by decreasing some of its flux parameters. We take all the flux parameters of the $(N-2)$ points in the blob to be parallel:

$$k_j^I \;=\; \hat{k}_0^I \;=\; k^I\,, \qquad j \;=\; 1,\ldots,N-2\,, \tag{233}$$

Further assume that all the GH charges in the black-hole blob obey $q_j = (-1)^{j+1}$, $j = 1, \ldots, N-2$. We therefore have

$$\begin{aligned} \widehat{Q}_I &= 2\,(N-1)(N-3)\,C_{IJK}\,k^J k^K\,, \\ \widehat{J}_R &= \tfrac{8}{3}\,(N-1)(N-2)(N-3)\,C_{IJK}\,k^I k^J k^K\,. \end{aligned} \tag{234}$$

Define:

$$\mu_i \;\equiv\; \tfrac{1}{6}\,(N-2-q_i)^{-1}\,C_{IJK}\sum_{\substack{j=1\\ j\neq i}}^{N-2}\Pi^{(I)}_{ij}\,\Pi^{(J)}_{ij}\,\Pi^{(K)}_{ij}\,\frac{q_j}{r_{ij}}\,, \tag{235}$$

then the bubble equations for this blob in isolation (*i.e.* with no additional bubbles, black holes or rings) are simply:

$$\mu_i \;=\; \sum_{I=1}^{3} k^I\,, \tag{236}$$

More generally, in any solution satisfying (233), if one finds a blob in which the μ_i are all equal to the same constant, μ_0, then the GH points in the blob must all be arranged in the same way as an isolated black hole, but with all the positions scaled by $\mu_0^{-1}(\sum_{I=1}^3 k^I)$.

Now consider the full set of N points with $\Delta, r_j \ll r_0$. In Section 9.2 we solved the last two bubble equations and determined Δ and r_0 in terms of the flux parameters. The remaining bubble equations are then:

$$(N-2-q_i)\,\mu_i + \frac{\alpha_i}{|\vec{r}_N - \vec{r}_i|} - \frac{\beta_i}{|\vec{r}_{(N-1)} - \vec{r}_i|} \;=\; \sum_{I=1}^{3}\left((N-2-q_i)\,k^I + \frac{d^I}{2}\right), \tag{237}$$

for $i = 1, \ldots, N-2$. Once again we use the multipole expansion in these equations:

$$(N-2-q_i)\,\mu_i \;+\; \frac{(\alpha_i - \beta_i)}{r_0} \;-\; \frac{\alpha_i\,\Delta}{r_0^2} \;=\; \sum_{I=1}^{3}\left((N-2-q_i)\,k^I + \frac{d^I}{2}\right), \tag{238}$$

It is elementary to show that:

$$\alpha_i - \beta_i \;=\; \tfrac{1}{8}\,(j_L - d^I\,\widehat{Q}_I) \;+\; \gamma \;-\; \tfrac{1}{8}\,(N-2-q_i)\,C_{IJK}\,d^I\,k^J\,X^K\,, \tag{239}$$

where X^I is defined in (223). If one now uses this identity, along with (228) and (231) in (238) one obtains:

$$\begin{aligned} (N-2-q_i)\,\mu_i \quad &- \quad \frac{1}{r_0}\,C_{IJK}\left[\tfrac{1}{8}\,(N-2-q_i)\,d^I\,k^J\,X^K \;-\; \left(1-\frac{\alpha_i}{\alpha_0}\right)\gamma\right] \\ &\approx \quad (N-2-q_i)\sum_{I=1}^{3} k^I\,. \end{aligned} \tag{240}$$

Finally, note that:

$$\alpha_0 - \alpha_i \;=\; Q\,(N-2-q_i)\,C_{IJK}\,[\tfrac{1}{32}(X^I - \tfrac{1}{Q}d^I)\,(X^J - \tfrac{1}{Q}d^J)\,k^K \;+\; \tfrac{1}{6}\,k^I\,k^J\,k^K]\,, \tag{241}$$

and so the bubble equations (237) reduce to:

$$\begin{aligned}
\mu_i \;&\approx\; \Big(\sum_{I=1}^{3} k^I\Big) \;+\; \frac{1}{r_0}\, C_{IJK}\, \Big[\tfrac{1}{8}\, d^I\, k^J\, X^K \\
&\qquad -\; \alpha_0^{-1}\, Q\, \gamma\, (\tfrac{1}{32}\, (X^I - \tfrac{1}{Q} d^I)\, (X^J - \tfrac{1}{Q} d^J)\, k^K \;+\; \tfrac{1}{6}\, k^I\, k^J\, k^K)\Big] \\
&\approx\; \Big(\sum_{I=1}^{3} k^I\Big) \;+\; \frac{1}{r_0}\, C_{IJK}\, \Big[\tfrac{1}{8}\, d^I\, k^J\, X^K \qquad (242) \\
&\qquad\qquad -\; \alpha_0^{-1}\, Q\, \gamma\, (\tfrac{1}{32}\, X^I\, X^J\, k^K + \tfrac{1}{6}\, k^I\, k^J\, k^K)\Big]\,, \qquad (243)
\end{aligned}$$

since we are assuming X^I is large compared to $Q^{-1} d^I$.

Observe that the right-hand side of (242) is independent of i, which means that the first $(N-2)$ GH points satisfy a scaled version of the equations (236) for a isolated, bubbled black hole. Indeed, if $\vec{r}_i^{\,BH}$ are the positions of a set of GH points satisfying (236) then we can solve (242) by scaling the black hole solution, $\vec{r}_i = \lambda^{-1} \vec{r}_i^{\,BH}$, where the scale factor is given by:

$$\begin{aligned}
\lambda \;&\approx\; 1 \;+\; \frac{1}{r_0}\, \Big(\sum_{I=1}^{3} k^I\Big)^{-1}\, C_{IJK}\, \Big[\tfrac{1}{8}\, d^I\, k^J\, X^K \\
&\qquad -\; \alpha_0^{-1}\, Q\, \gamma\, (\tfrac{1}{32}\, X^I\, X^J\, k^K \;+\; \tfrac{1}{6}\, k^I\, k^J\, k^K)\Big]\,. \qquad (244)
\end{aligned}$$

Notice that as one approaches the critical "merger" value, at which $\Omega = j_L - d^I\, \widehat{Q}_I = 0$, (244) implies that the distance, r_0, must also scale as λ^{-1}. Therefore the merger process will typically involve sending $r_0 \to 0$ while respecting the assumptions made in our approximations $(\Delta, r_i \ll r_0)$. The result will be a "scaling solution" in which all distances in the GH base are vanishing while preserving their relative sizes.

In [42] this picture of the generic merger process was verified by making quite a number of numerical computations[34]; we urge the curious reader to refer to that paper for more details. In Section 9.4 we will only present one very simple scaling solution, which illustrates the physics of these mergers.

An important exception to the foregoing analysis arises when the term proportional to r_0^{-1} in (242) vanishes to leading order. In particular, this happens if we violate one of the assumptions of our analysis, namely, if one has:

$$X^I \;\equiv\; 2\, f^I - d^I - 4\, (N-2)\, k^I \;\approx\; 0\,, \qquad (245)$$

[34] A merger was tracked through a range where the scale factor, λ, varied from about 4 to well over 600. It was also verified that this scaling behavior is not an artefact of axial symmetry. Moreover, in several numerical simulations the GH points of the black-hole blob were arranged along a symmetry axis but the bubbled ring approached the black-hole blob at various angles to this axis; the scaling behavior was essentially unmodified by varying the angle of approach.

to leading order order in $Q^{-1}d^I$. If X^I vanishes one can see that, to leading order, the merger condition is satisfied:

$$\begin{aligned}\Omega &\equiv j_L - d^I\,\widehat{Q}_I \\ &= \tfrac{1}{8}\,C_{IJK}\,d^I\,[X^J X^K - \tfrac{1}{3}\,Q^{-2}\,(4\,Q-1)\,d^J d^K - 16\,k^J k^K] \\ &\approx 0\,,\end{aligned} \tag{246}$$

and so one must have $r_0 \to 0$. However, the foregoing analysis is no longer valid, and so the merger will not necessarily result in a scaling solution.

An important example of this occurs when k^I, d^I and f^I are all parallel:

$$k^I \;=\; k\,u^I\,, \qquad d^I \;=\; d\,u^I\,, \qquad f^I \;=\; f\,u^I\,, \tag{247}$$

for some fixed u^I. Then the merger condition (246) is satisfied to leading order, only when $X \equiv (2\,f - d - 4\,(N-2)\,k)$ vanishes.

For non-parallel fluxes it is possible to satisfy the merger condition, (246), while keeping X^I large, and the result is a scaling solution.

Even if it looks like irreversible mergers progress until the final size on the base vanishes, this is an artifact of working in a classical limit an ignoring the quantization of the fluxes. After taking this into account we can see from (242) that r_0 cannot be taken continuously to zero because the d^I, f^I, X^I and k^I are integers of half-integers. Hence, the final result of an irreversible merger is a microstate of a high, but finite, redshift and whose throat only becomes infinite in the classical limit.

In order to find the maximum depth of the throat, one has to find the smallest allowed value for the size of the ensemble of GH points in the $\mathbb{R}^3$ base of the GH space. During the irreversible merger all the distances scale, the size of the ensemble of points will be approximately equal to the distance between the ring blob and the black hole blob, which is given by (231). Since $j_L - d^I\widehat{Q}_I$ is quantized, the minimal size of the ensemble of GH points is given by:

$$r|_{\min} \approx \frac{1}{d^1 + d^2 + d^3}\,. \tag{248}$$

More generally, in the scaling limit, the GH size of a solution with left-moving angular momentum J_L is

$$r|_{\min} \approx \frac{J_L}{d^1 + d^2 + d^3}\,. \tag{249}$$

Since the d^I scale like the square-roots of the ring charges, we can see that in the classical limit, $r|_{\min}$ becomes zero and the throat becomes infinite.

9.4 Numerical results for a simple merger

Given that most of the numerical investigations and most of the derivations we have discussed above use black hole microstate made from a very large number of points, it is quite hard to illustrate explicitly the details of a microstate merger.

To do this, it is much more pedagogical to investigate a black hole microstate that is made from three points, of GH charges $-n$, $2n+1$, and $-n$, and its merger with the black ring microstate of GH charges $-Q$ and $+Q$. This black-hole microstate can be obtained by redistributing the position of the GH points inside the black-hole blob considered in Section 9.3, putting all the $+1$ charges together and putting half of the -1 charges together on one side of the positive center and the other half on the other side[35]

We consider a configuration with 5 GH centers of charges

$$q_1 = -12,\ q_2 = 25,\ q_3 = -12,\ q_4 = -20,\ q_5 = 20\ . \tag{250}$$

The first three points give the black-hole "blob," which can be thought as coming from a blob of $N-2=49$ points upon redistributing the GH points as described above; the k^I parameters of the black hole points are

$$k^I_1 = q_1\hat{k}^I_0,\ k^I_2 = q_2\hat{k}^I_0,\ k^I_3 = q_3\hat{k}^I_0\ , \tag{251}$$

where $\hat{k}^I_0$ is the average of the k^I over the black-hole points, defined in (194). To merge the ring and the black hole microstates we have varied $\hat{k}^2_0$ keeping $\hat{k}^1_0$ and $\hat{k}^3_0$ fixed:

$$\hat{k}^1_0 = \frac{5}{2},\ \hat{k}^3_0 = \frac{1}{3}, \tag{252}$$

We have also kept fixed the ring parameters f^I and d^I:

$$d^1 = 100,\ d^2 = 130,\ d^3 = 80,\ f^1 = f^2 = 160,\ f^3 = 350 \tag{253}$$

The relation between these parameters and the k^I of the ring is given in (196), where $N-2$ (the sum of $|q_i|$ for the black hole points) is now $|q_1|+|q_2|+|q_3| = 49$.

[35]Since the k parameters on the black-hole points are the same, the bubble equations give no obstruction to moving black-hole centers of the same GH charge on top of each other.

	$\hat{k}_0^2$	$x_4 - x_3$	$\frac{x_4 - x_3}{x_2 - x_1}$	$\frac{x_2 - x_1}{x_3 - x_2}$	$\frac{x_2 - x_1}{x_5 - x_4}$	J_L	$\mathcal{H}$
0	3.0833	175.5	2225	1.001	2.987	215983	.275
1	3.1667	23.8	2069	1.001	3.215	29316	.278
2	3.175	8.65	2054	1.001	3.239	10650	.279
3	3.1775	4.10	2049	1.001	3.246	5050	.279
4	3.178	3.19	2048	1.001	3.248	3930	.279
5	3.17833	2.59	2048	1.001	3.249	3183	.279
6	3.17867	1.98	2047	1.001	3.250	2437	.279
7	3.1795	.463	2046	1.001	3.252	570	.279
8	3.17967	.160	2045	1.001	3.253	197	.279

Table 2: Distances between points in the scaling regime. The parameter $\mathcal{H} \equiv \frac{Q_1Q_2Q_3 - J_R^2/4}{Q_1Q_2Q_3}$ *measures how far away the angular momentum of the resulting solution is from the angular momentum of the maximally-spinning black hole with identical charges. The value of* $\hat{k}_0^2$ *is varied to produce the merger, and the other parameters of the configuration are kept fixed:* $Q = 20,\ q_1 = q_3 = -12,\ q_2 = 25,\ \hat{k}_0^1 = \frac{5}{2},\ \hat{k}_0^3 = \frac{1}{3},\ d^1 = 100,\ d^2 = 130,\ d^3 = 80,\ f^1 = f^2 = 160,\ f^3 = 350$. *Both the charges and* J_R *remain approximately constant, with* $J_R \approx 3.53 \times 10^7$

The charges and J_R angular momentum of the solutions are approximately

$$Q_1 \approx 68.4 \times 10^3,\ Q_2 \approx 55.8 \times 10^3,\ Q_3 \approx 112.8 \times 10^3,\ J_R \approx 3.53 \times 10^7, \tag{254}$$

while J_L goes to zero as the solution becomes deeper and deeper.

Solving the bubble equations (143) numerically, one obtains the positions x_i of the five points as a function of $\hat{k}_0^2$. As we can see from the table above, a very small increase in the value of $\hat{k}_0^2$ causes a huge change in the positions of the points on the base. If we were merging real black holes and real black rings, this increase would correspond to the black hole and the black ring merging. For the microstates, this results in the scaling described above: all the distances on the base become smaller, but their ratios remain fixed.

Checking analytically that these solutions have no closed timelike curves is not that straightforward, since the quantities in (141) have several hundred terms. However, in [42] it was found numerically that such closed timelike curves are absent, and that the equations (141) are satisfied throughout the scaling solution.

9.5 The metric structure of the deep microstates

The physical metric is given by (30) and (31) and the physical distances are related to the coordinate distances on the the $\mathbb{R}^3$ base of the GH space, $d\vec{y} \cdot d\vec{y}$ via:

$$ds^2 \ = \ (Z_1 Z_2 Z_3)^{1/3}\, V\, d\vec{y} \cdot d\vec{y}\,. \tag{255}$$

The physical lengths are thus determined by the functions, $Z_I V$, and if one has:

$$(Z_1 Z_2 Z_3)^{1/3} V \;\sim\; \frac{1}{r^2}\,, \tag{256}$$

then the solution looks is an $AdS_2 \times S^3$ black hole throat. In the region where the constants in the harmonic functions become important, this throat turns into an asymptotically flat $\mathbb{R}^{(4,1)}$ region. Near the GH centers that give the black-hole bubbles, the function $Z_1 Z_2 Z_3$ becomes constant. This corresponds to the black-hole throat "capping off". As the GH points get closer in the base, the region where (256) is valid becomes larger, and hence the throat becomes longer.

As one may intuitively expect, in a scaling solution the ring is always in the throat of the black hole. Indeed, the term "1" on the right hand side of (244) originates from the constant terms in L_I and M, defined in (130). In the scaling regime this term is sub-leading, which implies the ring is in a region where the 1 in the L_I (and hence the Z_I) is also sub-leading. Hence, the ring lies in the AdS throat of the black-hole blob.

Increasing the scale factor, λ, in (244) means that the bubbles localize in a smaller and smaller region of the GH base, which means that the throat is getting longer and longer. The physical circumference of the throat is fixed by the charges and the angular momentum, and remains finite even though the blob is shrinking on the GH base. Throughout the scaling the throat becomes deeper and deeper; the ring remains in the throat, and also descends deeper and deeper into it, in direct proportion to the overall depth of the throat.

On a more mechanistic level, the physical distance through the blob and the physical distance from the blob to the ring are controlled by integrals of the form:

$$\int (Z_1 Z_2 Z_3\, V^3)^{1/6}\, d\ell\,. \tag{257}$$

In the throat the behavior of this function is given by (256) and this integral is logarithmically divergent as $r \to 0$. However, the Z_I limit to finite values at $\vec{r} = \vec{r}_j$ and between two very close, neighboring GH points in the blob, the integral has a dominant contribution of the form

$$C_0 \int |(x - x_i)(x - x_j)|^{-1/2}\, dx\,, \tag{258}$$

for some constant, C_0, determined by the flux parameters. This integral is finite and indeed is equal to $C_0\,\pi$. Thus we see that the throat gets very long but then caps off with bubbles of finite physical size.

9.6 Are deep microstates dual to typical boundary microstates?

As we have seen in Section 9.5, the throats of the deep microstates become infinite in the classical limit. Nevertheless, taking into account flux quantization one can find that

the GH radius of microstates does not go all the way to zero, but to a finite value (248), which corresponds to setting $J_L = 1$.

One can estimate the energy gap of the solution by considering the lightest possible state at the bottom of the throat, and estimating its energy as seen from infinity. The lightest massive particle one can put on the bottom of the throat is not a Planck-mass object, but a Kaluza-Klein mode on the S^3. Its mass is

$$m_{KK} = \frac{1}{R_{S^3}} = \frac{1}{(Q_1 Q_2 Q_3)^{\frac{1}{6}}} \tag{259}$$

and therefore the mass gap in a microstate of size $r_{\min}$ in the GH base is:

$$\Delta E_{r_0} = m_{KK}\sqrt{g_{00}}|_{r=r_{\min}} = m_{KK}(Z_1 Z_2 Z_3)^{-1/3}|_{r=r_{\min}} = \frac{r_{\min}}{(Q_1 Q_5 Q_P)^{1/2}}. \tag{260}$$

For a ring-hole merger, $r_{\min}$ depends on the sum of the d^I, and so its relation with the total charges of the system is not straightforward. Nevertheless, we can consider a regime where $Q_1 \sim Q_5 > Q_P$, and in this regime the dipole charge that dominates the sum in (249) is $d^3 \approx \sqrt{\frac{Q_1 Q_5}{Q_P}}$. Hence

$$r_{\min} = \frac{J_L}{d^3} \approx J_L \sqrt{\frac{Q_P}{Q_1 Q_5}}\ , \tag{261}$$

Hence, the mass gap for a KK mode sitting on the bottom of the throat at $r \sim r_{\min}$ is

$$\Delta E_{r_{\min}} \approx \frac{J_L}{Q_1 Q_5}\ . \tag{262}$$

This M-theory frame calculation is done in the limit $Q_1 \sim Q_5 > Q_P$, which is the limit in which the solution, when put into the D1-D5-P duality frame, becomes asymptotically $AdS_3 \times S^3 \times T^4$. As shown in [45], in this limit $d^1 + d^2 + d^3 \approx d^3$, which justifies going from (249) to (261).

For $J_L = 1$, the mass gap computed in the bulk (262) matches the charge dependence of the mass gap of the black hole [98]. Moreover, this mass gap should also match the mass gap of the dual microstate in the D1-D5 CFT.

As it is well known (see [28, 29] for reviews) the states of this CFT can be characterized by various ways of breaking a long effective string of length $N_1 N_5$ into component strings. BPS momentum modes on these component strings carry J_R. The fermion zero modes of each component string allow it in addition to carry one unit of J_L. The typical CFT microstates that contribute to the entropy of the three-charge black hole have one component string [58]; microstates dual to objects that have a macroscopically large J_L have the effective string broken into many component strings [5, 7, 45].

Hence, the only way a system can have a large J_L is to be have many component strings. The CFT mass gap corresponds to exciting the longest component string, and is proportional to the inverse of its length.

The formula (262) immediately suggests what the dual of a deep microstate should be. Consider a long effective string of length N_1N_5 broken into J_L component strings of equal length. Each component string can carry one unit of left-moving angular momentum, totaling up to J_L. The length of each component string is

$$l_{\text{component}} = \frac{N_1N_5}{J_L} \ , \tag{263}$$

and hence the CFT mass gap is

$$\Delta E_{CFT} \approx \frac{J_L}{N_1N_5} \ . \tag{264}$$

This agrees with *both* the J_L dependence and the dependence on the charges of the gap computed in the bulk. While we have been cavalier about various numerical factors of order one, the agreement that we have found suggests that deep microstates of angular momentum J_L are dual to CFT states with J_L component strings. If this is true, then the deepest microstates, which have $J_L = 1$, correspond to states that have only one component string, of length N_1N_5. This is a feature that typical microstates of the three-charge black hole have, and the fact that deep microstates share this feature is quite remarkable.

Our analysis here has been rather heuristic. It would be very interesting to examine this issue in greater depth by finding, at least approximate solutions to the wave equation in these backgrounds, and performing an analysis along the lines of [5, 7].

10 Black Ring Microstates and Abysses

As we have seen in the previous sections, one of the key steps in understanding three-charge microstate geometries was the realization that they are bubbling geometries, which come from the geometric transition of three-charge brane configurations. Such a transition replaces the spatial $\mathbb{R}^4$ that is used to construct the black-hole and black-ring solutions by a topologically non-trivial hyper-Kähler manifold. The singular sources that define the original black holes or black rings are replaced by smooth topological fluxes threading non-trivial cycles.

For reasons of computational simplicity, the metrics on the hyper-Kähler base were usually chosen to be Gibbons-Hawking (GH) metrics and microstate solutions constructed using these metrics have been analyzed extensively. In particular, the asymptotic charges and angular momenta were computed and it was found in Section 8 that generic distributions of fluxes lead to microstate geometries whose charges correspond to maximally-

spinning classical black holes or black rings of zero horizon area. We typically refer to such microstates geometries as "zero-entropy microstate geometries[36]."

It is not known generically how to evade the restriction to zero-entropy microstates without introducing closed time-like curves (CTC's). At present the only systematic way of doing this is to use mergers of zero-entropy microstates to obtain microstates of objects with non-zero entropy. This technique was used in the previous section to construct the first microstate solutions that have the same charges and angular momenta as a three-charge black hole of classically large horizon area, that is, a "true" black hole from the perspective of classical general relativity.

The purpose of this section is to also use both mergers of two zero-entropy black-ring microstates, as well as other methods, to obtain the first microstates of black rings with a classical horizon area. Note that because of the infinite non-uniqueness of BPS black rings, a solution with black ring charges and angular momenta is not necessarily a black ring microstate. A microstate has (by definition) *all* the macroscopic features of the object it describes, and for black ring this includes not only the charges and angular momenta, but also the dipole charges.

One of the interesting, and probably defining features of the microstates geometries of true black holes is that they are scaling solutions or "deep microstates." That is, the "bubbles," or non-trivial topological cycles scale into a vanishingly small region in the GH base metric (while preserving the relative sizes of the cycles). In the physical, space-time geometry this corresponds to the cycles descending deeply into a black-hole-like throat. Thus the bubbled black-hole geometries look like a regular black hole, except that their throat is capped off by regular geometry deep down the throat. In the pervious section it was shown that, at least for $U(1) \times U(1)$ invariant geometries, the depth at which the capping-off occurs is set by the size of the smallest quantum of flux that one can place upon a single bubble. Moreover, it was shown that small, non-BPS fluctuations in the region of the cap have an energy (as measured from infinity) that matches the expected mass gap of typical states in the underlying D1-D5 conformal field theory (CFT). Thus these "deep microstates" should be interpreted as the holographic duals the long effective strings of the D1-D5 CFT.

Our purpose here is to study deep microstate geometries in more detail, focussing first on the mergers of bubbled supertube geometries that lead to microstate geometries of BPS black rings with a classically large horizon area (that is, "true" black rings). After reviewing some basic properties of bubbled geometries in Subsection 10.1, we begin in Subsection 10.2 by considering microstate geometries corresponding to a pair of supertubes and study the axially symmetric ($U(1) \times U(1)$ invariant) mergers that lead to microstate geometries of "true" black rings. In Subsection10.3 we compute the physical parameters

[36]One should, of course, remember that a microstate geometry is horizonless and smooth and necessarily has zero entropy. The phrase "zero-entropy microstate geometries" is meant to emphasize the fact that the corresponding classical black object with the same charges and angular momenta also has vanishing entropy.

of the black ring microstate solutions that result after the merger of two microstates. In Subsections 10.4 and 10.5 we find that te axially symmetric mergers results in scaling, or deep, geometries where the non-trivial cycles descend deeply into the AdS throat of what looks like a classical black ring. The non-trivial topology, once again, smoothly caps off this throat at a depth that is set by the quantum of flux on an individual cycle. We thus obtain the analogs for black rings of the results [42] that were found for black holes and are discussed in Section 9.

The reader who is not keen on the technical details of the construction, and only interested in the physics of smooth microstate solutions of *arbitrary* depth can skip directly to Subsection 10.6, where we construct the first such example by considering a scaling solution that is no longer axi-symmetric. This solution has the surprising feature that the depth of the throat can be controlled by a modulus and can be made arbitrarily large by fine-tuning this modulus [37] During this process the solution remains *completely smooth*. We will refer to such throats of arbitrary depth as *abysses*. The existence of abysses suggests that breaking the $U(1) \times U(1)$ invariance allows the construction of smooth horizonless geometries whose holographic duals in the CFT exhibit mass gaps and spectra with energy gaps that are arbitrarily small.

Before beginning, it is interesting to discuss the relation between the horizonless three-charge scaling configuration with black ring charges constructed in [119] and the solutions we construct here. From a four-dimensional perspective this configuration contains D6 and $\overline{\text{D6}}$ branes, like the solutions we consider here, but also contains D0 and D2 branes. These configurations (as well as those of [118]) are useful for understanding and counting black hole microstates in the intermediate regime of parameters where the D4 branes affect the geometry and the D0's are considered as probes. However, their fate in the regime of parameters where black holes and black rings have macroscopic horizons is unclear. Their naive M-theory lift has naked singularities corresponding to the D0 branes, and the full back-reacted lift is not known[38]. The solutions with only D6 and $\overline{\text{D6}}$ branes remain smooth in five dimensions, and hence give a valid description of microstates of black holes and black rings in the same region of the moduli space where the classical black holes and black rings also exist.

10.1 Bubbled Geometries

Before focussing on bubbled ring geometries, it is worthwhile reviewing some of the basics of bubbled geometries that we discussed in Subsection 7.2. First recall that the four-

[37]The solution we study is a five-dimensional, smooth solution that, from a four-dimensional perspective, corresponds to a "closed quiver" of D6 and anti-D6 branes [80].

[38]It is likely that because of the presence of D2 branes this lift will be more complicated than the solutions we consider in this section.

dimensional base metric has Gibbons-Hawking (GH) form:

$$ds_4^2 \;=\; V^{-1}\,(d\psi + \vec{A}\cdot d\vec{y})^2 \;+\; V\,(d\vec{y}\cdot d\vec{y})\,, \tag{265}$$

where $\vec{y}\in\mathbb{R}^3$ and

$$V \;=\; \sum_{j=1}^{N}\frac{q_j}{r_j}\,, \qquad \vec{\nabla}\times\vec{A} \;=\; \vec{\nabla}V\,, \tag{266}$$

with $r_j \equiv |\vec{y}-\vec{y}^{(j)}|$. In order for the GH metric to be regular, one must take $q_j\in\mathbb{Z}$ and for the metric to be asymptotic to that of flat $\mathbb{R}^4$ one must also impose

$$q_0 \;\equiv\; \sum_{j=1}^{N} q_j \;=\; 1\,. \tag{267}$$

The fluxes through the non-trivial two-cycles in this geometry are determined by harmonic functions:

$$K^I \;\equiv\; \sum_{j=1}^{N}\frac{k_j^I}{r_j}\,, \tag{268}$$

and by the flux parameters, k_j^I, in particular. There is a gauge equivalence $K^I \to K^I + c^I V$, or $k_j^I \to k_j^I + c^I q_j$ for any constant, c^I. It is therefore useful to define the gauge invariant flux parameters:

$$\tilde{k}_j^I \;\equiv\; k_j^I \;-\; q_j\,N\,k_0^I\,, \qquad \text{with} \qquad k_0^I \;\equiv\; \frac{1}{N}\sum_{j=1}^{N} k_j^I\,. \tag{269}$$

As explained in Section 7, the charges and angular momenta of a bubbled solution are can be obtained from the positions, $\vec{y}^{(j)}$, of the GH points via [40, 37, 42]:

$$Q_I \;=\; -\,2\,C_{IJK}\sum_{j=1}^{N} q_j^{-1}\,\tilde{k}_j^J\,\tilde{k}_j^K\,, \tag{270}$$

$$J_R \;\equiv\; J_1 + J_2 \;=\; \tfrac{4}{3}\,C_{IJK}\sum_{j=1}^{N} q_j^{-2}\,\tilde{k}_j^I\,\tilde{k}_j^J\,\tilde{k}_j^K\,, \tag{271}$$

$$J_L \;\equiv\; J_1 - J_2 \;=\; 8\,|\vec{D}|\,, \tag{272}$$

where N is the number of GH points and

$$\vec{D}_j \;\equiv\; \sum_I \tilde{k}_j^I\,\vec{y}^{(j)}\,, \qquad \vec{D} \;\equiv\; \sum_{j=1}^{N}\vec{D}_j\,. \tag{273}$$

It is convenient to define:

$$P_{ij} \;\equiv\; \tfrac{1}{6}\,C_{IJK}\,\Pi_{ij}^{(I)}\,\Pi_{ij}^{(J)}\,\Pi_{ij}^{(K)} \tag{274}$$

and

$$\vec{J}_{L\,ij} \;\equiv\; -\,8\,q_i\,q_j\,P_{ij}\,\hat{y}_{ij}\,, \qquad \text{where} \qquad \hat{y}_{ij} \;\equiv\; \frac{(\vec{y}^{(i)}-\vec{y}^{(j)})}{|\vec{y}^{(i)}-\vec{y}^{(j)}|}\,. \tag{275}$$

One then has [37]:

$$\vec{J}_L \;=\; \sum_{\substack{i,j=1\\ j\neq i}}^{N} \vec{J}_{L\,ij}\,, \tag{276}$$

and if the GH points are all co-linear then we may take $\hat{y}_{ij} = \pm 1$ and 276 reduces to a sum over $\pm P_{ij}$.

Finally, to eliminate CTC's near the GH points, this configuration must satisfy the bubble equations (143) obtained in section 7.3:

$$\sum_{\substack{j=1\\ j\neq i}}^{N} q_i\,q_j\,\frac{P_{ij}}{r_{ij}} \;=\; -\sum_{I=1}^{3}\tilde{k}_i^I\,, \tag{277}$$

where $r_{ij} = |\vec{y}^{(i)} - \vec{y}^{(j)}|$

In this section, we specifically wish to consider the situation where the bubbled geometry looks, at large scales, like a supertube or black ring. We therefore wish to take $q_1 = +1$ and locate this GH point at $\vec{y}^{(1)} = 0$ and will then assume that all the remaining GH points cluster a some distance, ρ from the origin. More specifically, we will typically assume that

$$r_{1j} \;\approx\; \rho\,, \qquad r_{ij} \;\ll\; \rho\,, \qquad i,j = 2,\ldots,N\,. \tag{278}$$

In this limit, the first bubble equation yields the approximate ring radius:

$$\rho \;\approx\; -\Big[\sum_{I=1}^{3}\tilde{k}_1^I\Big]^{-1}\sum_{j=2}^{N} q_j\,P_{1j}\,. \tag{279}$$

10.2 The axi-symmetric merger of two bubbled supertubes

10.2.1 The layout and physical parameters

We consider the simplest possible pair of bubbled rings in which each ring is bubbled by identical pairs of GH points of charges, $-Q$ and $+Q$. Thus the configuration will have:

$$q_1 \;=\; +1\,, \qquad q_2 \;=\; -\,Q\,, \qquad q_3 \;=\; +\,Q\,, \qquad q_4 \;=\; -\,Q\,, \qquad q_5 \;=\; +\,Q\,, \tag{280}$$

and we will denote the various distances by

$$\rho \;\equiv\; r_{12}\,, \qquad \sigma \;\equiv\; r_{34}\,, \qquad \Delta_1 \;\equiv\; r_{23}\,, \qquad \Delta_2 \;\equiv\; r_{45}\,. \tag{281}$$

This layout is depicted in Fig. 10. The Δ_j will represent the bubbled ring widths, and in the classical limit, $Q \to \infty$, one has $\Delta_j \to 0$. In this limit, ρ and $\rho + \sigma$ represent the

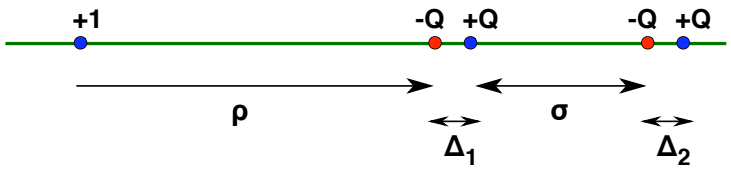

Figure 10: The layout of GH points for two bubbled supertubes.

classical supertube radii. The classical un-bubbled solution to which this bubbled solution corresponds was first constructed in [64, 85].

As usual we denote the flux parameters by

$$\Pi^{(I)}_{ij} \;=\; \Big(\frac{k^I_j}{q_j} \;-\; \frac{k^I_i}{q_i}\Big)\,, \tag{282}$$

but there is a more natural, gauge invariant basis of flux parameters given by:

$$\begin{aligned} d^I_1 \;&\equiv\; 2\,(k^I_2 \;+\; k^I_3)\,, \qquad f^I_1 \;\equiv\; 2\,k^I_1 \;+\; (1+\tfrac{1}{Q})\,k^I_2 \;+\; (1-\tfrac{1}{Q})\,k^I_3\,,\\ d^I_2 \;&\equiv\; 2\,(k^I_4 \;+\; k^I_5)\,, \qquad f^I_2 \;\equiv\; 2\,k^I_1 \;+\; (1+\tfrac{1}{Q})\,k^I_4 \;+\; (1-\tfrac{1}{Q})\,k^I_5\,. \end{aligned} \tag{283}$$

In the classical supertube limit, where $\Delta_j \to 0$, the d^I reduce to the number, n^I, of M5 branes around the ring profile. In the GH metric these supertubes are point-like in the $\mathbb{R}^3$ base and run around the $U(1)$ fiber. The parameters, f^I_1 and f^I_2, are a little more physically ambiguous but we have chosen them to be the gauge-invariant combinations of flux parameters that are made out of the flux parameters associated to the two separate rings.

It is also easy to see how to define the d^I_a more generally in terms of the cohomology. Recall that the homology cycle, Δ_{ij}, can be defined by the $U(1)$ fiber running along any curve between q_i and q_j. The fluxes through Δ_{23} and Δ_{45} are simply $\frac{Q}{2}d^I_1$ and $\frac{Q}{2}d^I_2$ respectively. We also claim that Δ_{23} and Δ_{45} are homologous to the Gaussian surfaces that measure the M5-brane fluxes in the classical, supertube limit. To see this, first recall that for the GH points aligned along the z-axis we may take:

$$\vec{A}\cdot d\vec{y} \;=\; \sum_{j=1}^{5} q_j \frac{(z-z_j)}{r_j}\,d\phi\,. \tag{284}$$

where ϕ is the angle in the (x,y) plane. In particular, if $V = \frac{1}{r}$ and θ denotes the polar angle away from the z-axis then the GH metric reduces to that of $\mathbb{R}^4 = \mathbb{R}^2\times\mathbb{R}^2$:

$$ds^2_4 \;=\; (du^2 \;+\; u^2\,d\theta_1^2) \;+\; (dv^2 \;+\; v^2\,d\theta_2^2)\,, \tag{285}$$

via the coordinate transformation:

$$u \;=\; \tfrac{1}{4}\, r^2\, \cos\tfrac{\theta}{2}\,, \qquad \theta_1 \;=\; \tfrac{1}{2}\,(\psi+\phi)\,, \tag{286}$$

$$v \;=\; \tfrac{1}{4}\, r^2\, \sin\tfrac{\theta}{2}\,, \qquad \theta_2 \;=\; \tfrac{1}{2}\,(\psi-\phi)\,. \tag{287}$$

Now observe that if one moves along the z-axis then the $U(1)$ fiber direction, $(d\psi + A)$, is equal to $2\,d\theta_1 = d\psi + d\phi$ in the "long intervals" from q_1 to q_2, from q_3 to q_4 and from q_5 to infinity. In the supertube limit, the $U(1)$ fiber, and hence the supertube, lies in the (u, θ_1) plane. The Gaussian surfaces used to define M5-brane charge can be chosen to so that θ_1 is fixed and θ_2 is varying. This means they cannot involve Δ_{12} and Δ_{34}, which necessarily involve the fiber direction with co-tangent, $(d\psi + A) \sim d\theta_1$, and so the M5-brane Gaussian surfaces can only be related to Δ_{23} and Δ_{45}.

The charges and angular momenta of individual black rings are given by:

$$Q_I^{(a)} \;=\; C_{IJK}\, d_a^J\, f_a^K\,, \tag{288}$$

$$j_R^{(a)} \;\equiv\; \tfrac{1}{2}\, C_{IJK}\,(f_a^I f_a^J d_a^K \;+\; f_a^I d_a^J d_a^K) \;-\; \tfrac{1}{24}\,(1-Q^{-2})\, C_{IJK}\, d_a^I d_a^J d_a^K\,, \tag{289}$$

$$j_L^{(a)} \;\equiv\; \tfrac{1}{2}\, C_{IJK}\,(d_a^I f_a^J f_a^K \;-\; f_a^I d_a^J d_a^K) \;+\; \Big(\frac{3\,Q^2 - 4\,Q + 1}{24\,Q^2}\Big)\, C_{IJK}\, d_a^I d_a^J d_a^K\,, \tag{290}$$

for $a = 1, 2$.

For the configuration described above and depicted in Fig. 10 we have:

$$Q_I \;=\; Q_I^{(1)} \;+\; Q_I^{(2)} \;+\; C_{IJK}\, d_1^J\, d_2^K\,, \tag{291}$$

$$J_R \;=\; j_R^{(1)} \;+\; j_R^{(2)} \;+\; d_1^I\, Q_I^{(2)} \;+\; d_2^I\, Q_I^{(1)} \;+\; \tfrac{1}{2}\, C_{IJK}\, d_1^I\, d_2^J\,(d_1^K + d_2^K)\,, \tag{292}$$

$$J_L \;=\; j_L^{(1)} \;+\; j_L^{(2)} \;+\; d_1^I\, Q_I^{(2)} \;-\; d_2^I\, Q_I^{(1)} \;+\; \tfrac{1}{2}\, C_{IJK}\, d_1^I\, d_2^J\,(d_1^K - d_2^K)\,, \tag{293}$$

It is useful to introduce the flux vectors

$$Y^I \;\equiv\; (f_2^I - f_1^I - \tfrac{1}{2}\,(d_2^I - d_1^I))\,, \tag{294}$$

and the combination of fluxes:

$$\widehat{P} \;\equiv\; (P_{24} \;-\; P_{25} \;-\; P_{34} \;+\; P_{35}) \;=\; \tfrac{1}{8\,Q^2}\, C_{IJK}\, d_1^I\, d_2^J\, Y^K\,. \tag{295}$$

Note that $\widehat{P}$ measures the total flux running between the pairs of points that define the two rings. The interaction part of the left-handed angular momentum can now be written:

$$\begin{aligned} J_L^{int} \;&\equiv\; d_1^I\, Q_I^{(2)} \;-\; d_2^I\, Q_I^{(1)} \;+\; \tfrac{1}{2}\, C_{IJK}\, d_1^I\, d_2^J\,(d_1^K - d_2^K) \\ &=\; 8\,Q^2\,\widehat{P} \;=\; C_{IJK}\, d_1^I\, d_2^J\, Y^K\,. \end{aligned} \tag{296}$$

From a four-dimensional perspective, the angular momentum J_L^{int} corresponds to the Poynting vector coming from the interaction of the electric fields of one ring with the magnetic fields of the other. We will see in the next sub-section that this controls the merger of the two rings.

10.3 Classical limits and their entropy

For a single, classical black ring, the entropy is given by

$$S \;=\; \pi\sqrt{\mathcal{M}} \tag{297}$$

The function $\mathcal{M}$, given in equation (61), can be rewritten as

$$\begin{aligned}\mathcal{M} \;&=\; 2\,d^1d^2Q_1Q_2 + 2\,d^1d^3Q_1Q_3 + 2\,d^2d^3Q_2Q_3 - (d^1Q_1)^2 - (d^2Q_2)^2 - (d^3Q_3)^2 \qquad (298)\\ &-\; d^1d^2d^3\,[4\,J_L \;+\; 2\,(d^1Q_1 + d^2Q_2 + d^3Q_3) \;-\; 3\,d^1d^2d^3]\,, \qquad (299)\end{aligned}$$

where $J_L > 0$, the d^I are the numbers of M5 branes and the Q_I are the electric charges measured from infinity. One also has the following relation between the angular momentum, J_L, and the classical embedding radius, R, measured in $\mathbb{R}^2$:

$$J_L \;=\; (d^1 + d^2 + d^3)\,R^2\,. \tag{300}$$

If one substitutes the expressions, (145) and (290), for the charges and for the angular momentum of a single, bubbled ring into (298), one obtains a simple expression:

$$\mathcal{M} \;=\; \Big(\frac{4\,Q-1}{Q^2}\Big)\,(d^1d^2d^3)^2\,. \tag{301}$$

Observe that this vanishes as $Q \to \infty$. This is the "classical limit" where the bubbled ring collapses back to the standard, classical ring. Therefore, the classical object corresponding to this simple, bubbled configuration has $\mathcal{M} = 0$ and is thus a supertube.

For a bubbled ring, the relation, (300), emerges from the bubble equations as:

$$J_L \;=\; 4\,(d^1 + d^2 + d^3)\,\rho\,. \tag{302}$$

where ρ is the ring radius measured in the GH base, and the change of variable (286) leads to $\rho = \frac{1}{4}R^2$.

If one merges two bubbled supertubes so as to obtain a single bubbled ring, one has an object with M5 brane charge given by $d^I = d^I_1 + d^I_2$ and with charges and angular momenta given by (291),(292) and (293). To obtain the entropy of the corresponding classical object, one substitutes these expressions into (298) and the result is:

$$\begin{aligned}\mathcal{M} \;&=\; -(\epsilon_{IJK}\,d^I_1d^J_2Y^K)^2 \;-\; 4\Big[(d^1_1 + d^1_2)(d^2_1d^3_1d^1_2 + d^2_2d^3_2d^1_1)\,Y^2\,Y^3\\ &+\; (d^2_1 + d^2_2)(d^1_1d^3_1d^2_2 + d^1_2d^3_2d^2_1)\,Y^1\,Y^3 + (d^3_1 + d^3_2)(d^1_1d^2_1d^3_2 + d^1_2d^2_2d^3_1)\,Y^1\,Y^2\Big]\\ &-\; \tfrac{2}{3}\,(C_{IJK}\,(d^I_1 + d^I_2)(d^J_1 + d^J_2)(d^K_1 + d^K_2))\,(C_{ABC}\,d^A_1d^B_2Y^C)\\ &+\; (\tfrac{4\,Q-1}{36\,Q^2})(C_{IJK}\,(d^I_1 + d^I_2)(d^J_1 + d^J_2)(d^K_2 + d^K_2))(C_{ABC}\,(d^A_1d^B_1d^C_1 + d^A_2d^B_2d^C_2))\,.\end{aligned}$$

Note that if this is generically non-vanishing as $Q \to \infty$. However, if $Y^I = 0$ then it does go to zero as $Q \to \infty$.

Putting it somewhat differently, if $Y^I = 0$ then the merged ring has an effective d^I and f^I given by:

$$d^I \;=\; d_1^I \;+\; d_2^I\,, \qquad f^I \;=\; f_1^I \;+\; \tfrac{1}{2}\,d_2^I \;=\; f_2^I \;+\; \tfrac{1}{2}\,d_1^I\,. \tag{303}$$

The fact that one adds the d_a^I follows from the considerations in Subsection 10.2, and the formula for f^I is obtained from (291) and (288), using $Y^I = 0$. Now observe that for large Q, one has

$$j_L^{(a)} \;\approx\; \tfrac{1}{2}\,C_{IJK}\,d_a^I(f_a^J - \tfrac{1}{2}\,d_a^J)\,(f_a^K - \tfrac{1}{2}\,d_a^K) \;=\; \tfrac{1}{2}\,C_{IJK}\,d_a^I(f^J - \tfrac{1}{2}\,d^J)\,(f^K - \tfrac{1}{2}\,d^K)\,. \tag{304}$$

It then follows that when $Y^I = 0$ the angular momentum, J_L, for the merged ring is given by:

$$J_L \;=\; j_L^{(1)} \;+\; j_L^{(2)} \;+\; C_{IJK}\,d_1^I\,d_2^J\,Y^K \;=\; j_L^{(1)} \;+\; j_L^{(2)} \tag{305}$$

$$\approx\; \tfrac{1}{2}\,C_{IJK}\,d^I(f^J - \tfrac{1}{2}\,d^J)\,(f^K - \tfrac{1}{2}\,d^K)\,, \tag{306}$$

which is the angular momentum, J_L, for a bubbled ring or supertube of charges d^I and Q_I. In other words the merged configuration still has a maximal value of J_L and the corresponding classical object still has vanishing horizon area. If $Y^I \neq 0$ then the final angular momentum will generically be less than this maximal value[39].

10.4 Solving the bubble equations

For the configuration depicted in Fig. 10, there are four independent bubble equations (143). If one adds the equations for $i = 2, 3$ and $i = 4, 5$ then eliminates terms with denominators $r_{23} = \Delta_1$ and $r_{45} = \Delta_2$, one obtains:

$$\begin{aligned} Q\,\Big(\frac{P_{12}}{\rho} - \frac{P_{13}}{\rho+\Delta_1}\Big) \;+\; Q^2\,\Lambda \quad &=\quad -\tfrac{1}{2}\sum_{I=1}^{3} d_1^I \\ Q\,\Big(\frac{P_{14}}{\rho+\sigma+\Delta_1} - \frac{P_{15}}{\rho+\sigma+\Delta_1+\Delta_2}\Big) \;-\; Q^2\,\Lambda \quad &=\quad -\tfrac{1}{2}\sum_{I=1}^{3} d_2^I\,. \end{aligned} \tag{307}$$

where

$$\Lambda \;\equiv\; \frac{P_{24}}{\sigma+\Delta_1} - \frac{P_{34}}{\sigma} - \frac{P_{25}}{\sigma+\Delta_1+\Delta_2} + \frac{P_{35}}{\sigma+\Delta_2}\,. \tag{308}$$

For two bubbled rings with $\Delta_j \ll \rho, \sigma$, assuming that all other terms in the multipole expansion are sub-leading, these equations reduce to:

$$\frac{Q\,(P_{12} - P_{13})}{\rho} \;+\; \frac{Q^2\,\widehat{P}}{\sigma} \quad =\quad -\tfrac{1}{2}\sum_{I=1}^{3} d_1^I$$

[39]This is not obvious from (303) because one must also require the absence of CTC's in the solution. This comment is therefore based primarily on the essential physics of mergers as well as experience with a number of examples.

$$\frac{Q\,(P_{14}-P_{15})}{\rho+\sigma}\;-\;\frac{Q^2\,\widehat{P}}{\sigma}\quad=\quad-\tfrac{1}{2}\sum_{I=1}^{3}d_2^I\,. \tag{309}$$

For two generic bubbled rings to merge one must have $\sigma\to 0$ and so the merger condition is $\widehat{P}\to 0$, but with $\sigma^{-1}\widehat{P}$ remaining finite. Note that this means that the interaction part of the left-handed angular momentum, J_L^{int}, must vanish. More generally, for a solution in which Δ_j and σ get small simultaneously, one must have $\widehat{P}\to 0$, but with Λ remaining finite. Either way, the location, ρ_0, of the merged object is given by:

$$\begin{aligned}\rho_0\quad&=\quad-2\,Q\left[\sum_{I=1}^{3}(d_1^I+d_2^I)\right]^{-1}(P_{12}-P_{13}+P_{14}-P_{15})\\ &=\quad\tfrac{1}{4}\left[\sum_{I=1}^{3}(d_1^I+d_2^I)\right]^{-1}\left(j_L^{(1)}\;+\;j_L^{(2)}\;+\;\tfrac{1}{6\,Q}\,C_{IJK}\,(d_1^Id_1^Jd_1^K+d_2^Id_2^Jd_2^K)\right),\end{aligned} \tag{310}$$

which is equivalent to (302) for the combined object.

Conversely, if one has $\widehat{P}\to 0$ one can obtain the merger solution, and a second solution in which σ remains finite. One then has:

$$\begin{aligned}\rho\quad&=\quad-2\,Q\left[\sum_{I=1}^{3}d_1^I\right]^{-1}(P_{12}-P_{13})\;=\;\tfrac{1}{4}\left[\sum_{I=1}^{3}d_1^I\right]^{-1}\left(j_L^{(1)}\;+\;\tfrac{1}{6\,Q}\,C_{IJK}\,d_1^Id_1^Jd_1^K\right),\\ \rho+\sigma\quad&=\quad-2\,Q\left[\sum_{I=1}^{3}d_2^I\right]^{-1}(P_{14}-P_{15})\;=\;\tfrac{1}{4}\left[\sum_{I=1}^{3}d_2^I\right]^{-1}\left(j_L^{(2)}\;+\;\tfrac{1}{6\,Q}\,C_{IJK}\,d_2^Id_2^Jd_2^K\right),\end{aligned} \tag{311}$$

Note that these are essentially the radii given by (302) for each of the two rings separately. Indeed, the limit $\widehat{P}\to 0$ corresponds to the vanishing of the "interaction part" of J_L.

In the foregoing merger analysis we have assumed that $\Delta_j\ll\rho,\sigma$ and we have dropped terms from the multipole expansions of the denominators in (307). This means that the fluxes through the rings, $\Pi_{23}^{(I)}$ and $\Pi_{45}^{(I)}$, must be much less than the other fluxes, and so $Q^{-1}d_a^I$ must be small compared to f_a^I and d_a^I. Thus we should consistently drop terms that are sub-leading in $Q^{-1}d_a^I$, like the last terms in (310) and (311). Such terms also appear as corrections coming from the multipole expansions [42].

10.5 Scaling solutions

A scaling solution is most simply defined to be a bubble configuration where there is a subset, $\mathcal{S}$, of the GH points that are uniformly approaching one another as some control parameter or, perhaps a modulus, is adjusted to a critical value. That is, one has

$$r_{ij}\;\to\;\lambda\,r_{ij}\,,\qquad i,j\in\mathcal{S}\,, \tag{312}$$

with $\lambda\to 0$. Physically, if the total charge of the GH points in $\mathcal{S}$ is non-zero, this means that these GH points are descending into an arbitrarily deep black-hole-like throat and

that the red-shifts of excitations localized around these points are going to infinity. Such black-hole microstates are called "Deep Microstates." They were discovered in [42] via the study of mergers of black holes and black rings [75], and are reviewed in Section 9. In particular, scaling solutions were shown to be associated to microstates of black holes of non-zero horizon area and it was also argued (using the dual CFT) that these deep microstates belong to the same sector as the *typical* microstates of the black hole.

In this section we examine the corresponding story when the total GH charge in $\mathcal{S}$ is zero. One then expects to obtain scaling solutions corresponding to deep microstates of black rings with non-zero horizon area. This is, indeed what we find.

So far, the study of scaling solutions has largely focussed on $U(1) \times U(1)$ invariant configurations. This is largely because such solutions are intrinsically simpler and, for fixed fluxes, there are finitely many, discrete solutions that are $U(1) \times U(1)$ invariant. Moreover, in scaling solutions with such a symmetry, the depth of the throat is controlled by the choice of the quantized fluxes on bubbles [42], like $\widehat{P}$ in Section 10.2. Thus the size of the flux quanta provides a cut-off for the maximum depth of the throat. However, one can easily break the $U(1) \times U(1)$ symmetry to $U(1)$ by letting the GH points move to arbitrary points, $\vec{r}_i$, in $\mathbb{R}^3$ and then a subset of the angles between the vectors, $\vec{r}_{ij} = \vec{r}_j - \vec{r}_i$, become continuous moduli of the solutions. If the initial fluxes lie in the right domain then one can find scaling solutions at special points, or on special surfaces of the moduli space. Thus, we can make the black-hole, or black-ring throat arbitrarily deep by tuning the moduli. In practice, we find (numerically) that this tuning has to be extremely sharp and that the throat depth varies by many orders of magnitude for tiny (micro-radian) variations of the angles.

10.5.1 Axi-symmetric scaling solutions

Since the $U(1) \times U(1)$ invariant solutions are discrete for given fluxes, we can achieve an axi-symmetric scaling solution only by delicate adjustment of the fluxes. In particular, the easiest way to find such a scaling solution is via the merger of two bubbled supertubes as described in Section 10.2. Specifically, we need $J_L^{int} \to 0$, which means that the fluxes need to be adjusted so that $\widehat{P} \to 0$. To get a deep microstate, the expression for the classical horizon area, (303), shows that we must do this in such a manner that Y^I remains finite and so the merger condition, (296), implies that we must tune the f^I or the d_a^I so that Y^I is finite but orthogonal to $C_{IJK} d_1^J d_2^K$.

It is relatively easy to see that there are scaling solutions that arise through mergers of bubbled supertubes. We consider, once again, the configuration in Fig. 10 where $\Delta_j, \sigma \to 0$. There are four independent bubble equations, (143), to satisfy. (Remember that the sum of the five bubble equations is trivial.) The first equation is precisely the same as the sum of the two equations in (307) and it determines the position, ρ_0, of the merger, as in (310). For the scaled merging of bubbled supertubes we expect that $\Delta_j \ll \sigma$ during the merger and so the three remaining, independent bubble equations have the

form:

$$\begin{aligned}
-\frac{P_{25}}{\sigma+\Delta_1+\Delta_2} - \frac{P_{23}}{\Delta_1} + \frac{P_{24}}{\sigma+\Delta_1} &\approx \frac{(P_{24}-P_{25})}{\sigma} - \frac{P_{23}}{\Delta_1} &&= C_1\,,\\
\frac{P_{23}}{\Delta_1} + \frac{P_{35}}{\sigma+\Delta_2} - \frac{P_{34}}{\sigma} &\approx \frac{(P_{35}-P_{34})}{\sigma} + \frac{P_{23}}{\Delta_1} &&= C_2\,,\\
-\frac{P_{24}}{\sigma+\Delta_1} + \frac{P_{34}}{\sigma} - \frac{P_{45}}{\Delta_2} &\approx \frac{(P_{34}-P_{24})}{\sigma} - \frac{P_{45}}{\Delta_2} &&= C_3\,,
\end{aligned} \tag{313}$$

where the C_j contain terms involving the fluxes, Q and ρ_0. The important point about (313) is that we have explicitly shown the terms that grow large as $\Delta_j, \sigma \to 0$. For the scaling solution we need:

$$\sigma \;=\; \lambda\,\sigma^{(0)}\,, \qquad \Delta_a \;=\; \lambda\,\Delta_a^{(0)}\,, \qquad \lambda \to 0\,. \tag{314}$$

This means that, to leading order as $\lambda \to 0$:

$$\frac{\sigma^{(0)}}{\Delta_1^{(0)}} \;\approx\; \frac{(P_{24}-P_{25})}{P_{23}} \;\approx\; \frac{(P_{34}-P_{35})}{P_{23}}\,, \qquad \frac{\sigma^{(0)}}{\Delta_2^{(0)}} \;\approx\; \frac{(P_{34}-P_{24})}{P_{45}}\,. \tag{315}$$

In particular there is no conflict between the first and second equations in (313) because $\widehat{P} \to 0$. The foregoing solution becomes more and more accurate for smaller values of λ and given this solution one can then easily find the solution for finite, larger values of λ using perturbation theory.

This is not necessarily the only scaling solution with the configuration shown in Fig. 10. Indeed, numerical solutions show that there is often another one in which the Δ_j and σ are of approximately the same order. However in all the examples of this second solution that we have found, there are large regions of CTC's. On the other hand, the scaling solutions that we have found based upon mergers of bubbled supertubes appear to be free of CTC's. We will discuss this more in Subsection 10.6.

10.5.2 Numerical results for axi-symmetric scaling solutions

In order to see the scaling solutions explicitly, and verify that there are no CTC's we constructed several numerical examples and we now discuss a representative case.

It is useful to define:

$$X_a^I \;\equiv\; f_a^I \;-\; \tfrac{1}{2}\,d_a^I\,. \tag{316}$$

We then take $Q = 105$ and:

$$\begin{aligned}
d_1^I &= (\,50\,,\,60\,,\,40\,)\,, \quad X_1^I \;=\; (\,110\,,\,560\,,\,50\,)\,,\\
d_2^I &= (\,80\,,\,50\,,\,45\,)\,, \quad X_2^I \;=\; (\,x\,,\,270\,,\,280\,)\,,
\end{aligned} \tag{317}$$

where x is varied from about 64 up to its merger value of $x \approx 90.3$. The results are shown in Fig. 11. As is evident from the graph, there are three sets of solutions to the bubble

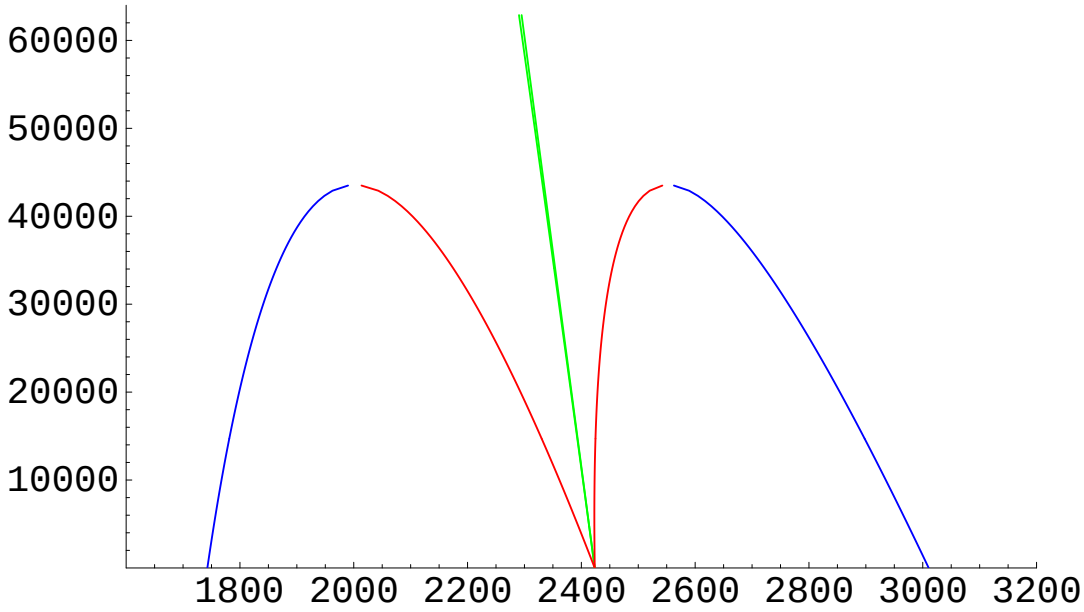

Figure 11: Solutions of the bubble equations for the configuration shown in Fig. 10. The plot shows the ring positions, ρ and σ, along the horizontal axis with $|J_L^{int}|$ plotted on the vertical axis. The separations, Δ_j, are too small to resolve. There are three branches: (i) The single, nearly vertical line in the center (in green) for which all four GH points remain extremely close together; (ii) The two outermost curves (in blue) where the two rings become progressively more widely spaced as $J_L^{int} \to 0$; (iii) The two curves (in red) that meet branch (ii) and show the scaling merger in which the two rings meet at $J_L^{int} = 0$.

equations. Branch (i) exists for all values of J_L^{int} and has all four GH points in a very close cluster that scales as $J_L^{int} \to 0$. This appears as a very steep line at the center of Fig. 11. Branches (ii) and (iii) only appear at a bifurcation point when one has $|J_L^{int}| \approx 43500$ or $x \approx 71.7$, and represent solutions in which the four GH points separate into two sets of very close pairs. On branch (ii) the two pairs move apart as $J_L^{int} \to 0$ and the locations of the two bubbled rings is given by (311). Branch (iii) is the scaling merger solution at ρ_0 given by (310) and is described by (314) and (315).

We have done extensive numerical searches for CTC's in all these solutions and we find that branch (i) is completely unphysical, with large regions of CTCs, but that branches (ii) and (iii) are physical and have no CTC's.

Finally, one can use (298) or (303) to compute the horizon area, $\mathcal{M}$, of a classical black ring with the same charges and angular momenta as the merged configuration. The absolute number does not immediately convey useful information. On the other hand, we can compare this to the "maximal horizon area," $\mathcal{M}_0$, of a black ring with the same

values of Q_I and d^I, but with $J_L = 0$. For the configuration in (317) we find:

$$\mathcal{R} \equiv \frac{\mathcal{M}}{\mathcal{M}_0} \approx 0.14\,, \tag{318}$$

Thus the the result of this merger of two bubbled supertubes is a microstate of a black ring with a non-vanishing horizon area.

We have studied several other such mergers with different values of flux parameters and found a number of solutions that are free of CTC's and have even higher values of $\mathcal{R}$. Indeed, one can arrange a very high value of $\mathcal{R}$ if one takes the outer ring to rotate in the opposite direction to the inner ring. One can achieve this in the foregoing example, (317), by taking, for example,

$$X_2^I = (-300\,,\, 270\,,\, 531.27)\,, \tag{319}$$

while leaving all the other parameters unchanged. This configuration is very close to the merger point and has $\mathcal{R} \approx 0.638$. As one would expect, one generates more entropy by merging states whose angular momenta are opposed to one another.

10.6 Abysses and closed quivers.

Thus far we have primarily focussed on $U(1) \times U(1)$ invariant scaling solutions. It is relatively easy to modify the analysis above to obtain scaling solutions in which the five GH points no longer lie on an axis. It is, however, even simpler to find scaling solutions based upon four GH points, and this is what we will focus on here.

Consider four charges laid out as in Fig. 12 with:

$$q_1 = +1\,, \qquad q_2 = 2\,Q\,, \qquad q_3 = -Q\,, \qquad q_4 = -Q\,. \tag{320}$$

The general bubble equations take the form:

$$\begin{aligned}
\frac{2\,Q\,P_{12}}{r_{12}} - \frac{Q\,P_{13}}{r_{13}} - \frac{Q\,P_{14}}{r_{14}} &= -\sum_{I=1}^{3} \tilde{k}_1^I \quad = \quad C_1\,,\\
-\frac{2\,Q\,P_{12}}{r_{12}} - \frac{2\,Q^2\,P_{23}}{r_{23}} - \frac{2\,Q^2\,P_{24}}{r_{24}} &= -\sum_{I=1}^{3} \tilde{k}_2^I \quad = \quad C_2\,,\\
\frac{Q\,P_{13}}{r_{13}} + \frac{2\,Q^2\,P_{23}}{r_{23}} + \frac{Q^2\,P_{34}}{r_{34}} &= -\sum_{I=1}^{3} \tilde{k}_3^I \quad = \quad C_3\,,\\
\frac{Q\,P_{14}}{r_{14}} + \frac{2\,Q^2\,P_{24}}{r_{24}} - \frac{Q^2\,P_{34}}{r_{34}} &= -\sum_{I=1}^{3} \tilde{k}_4^I \quad = \quad C_4\,,
\end{aligned} \tag{321}$$

To obtain a scaling solution whose classical limit is a ring, the triangle defined by points $2, 3$ and 4 should collapse so that:

$$r_{1j} \approx \rho\,, \qquad r_{ij} \ll \rho\,, \qquad i,j = 2,3,4\,. \tag{322}$$

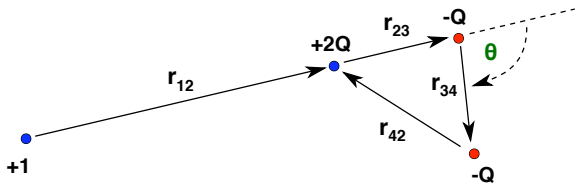

Figure 12: The layout of GH points for a triangular scaling solution.

Indeed, for a scaling solution in which $r_{ij} \to 0$ for $i, j = 2, 3, 4$, the bubble equations (321) require that:

$$r_{ij} \;\to\; (-1)^{i+j+1} \lambda \, q_i \, q_j \, P_{ij} \,, \qquad 2 \leq i < j \leq 4 \,, \tag{323}$$

with $\lambda \to 0$. In other words, the fluxes define the lengths of the sides and hence the angles in the triangles. One then has:

$$\vec{J}_{L\,ij} \;=\; -\,8\,(-1)^{i+j+1} \lambda \, \vec{r}_{ij} \,, \qquad 2 \leq i < j \leq 4 \,, \tag{324}$$

where $\vec{r}_{ij} \equiv (\vec{y}^{(i)} - \vec{y}^{(j)})$. It follows that

$$\vec{J}_L^{\,int} \;=\; \sum_{i,j=2}^{4} \vec{J}_{L\,ij} \;\to\; -\,16\,\lambda\,(\vec{r}_{23} + \vec{r}_{34} - \vec{r}_{24}) \;\equiv\; 0 \,, \tag{325}$$

because these vectors define the sides of the triangle. The last bubble equation then yields:

$$\rho \;\approx\; 2\,Q \left[\sum_{I=1}^{3} d^I \right]^{-1} (P_{12} \;-\; 2\,P_{13} \;+\; P_{14}) \,, \tag{326}$$

where

$$d^I \;\equiv\; 2\,(k_2^I \;+\; k_3^I \;+\; k_4^I) \,. \tag{327}$$

Moreover, one also finds that the combination of fluxes in (326) is exactly the non-vanishing part of J_L and so one, once again, recovers (302).

Thus we find scaling solutions for generic values of fluxes: The only constraint is that the $|q_i q_j P_{ij}|$ must satisfy the triangle inequalities. Now recall that only three of the equations in (321) are independent. One of them fixes ρ and the others fix the lengths of two sides of the triangle in terms of the length of the third side. Thus we may view the angle, θ, in Fig. 12 as a modulus of the solution. The scaling solution then appears when the angle, θ, is tuned so that the triangle has the shape determined by the fluxes as in (323). The new feature of this class of solutions is that we are no longer fine-tuning a quantized flux parameter in order to approach the scaling limit. For these triangular scaling solutions, one can pick the quantized fluxes and then the scaling solution appears as a *modulus* is tuned to a critical value.

Obviously, not all of these triangular scaling solutions will be free of CTC's and this will put further constraints on the flux parameters. However, we have found a number of numerical examples that exhibit scaling at the critical value of θ and reveal no CTC's under careful numerical scrutiny of the solution. One such example has the following parameters:

$$\begin{array}{rcl} q_i & = & (1\,, 210\,, -105\,, -105)\,, \quad k_i^1 \;=\; (0\,, 525\,, 1200\,, 2210)\,, \\ k_i^2 & = & (0\,, -20000\,, 16000\,, 7887)\,, \quad k_i^3 \;=\; (0\,, 6400\,, 1613\,, 7900)\,, \end{array} \tag{328}$$

where, $i = 1, \ldots, 4$. Define $\Gamma_{ij} \;=\; q_i q_j P_{ij}$ then we have:

$$\Gamma_{23} \;=\; 8.0446 \times 10^8\,, \quad \Gamma_{34} \;=\; 4.9063 \times 10^8\,, \quad \Gamma_{24} \;=\; -\,1.1046 \times 10^9\,. \tag{329}$$

Note that the magnitudes of these fluxes all satisfy the triangle inequalities

$$|\Gamma_{ij}| \;\leq\; |\Gamma_{ik}| \;+\; |\Gamma_{kj}|\,. \tag{330}$$

By solving the bubble equations numerically, we find the overall size of the ring blob depends on the shape of the triangle formed by the three charges. In Table 2 we show how the size of the triangle changes as we vary the angle, θ.

The total dipole charges of this merger solution are given by:

$$d^I \;\equiv\; 2 \sum_{j=1}^{3} k_j^I\,, \tag{331}$$

while the electric charges and angular momenta can be obtained from (145,151) and (152). From these one can obtain the horizon area ratio, $\mathcal{R}$, in (318) for the corresponding classical black-ring solutions and here we find $\mathcal{R} \approx 0.103$. Thus this scaling solution represents a microstate of a true black ring.

$\pi - \theta$	r_{12}	r_{23}	r_{34}	r_{24}	r_{34}/r_{23}	r_{24}/r_{23}
0	580.889	28.601	19.150	47.751	.66954	1.6695
.2	532.623	27.820	18.577	46.175	.66776	1.6598
.4	537.742	25.439	16.851	41.482	.66238	1.6306
.6	546.005	21.341	13.943	33.779	.65333	1.5828
.8	557.025	15.323	9.8136	23.251	.64046	1.5174
1	570.302	7.0865	4.4196	10.178	.62366	1.4363
1.1	577.612	2.0172	1.2381	2.8049	.61375	1.3905
1.13	579.878	.36089	.22035	.49664	.61058	1.3762
1.136	580.335	.021823	.013311	.029969	.60993	1.3732
1.13635	580.361	1.963×10^{-3}	1.197×10^{-3}	2.695×10^{-3}	.60990	1.3731
1.136383	580.364	9.008×10^{-5}	5.494×10^{-5}	1.237×10^{-5}	.60989	1.3731
1.136384586	580.364	6.289×10^{-8}	3.836×10^{-8}	8.635×10^{-8}	.60989	1.3731
1.1363845871	580.364	4.573×10^{-10}	2.789×10^{-10}	6.279×10^{-10}	.60989	1.3731
1.136384587108	580.364	3.207×10^{-12}	1.956×10^{-12}	4.403×10^{-12}	.60989	1.3731

Table 3: This table shows the distances, r_{ij}, between point i and point j in the triangle solution as a function of the modulus, θ. (See Fig. 12.) The angle, θ, is the angle between $\vec{r}_{23}$ and $\vec{r}_{34}$ and it is varied to produce the merger at $\theta = \theta_c$ (given below), while all the other parameters are kept fixed. One should also note that the ratios of the distances at merger are precisely the ratios of the fluxes: $|\Gamma_{34}/\Gamma_{23}| \approx 0.609893$ and $|\Gamma_{24}/\Gamma_{23}| \approx 1.37308$.

As the angle θ is changed towards a critical angle, given by

$$\pi - \theta_c \approx 1.13638458710805705... \tag{332}$$

the distances inside the ring blob as measured on the base (r_{23}, r_{34}, r_{24}) shrink as well, such that

$$r_{ij} \sim \theta - \theta_c \tag{333}$$

We have checked at great length that this solution is free of closed timelike curves and has a global time function. The details of this are given in the Appendix of [43].

As explained in [42] and reviewed in section 9 and in the previous subsection, during the scaling (333) the physical distances between the points that form the cap remains the same, while the throat becomes longer and longer[40]. The structure of the cap remains self-similar, the curvature is bounded above by a cap-dependent value that is parametrically smaller than the Planck size. Hence, supergravity is a valid description of the scaling solution for any throat depth! Interestingly-enough, as $\theta \to \theta_c$, the length of the throat

[40]We have also checked this explicitly for the solution presented in Table 2.

diverges, and the solution becomes an "abyss" that increasingly resembles the naive black hole solution.

From a four-dimensional perspective, the solutions we consider here correspond to multi-centered configurations of D6 and $\overline{\text{D6}}$ branes. The fact that four-dimensional multi-center solutions can collapse has been known for quite a while [80] and has been associated to the existence of "closed quivers" in the gauge theory describing these configurations. The discussion of fluxes and angular momenta presented above can also be obtained from the more general analysis of multi-black hole four-dimensional solutions, upon restricting to D6 $-$ $\overline{\text{D6}}$ configurations.

It is also possible to argue from a four-dimensional perspective that even if the points of the quiver appear to collapse, in fact the distance between these points remains fixed[41]. The four-dimensional metric is

$$ds^2_{4D} = -\mathcal{Q}^{-1/2}(dt+\omega)^2 + \mathcal{Q}^{1/2}(ds^2_{\mathbb{R}^3}) \tag{334}$$

where

$$\mathcal{Q} \;\equiv\; Z_1\, Z_2\, Z_3\, V \;-\; \mu^2\, V^2 \;\geq\; 0\,. \tag{335}$$

In a scaling solution where the distances between the centers in the flat $\mathbb{R}^3$ metric scales like Λ, the value of the function $\mathcal{Q}$ in the region of the centers scales like $1/\Lambda^2$, when the total charge of the scaling centers is that of a black hole of nonzero entropy. Hence, the physical distance between the scaling centers remains constant. This four-dimensional analysis also implies that only centers whose total charge corresponds to a black hole or a black ring of finite horizon area can form a deep (abyssal) microstate.

Of course, from a four-dimensional perspective all the GH centers are naked singularities, and one could object that the distances between these centers are ill-defined. However, the four-dimensional results are useful because they complement those obtained from the full five-dimensional solution: the physical distance between the centers remains fixed throughout the scaling, and the apparent collapse of the centers manifests itself as the appearance of a throat.

11 Entropy Enhancement

There is a significant body of evidence that supports the idea that, within string theory, one can resolve BPS black hole singularities in terms of regular, horizonless *microstate geometries*. These geometries describe the microstates of black holes in the same regime of parameters where the classical black hole exists (see [14, 15, 16, 17] for reviews). One of the primary issues in proving this idea is whether the known microstate geometries represent typical black hole microstates or whether they are somehow confined to a peculiar atypical sub-sector of the Hilbert space.

[41] We thank Eric Gimon for pointing out this argument to us.

To refine this issue, one should first note that in the large-N limit, bulk classical geometries describe, to arbitrary accuracy, bulk quantum states that are dual to coherent states within the Hilbert space of states of the dual CFT. Coherent states can always be used to provide a basis for the Hilbert space, but this may not be so for the "semi-classical states" described by classical geometries. Indeed, as one finds with two-charge geometries, some of the boundary coherent states in such a basis will be dual to geometries that have string-scale features and for which the supergravity approximation breaks down or is, at best, a heuristic guide.

These issues are, however, not directly relevant if one's goal is to argue that the entropy of a black hole comes from horizon-sized, horizonless configurations that have unitary scattering and hence no information loss: For this, the relevant question is whether the states corresponding to such smooth microstate geometries are suitably dense within the Hilbert space of states. Indeed, in the vicinity a single, smooth microstate geometry that is well-described in supergravity there might exist a vast (but controlled) number of quantum microstates that have the same essential features (such as size, absence of horizon and sub-leading dipole fields). Thus the classical microstate geometry would act as a representative of these quantum microstates.

Hence, in counting semi-classical microstate geometries the first goal is to get the correct dependence of the number geometries as a function of the charges. For BPS black holes in five dimensions, this means one must have:

$$S \sim \log(N) \sim \sqrt{Q_1\, Q_2\, Q_3}\,. \tag{336}$$

If $N_{quantum}$ and N_{geom} respectively represent the number of quantum states and the number of semi-classical, microstate geometries that are valid in the supergravity approximation, then one can recover (336), if $\log(N_{geom})$ and $\log(N_{quantum})$ have the same growth to leading order in the charges[42].

A subsequent goal is to get the correct coefficient, $S = 2\pi\sqrt{Q_1 Q_2 Q_3}$, which amounts to predicting the correct central charge for the underlying conformal field theory. On the other hand, if one restricts oneself to a finite fraction of the degrees of freedom (with, perhaps, a lower central charge) and obtains horizon-sized, horizonless black-hole microstates with unitary scattering, it seems very implausible that restoring the rest of the degrees of freedom will drastically change the macroscopic features of these microstates. In particular, it is very unlikely that restoring such degrees of freedom will generate a horizon.

Thus, establishing that black holes in string theory are ensembles of horizonless configurations with unitary scattering is not as demanding as it might, at first, seem, and could reduce to showing that a semi-classical counting of smooth, horizonless, classical microstate geometries gives a black-hole-like, or macroscopic, entropy (336). Indeed, it

[42] In this sense, "suitably dense" can, in fact, amount to an extremely sparse relative population.

is our purpose here to display a mechanism by which smooth microstates of such a large entropy can arise.

In [42, 43] it was argued that the deep, or scaling, microstate geometries are the gravitational duals of states that belong to the "typical sector" of the D1-D5-P CFT. This was based upon the fact that a typical excitation of the gravitational system had precisely the correct energy to be the dual of an excitation in the sector of the CFT that contributes maximally to the entropy. In particular, the gravitational red-shift of the throat provides a critical factor in arriving at the proper excitation energies. Thus deep, or scaling geometries [42, 43, 80] will be one of the crucial ingredients in accounting for the entropy of black holes using microstate geometries.

Another important ingredient in our discussion will be the fact that two-charge supertubes [22], which can have arbitrary shapes, give smooth supergravity solutions in the duality frame in which they have D1 and D5 charges [5, 7]. This has been very useful in matching the entropy of two-charge smooth supergravity solutions to that of the dual CFT and served as one of the motivations of the formulation of the fuzzball proposal. However, even if supertubes can have arbitrary shapes, and hence a lot of entropy, their naive quantization cannot hope to account for the entropy of a black hole with a non-trivial, macroscopic horizon (336). Indeed, as found in [124, 125, 126], since supertubes only carry two charges, their entropy scales like:

$$S \sim \sqrt{Q_1 Q_2}\,. \tag{337}$$

The new insight here comes from considering supertubes in the background of a scaling geometry. We generalize the analysis of [124], and use the supertube DBI–WZ action to count states of quantized supertubes in non-trivial background geometries. We find that, for the purposes of entropy counting, the supertube charges Q_I that appear in (337) are replaced by the local effective charges of the supertube, Q_I^{eff}, which are a combination of the supertube charges and terms coming from the interaction between the supertube magnetic dipole moment and the background magnetic dipole fields.

If there are strong magnetic fluxes in the background, as there are in a deep, bubbled microstate geometries, these effective charges can be *much larger* than the asymptotic charges of the configuration, and can thus lead to a very large entropy enhancement! Indeed, one finds that if the supertube is put in certain deep scaling solutions, the effective charges can diverge if the supertube is suitably localized or if the length of the throat goes to infinity. Of course, this divergence is merely the result of not considering the back-reaction of the wiggly supertube on its background: Once this back-reaction is taken into account, the supertube will delocalize and the fine balance needed to create extremely deep scaling solutions might be destroyed if the tube wiggles too much.

Hence, we expect a huge range of possibilities in the the semi-classical configuration space, from very shallow solutions to very deep solutions. In very shallow solutions, the supertubes can oscillate a lot, but they will not have their entropy enhanced and for very

deep solutions the supertube will have vastly enhanced charges but, if the solution is to remain deep, the supertube will be very limited in its oscillations. One can thus imagine that the solutions with most of the entropy will be intermediate, neither too shallow (so as to obtain effective charge enhancement), nor too deep (to alow the supertube to fluctuate significantly). To fully support this intuition one will need to construct the full back-reacted supergravity solution for wiggly supertubes in bubbling three-charge backgrounds. Even though we do not yet have such solutions, it is possible to use the AdS-CFT correspondence to estimate the depth of the bulk microstate solutions dual to states in the typical sector of the dual CFT [42]. We will use this result to determine the depth of the typical throat and then argue that the effective supertube charges corresponding to this throat depth yields an enhanced supertube entropy that is macroscopic (336).

It is interesting to note that entropy enhancement is not just a red-shift effect: There is no entropy enhancement unless there are strong background magnetic fluxes. A three-charge BPS black hole will not enhance the entropy of supertubes: it is only solutions that have dipole charges, like bubbled black holes or black rings that can generate supertube entropy enhancement.

The last ingredient that we use is the generalized spectral flow transformation [127][43] that enables us to start from a simple, bubbled black hole microstate geometry [36, 37] and generate a bubbled geometry in which one or several of the Gibbons-Hawking (GH) centers are transformed into smooth two-charge supertubes. Indeed, from a six-dimensional perspective (in a IIB duality frame in which the solution has D1-D5-P charges) this mapping is simply a coordinate transformation. One can then study the particular class of fluctuating microstate geometries that result from allowing the supertube component to oscillate in the deep bubbled geometries. The naive expectation is that one would recover an entropy of the form (337) but, as we indicated, the Q_I are replaced by the enhanced Q_I^{eff}, and the entropy of these supertubes can become "macroscopic" in that it corresponds to the entropy of a black hole with a macroscopic horizon. One can then undo the spectral flow to argue that this entropy is present in the BPS fluctuations of three-charge bubbling solutions in *any* duality frame. In fact, spectrally flowing configurations with oscillating supertubes into other duality frames is not strictly speaking necessary for the purpose of illustrating entropy enhancement and arguing that smooth solutions can give macroscopically large entropy. After all, one could do the full analysis in the D1-D5-P duality frame and consider smooth black hole microstates containing both GH centers and supertubes. Nevertheless, since such solutions have not been studied in the past in great detail, it is easiest to construct them by spectrally flowing multi-center GH solutions, which have been studied much more and are better understood.

The fluctuations we consider do not represent the most general, regular fluctuation of the geometry, but as we outlined earlier, this is not the point: They represent a sub-sector of the possible fluctuations whose Hilbert space has entropy that grows much faster than

[43] See [32, 128] for relevant earlier work.

(337) and indeed might grow as fast as (336). Thus we believe that these microstate geometries may be capturing generic states of the CFT for black holes and black rings with non-zero horizon area and capturing enough of them to account for that horizon area, up to overall numerical factors. The fact that we are only looking at a special class of fluctuations means that we are necessarily restricting the degrees of freedom of the fluctuations and so one would not expect, at the first pass, to recover the correct numerical factors in (336). The important progress here is that we see how microstate geometries may indeed capture enough entropy to account for macroscopic horizons and for their dependence upon charges.

It is also interesting to note that a similar conclusion – that deep, scaling, horizonless configurations can give a macroscopic (black-hole-like) entropy – was also reached in [118, 119] and [129]. In [118, 119] this was done by considering D0 branes in a background of D6 branes with world-volume fluxes, in the regime of parameters where the D0 branes do not back-react. In [129], a similar result was obtained by studying the quiver quantum mechanics of multiple D6 branes, in the regime where the branes do not back-react, but form a finite-sized configuration. Since these computations were performed in a regime in which the gravitational back-reaction of all or some of the branes is neglected, it is not clear how the configurations that give the black hole entropy will develop in the regime of parameters in which the classical black hole exists, and *all* the branes back-react on the geometry. Their size will continue increasing at the same rate as the would-be black hole horizon, and since they are made from primitive branes, it is very unlikely they will develop a horizon. Hence these two calculations do suggest that the black hole entropy comes from horizonless configurations. However, since the D0 branes give rise to naked singularities, the naive strong-coupling extrapolation of these microstate configurations will not be reliable when the classical black hole exists.

The microstates that we consider here are also counted in a regime of parameters in which some of their components, *i.e.* the supertubes, are treated as probes and described by their DBI–WZ action, and hence do not back-react on the geometry. However, unlike the configurations mentioned above, we understand very well what the supertubes become in the regime of parameters where the black hole exists: They give rise to smooth horizonless microstate solutions. Indeed, as we have shown in [130], the DBI–WZ description of supertubes gives configurations that in the D1-D5-P duality frame are smooth in supergravity. Hence, our entropy calculation is expected to extend to the regime of parameters where the classical black hole exists.

11.1 Fluctuating supertubes in non-trivial backgrounds

Three-charge bubbling solutions that have the same charges and dipole moments as black holes and black rings are determined by specifying a four-dimensional base space, and solving a set of linear equations to determine the warp factors, and the other parameters of the solution [53].

In the duality frame where the charges of the solutions correspond to D0 branes, D4 branes and F1 strings, the metric and the dilaton have the form:

$$\begin{aligned} ds_{10}^2 &= -\frac{1}{Z_3\sqrt{Z_1 Z_2}}\,(dt+k)^2 + \sqrt{Z_1 Z_2}\,ds_4^2 + \frac{\sqrt{Z_1 Z_2}}{Z_3}\,dx_5^2 + \sqrt{\frac{Z_1}{Z_2}}\,(dx_1^2+dx_2^2+dx_3^2+dx_4^2)\,, \\ \Phi &= \frac{1}{4}\log\left(\frac{Z_1^3}{Z_2 Z_3^2}\right), \end{aligned} \tag{338}$$

where we parameterize the S^1 of the F1 string by x^5, and the T_4 of the D4 world-volume by x_i, $i = 1, \ldots, 4$. The warp factors Z_1, Z_2, Z_3 correspond to D0, D4 and F1 charges respectively.

As we explained in Section 6, when the four-dimensional base of the solution is a multi-center Gibbons-Hawking (Taub-NUT) space,

$$ds_4^2 \;=\; V^{-1}\,(d\psi + A)^2 \;+\; V\,d\vec{y}\cdot d\vec{y}\,, \tag{339}$$

the full solution can be determined in terms of eight harmonic functions, V, K^I, L_I, M $(I = 1, 2, 3)$ on the $\mathbb{R}^3$ spanned by (y_1, y_2, y_3). As shown in [130], the RR potentials are given by

$$C^{(1)} = (Z_1^{-1} - 1)dt + Z_1^{-1}k - \zeta^{(1)}\,, \tag{340}$$

$$C^{(3)} = -Z_3^{-1}(dt+k)\wedge\zeta^{(1)}\wedge dx_5 - dt\wedge A^{(3)}\wedge dx_5 + (\nu_a + V^{-1}K^3\xi_a^{(1)})\Omega_-^{(a)}\wedge dx_5\,, \tag{341}$$

where

$$\vec{\nabla}\times\vec{\nu} = -\vec{\nabla}L_2 \qquad \text{and} \qquad \Omega_-^{(a)} = (d\psi + A)\wedge dy^a - \frac{1}{2}\epsilon_{abc}dy^b\wedge dy^c\,. \tag{342}$$

$$\zeta^{(I)} \;=\; V^{-1}K^I\,(d\psi + A) \;+\; \xi^I\,, \qquad \vec{\nabla}\times\vec{\xi^I} \;\equiv\; -\,\vec{\nabla}K^I\,. \tag{343}$$

The functions, Z_I, and the angular momentum one-form, k, are

$$Z_I \;=\; \tfrac{1}{2}V^{-1}\,C_{IJK}K^JK^K \;+\; L_I\,, \qquad k \;=\; \mu(d\psi + A) \;+\; \omega\,, \tag{344}$$

where

$$\mu \;=\; \tfrac{1}{6}\,V^{-2}\,C_{IJK}\,K^IK^JK^K \;+\; \tfrac{1}{2}\,V^{-1}\,K^IL_I \;+\; M\,. \tag{345}$$

and the one form, $\omega = \vec{\omega}\cdot d\vec{x}$, is given by the solution of the equation

$$\vec{\nabla}\times\vec{\omega} \;=\; V\vec{\nabla}M - M\vec{\nabla}V \;+\; \tfrac{1}{2}(K^I\vec{\nabla}L_I - L_I\vec{\nabla}K^I)\,. \tag{346}$$

We take the harmonic functions to have the form:

$$V \;=\; \epsilon_0 \;+\; \sum_{j=1}^{N}\frac{q_j}{r_j}\,, \qquad K^I \;=\; \kappa_0^I \;+\; \sum_{j=1}^{N}\frac{k_j^I}{r_j}\,, \tag{347}$$

$$L_I \;=\; l_0^I \;+\; \sum_{j=1}^{N}\frac{l_j^I}{r_j}\,, \qquad M \;=\; m_0 \;+\; \sum_{j=1}^{N}\frac{m_j}{r_j}\,, \tag{348}$$

where $r_j = |\vec{y} - \vec{y}_j|$, for N Gibbons-Hawking (GH) points located at $\vec{y}_j$. To ensure that the solution is regular (up to $\mathbb{Z}_{q_j}$ orbifold singularities) at $r_j \to 0$ we must have $q_j \in \mathbb{Z}$ and

$$l^I_j \;=\; -\tfrac{1}{2}\, q_j^{-1}\, C_{IJK} k^J_j k^K_j\,, \qquad m_j = \tfrac{1}{2}\, q_j^{-2}\, k^1_j k^2_j k^3_j\,, \qquad j = 1, \ldots, N\,. \tag{349}$$

As shown in [127], the spectral flow transformation:

$$\begin{aligned}
\widetilde{L}_I &= L_I \;-\; 2\,\gamma_I\, M\,, \qquad \widetilde{M} \;=\; M\,, \qquad \vec{\tilde{\omega}} \;=\; \vec{\omega}\,, && (350)\\
\widetilde{K}^I &= K^I \;-\; C^{IJK}\,\gamma_J\, L_K \;+\; C^{IJK}\,\gamma_J\,\gamma_K\, M\,, && (351)\\
\widetilde{V} &= V + \gamma_I\, K^I - \tfrac{1}{2}\, C^{IJK} V\,\gamma_I\,\gamma_J\, L_K + \tfrac{1}{3}\, C^{IJK}\gamma_I\,\gamma_J\,\gamma_K\, M\,, && (352)
\end{aligned}$$

transforms solution to solutions, and can change a GH centers into other GH centers, or two-charge supertubes[44]. This can be arranged to happen at the N^{th} GH point by choosing:

$$\gamma_{1,3} = 0\,, \qquad\qquad \gamma_2 = \gamma \;=\; -\,\frac{q_N}{k^2_N}\,, \tag{353}$$

which induces the following changes:

$$\begin{aligned}
\widetilde{Z}_1 &= \frac{V}{\widetilde{V}}\, Z_1\,, \qquad \widetilde{Z}_3 \;=\; \frac{V}{\widetilde{V}}\, Z_3\,, \qquad \widetilde{Z}_2 \;=\; \frac{\widetilde{V}}{V}\, Z_2 \;-\; 2\gamma\mu \;+\; \gamma^2\, \frac{Z_1\, Z_3}{\widetilde{V}}\,,\\
\tilde{\mu} &= \frac{V}{\widetilde{V}}\left(\mu \;-\; \gamma\, \frac{Z_1\, Z_3}{\widetilde{V}}\right), \qquad \widetilde{V} \;=\; V \;+\; \gamma\, K^2\,. && (354)
\end{aligned}$$

As explained in [127], the dipole charge and "bare" electric charges of the resulting supertube are given by the coefficients of the divergent terms in $\widetilde{K}^2$, $\widetilde{L}_1$ and $\widetilde{L}_3$. We define the "effective" charges of the supertube by the divergence of the electric potentials, Z_I, near the supertube:

$$Q_1^{eff} \;\equiv\; 4 \lim_{r_N \to 0} r_N\, \widetilde{Z}_1 \;=\; 4\, q_N\, (\widetilde{V}^{-1}\, Z_1)|_{r_N=0} \;=\; 4\tilde{\ell}^1_N \;+\; 4\tilde{k}^2_N (\widetilde{V}^{-1}\widetilde{K}^3)|_{r_N=0}\,, \tag{355}$$

and similarly for Q_3^{eff}. As we will see later, these are the charges that determine the entropy of supertubes, and since $(\widetilde{V}^{-1}\widetilde{K}^3)$ depends critically on the position of the supertube, the effective charges can be much larger than the asymptotic charges of the system. This is the crucial ingredient of the entropy enhancement mechanism.

11.2 The probe calculation

Consider a probe supertube with D0 and F1 charges and D2 dipole charge in the three-charge solution with a Gibbons-Hawking base described above. We choose the supertube

[44] From a four-dimensional perspective this corresponds to transforming a primitive D6 brane into a primitive D4 brane.

world-volume coordinates ξ to be $(t, \theta = \psi, z = x^5)$, where ψ is the $U(1)$ fiber of the GH base.

The DBI–WZ action of the supertube is:

$$\begin{aligned} S &= T_{D2} \int d^3\xi \left\{ \left[\left(\frac{1}{Z_1} - 1 \right) \mathcal{F}_{z\theta} + \frac{K^3}{Z_1 V} + (\mathcal{F}_{tz} - 1) \left(\frac{\mu}{Z_1} - \frac{K^1}{V} \right) \right] \right. \\ &- \left. \left[\frac{1}{V^2 Z_1^2} [(K^3 - V(\mu(1 - \mathcal{F}_{tz}) - \mathcal{F}_{z\theta}))^2 + V Z_1 Z_2 (1 - \mathcal{F}_{tz})(2 - Z_3(1 - \mathcal{F}_{tz}))] \right]^{1/2} \right\}, \end{aligned} \tag{356}$$

where $2\pi\alpha' F \equiv \mathcal{F} = \mathcal{F}_{tz} dt \wedge dz + \mathcal{F}_{z\theta} dz \wedge d\theta$ is the world-volume gauge field of the D2 brane. Our goal is to semi-classically quantize BPS fluctuations around certain supertube configurations, and compute their entropy. Supersymmetry requires that these fluctuations be independent of t and z, and that $\mathcal{F}_{tz} = 1$.

All the fluctuations of the supertube lead to similar values for the entropy, but for the purpose of illustrating entropy enhancement it is best to focus on the fluctuations in the four torus directions:

$$x_i \to x_i + \eta_i(t, \theta) \qquad i = 1 \ldots 4. \tag{357}$$

Since the BPS modes are independent of z, it is convenient to work with a Lagrangian density that has already been integrated over the z direction, which gives the conjugate momenta for the excitations η_i:

$$\Pi_i = \left(\frac{\partial}{\partial \dot{\eta}_i} \int_0^{2\pi L_z} \mathcal{L}_{WZ} + \mathcal{L}_{DBI} \right)_{\dot{\eta}_i = 0,\ \mathcal{F}_{tz} = 1} = 2\pi L_z T_{D2}\, \eta_i' \,, \tag{358}$$

where $\dot{\eta}_i \equiv \frac{\partial \eta_i}{\partial t}$ and $\eta_i' \equiv \frac{\partial \eta_i}{\partial \theta}$. To semi-classically quantize the BPS oscillations we impose the canonical commutation relations:

$$[\eta_j(t, \theta),\ \Pi_k(t, \theta')] = i \delta_{jk} \delta(\theta - \theta') \,. \tag{359}$$

A supertube with dipole charge n_2 can be thought of as wrapped n_2 times around the θ circle. To find the correct mode expansion it is not enough to focus on the BPS modes alone, even if one only wants to count the entropy coming from these modes. Both the BPS and non-BPS modes contribute to the delta-function in (359) and the inclusion of both contributions is essential to the proper normalization of the modes[45]. The result is simply an extra factor of $\sqrt{2}$ in the coefficient of the BPS mode expansion compared to the naive expansion that neglects non-BPS modes:

$$\eta_i = \eta_i^{\,\mathrm{BPS}} + \eta_i^{\,\mathrm{nonBPS}} = \frac{1}{\sqrt{8\pi^2 T_{D2} L_z}} \sum_{k>0} \left[e^{ik\theta/n_2} \frac{(a_k^i)^\dagger}{\sqrt{|k|}} + \mathrm{h.c.} \right] + \eta_i^{\,\mathrm{nonBPS}} \,. \tag{360}$$

[45] This subtlety is correctly taken into account in [124], but not in [125].

The creation and annihilation operators, $(a_k^i)^\dagger$ and a_k^i, for the modes in the $k^{\rm th}$ harmonic satisfy canonical commutation relations:

$$[a_k^i, (a_{k'}^j)^\dagger] = \delta^{ij}\delta_{k,k'}\,. \tag{361}$$

The D0 and F1 quantized charges of the supertube are:

$$Q_1 = \frac{T_{D2}}{T_{D0}}\int_0^{2\pi L_z} dz \int_0^{2\pi n_2} d\theta\, \mathcal{F}_{z\theta} = 4\pi^2 \frac{T_{D2}}{T_{D0}} L_z n_2 \mathcal{F}_{z\theta} \tag{362}$$

$$Q_3 = \frac{T_{D2}}{T_{F1}}\int_0^{2\pi n_2} d\theta \left[-\frac{K^1}{V} + \frac{1}{\mathcal{F}_{z\theta} + V^{-1}K^3}\left(\frac{Z_2}{V} + (\eta')^2\right)\right] \tag{363}$$

Substituting (360) into (363) and rearranging using (362) leads to:

$$\begin{aligned}\sum_{i=1}^4 \sum_{k>0} k (a_k^i)^\dagger a_k^i &= L_z T_{D2}\int_0^{2\pi n_2} d\theta \int_0^{2\pi n_2} d\theta' \sum_{i=1}^4 \eta_i' \eta_i' \\ &= \left[Q_1 + 2\pi T_{F1} L_z n_2 \frac{K^3}{V}\right]\left[Q_3 + \frac{2\pi T_{D2}}{T_{F1}} n_2 \frac{K^1}{V}\right] - 4\pi^2 T_{D2} L_z n_2^2 \frac{Z_2}{V}\,,\end{aligned} \tag{364}$$

where the integrals over θ and θ' are precisely those appearing in each of (362) and (363). This is the result we have been seeking. The left hand side of (364) can be thought of as the total energy L_0 of a set of four harmonic oscillators in $1+1$ dimensions. For large L_0, the entropy coming from the different ways of distributing this energy to various modes of these oscillators is given by the Cardy formula:

$$S = 2\pi\sqrt{\frac{cL_0}{6}}. \tag{365}$$

Since we count BPS excitations, there will be also 4 fermionic degrees of freedom, and the central charge associated to the torus oscillations will be $c = 4 + 2 = 6$, giving the entropy:

$$S = 2\pi\sqrt{\left[Q_1 + n_2\frac{K^3}{V}\right]\left[Q_3 + n_2\frac{K^1}{V}\right] - n_2^2\frac{Z_2}{V}} = 2\pi\sqrt{Q_1^{eff}\, Q_3^{eff} \;-\; n_2^2\frac{Z_2}{V}}\,, \tag{366}$$

where to render the equations simple we have chosen a system of units in which $2\pi T_{F1} L_z = L_z/\alpha' = 1$ and $2\pi T_{D2}/T_{F1} = (g_s\sqrt{\alpha'})^{-1} = 1$. We will use this convention throughout this Section. Equation (364) has two important consequences. First, for a supertube with a given set of BPS modes, this equation is nothing but a "radius formula" that determines its size by fixing, in the spatial base, the location of the $U(1)$ fiber that it wraps. When the supertube is maximally spinning, and has no BPS modes, this equation simply becomes the radius formula of the maximally spinning supertube [130]. The second

result is that this formula also determines the capacity of the supertube to store entropy: In flat space, this capacity is determined by the asymptotic charges, Q_1 and Q_3, whereas, in a more general background, the capacity to store entropy is determined by Q_1^{eff} and Q_3^{eff}. In certain backgrounds, the latter can be made much larger than the former and so a supertube of given asymptotic charges can have a lot more modes and thus store a lot more entropy by the simple expedient of migrating to a location where the effective charges are very large. We will discuss this further below.

Clearly, for bubbling backgrounds, and even for black ring backgrounds, the right hand side of (364) can diverge, and one naively gets an infinite value for the entropy. Nevertheless, as we mentioned in the introduction, this calculation is done in the approximation that the supertube does not back-react on the background, and taking this back-reaction into account will modify this naive conclusion.

For a supertube that is not along the GH fiber, equation (366) is still correct, except that the Q_I^{eff} are no longer given by (355) but by:

$$Q_1^{eff} \equiv Q_1 + n_2 \tilde{\zeta}^{(1)}, \qquad Q_3^{eff} \equiv Q_3 + n_2 \tilde{\zeta}^{(2)}. \tag{367}$$

where $\tilde{\zeta}^{(I)}$ are the pull-backs onto the supertube of the spacetime one-forms $\zeta^{(I)}$ defined in (343).

We have also explicitly calculated the supertube entropy in a general three-charge black-ring background, where the supertube oscillates both in the T^4, and in two of the transverse $\mathbb{R}^4$ directions. The result is identical to (366), except that now there are six possible bosonic modes (and thus after we include the corresponding fermions the central charge of the system is $c = 9$). The explicit answer for the entropy[46] is:

$$S = 2\pi\sqrt{\frac{cL_0}{6}} = 2\pi\sqrt{\frac{3}{2}}\sqrt{[(Q_1 - 2n_2q_3(1+y)]\,[Q_3 - 2n_2q_1(1+y)] - n_2^2 Z_2 R^2 \frac{(y^2-1)}{(x-y)^2}}\,, \tag{368}$$

Based on this result, we expect that upon including the four bosonic shape modes in the transverse space, as well as the fermionic counterparts of all the eight bosonic modes, the central charge c should jump from 6 to 12, and equation (366) to be modified accordingly. We have also explicitly computed the entropy coming from arbitrary shape modes, and the formulas do display entropy enhancement (they diverge near $y = -\infty$ for the black ring). However, the complete expressions are rather unilluminating, and we leave their study for later investigation [130]. Our calculation agrees with the entropy of supertubes in flat space-time, computed using similar methods in [124, 125], and using different methods in [126].

It is also possible to compute the angular momentum of a supertube that has a very large number of BPS modes turned on. From the T_{0i} components of the energy momentum

[46] Using the conventions of [15].

tensor we find

$$J^{ij} = \frac{1}{2\pi}\int_0^{2\pi n_2} d\theta(\eta_i\Pi_j - \eta_j\Pi_i) \tag{369}$$

and the angular momentum of the tube along the GH fiber is

$$J = \frac{Q_1Q_3}{n_2} - \frac{Q_1^{eff}\,Q_3^{eff}}{n_2} + n_2\frac{Z_2}{V}. \tag{370}$$

From this identity we may simply re-write (366) as

$$S \;=\; 2\pi\sqrt{Q_1^{eff}\,Q_3^{eff} \;-\; n_2^2\frac{Z_2}{V}} \;=\; 2\pi\sqrt{Q_1Q_3 - n_2J}\,. \tag{371}$$

Hence, in a certain sense, (366) is the same as the entropy formula for a supertube in empty space and it naively appears that entropy enhancement has gone away. It has not. The important point is that (370) implies that it is possible for J to become extremely large and negative as the number of BPS modes on the tube increases[47]. In flat space, $|J|$ is limited by $|Q_1Q_3|$ but in a general background our Born-Infeld analysis (equations (364) and (370)) imply that the upper bound is the same but there is no lower bound.

From the supergravity perspective, the limits on J usually emerge from requiring that there are no CTC's near the supertube. This is a local condition set by the local behavior of the metric, and particularly by the Z_I, near the supertube. Although we do not have the explicit solution, our analysis suggests that the lower limit of the angular momentum of the supertube is controlled by Q_1^{eff} and Q_3^{eff} as opposed to Q_1 and Q_3. Thus entropy enhancement can occur if the supertube moves to a region where Q_1^{eff} and Q_3^{eff} are extremely large and then a vast number of modes can be supported on a supertube (of fixed Q_1 and Q_3) by making J large and negative. We therefore expect the corresponding supergravity solution to be CTC-free provided that $|n_2J| < Q_1^{eff}Q_3^{eff}$.

One should thus think of a supertube of given n_2, Q_1 and Q_3 as being able to store a certain number of modes before it over-spins. The "storage capacity" of the supertube is determined by the local conditions around the supertube and, specifically, by n_2, Q_1^{eff} and Q_3^{eff}. Magnetic dipole interactions, like those evident in bubbling backgrounds, can thus greatly modify the capacity of a given supertube to store entropy.

11.3 Entropy Enhancement - the Proposal

As we have seen, the entropy of a supertube, and hence the entropy of a fluctuating geometry, depends upon the *local* effective charges and not upon the asymptotic charges measured at infinity. In the derivation of (364) we started with a maximally spinning, round supertube with zero entropy and perturbed around it. For the maximally spinning

[47]This is not unexpected: As in flat space, every BPS mode on the supertube takes away one quantum of angular momentum of the tube.

tube, the equilibrium position is determined by the vanishing of the right-hand side. Upon adding wiggles to the tube, the right hand side no longer vanishes and the imperfect cancelation is responsible for the entropy.

It is interesting to ask how much entropy can equation (364) accommodate. The answer is not so simple. At first glance one might say that the both terms in the right hand side of (364) can be divergent, and hence the entropy of the fluctuating tube is infinite. Nevertheless, one can see that the leading order divergent terms in $Q_1^{eff}\,Q_3^{eff}$ and in $n_2^2 Z_2/V$ come entirely from bulk supergravity fields, and exactly cancel, both for the supertube in GH background and for the supertube near a black ring (368).

It is likely that this partial cancelation is an artefact of the extremely symmetric form of the solution, and that in a more general solution such cancellation may not take place. In particular, both Q_1^{eff} and Q_3^{eff} are integrals of "effective charge" densities on the supertube world-volume, and the right hand side of equation (364) should be written as

$$Q_1^{eff}\,Q_3^{eff} - n_2^2\frac{Z_2}{V} = \int \rho_1^{eff} d\theta \int \rho_3^{eff} d\theta - \int \rho_1^{eff}\,\rho_3^{eff} d\theta \tag{372}$$

If this generalized formula is correct, certain density and shape modes will disturb the balance between the product of integrals and the integral of the product, and the leading behavior of the entropy will still be of the order

$$S \;\sim\; \sqrt{Q_1^{eff}\,Q_2^{eff}}\,. \tag{373}$$

Regardless of this, the next-to-leading divergent terms in (366) are a combination of supertube world-volume terms and bulk supergravity fields. In a scaling solution, or when the tube is close to the black ring, these terms can diverge, giving naively an infinite entropy. As we discussed above, we expect the back-reaction of the supertubes to render this entropy finite.

The idea of *entropy enhancement* is that one can find backgrounds in which the effective charges of a two-charge supertube can be made far larger than the asymptotic charges of the solution, and that, in the right circumstances, the oscillations of this humble supertube could give rise to an entropy that grows with the asymptotic charges much faster than $\sqrt{Q^2}$ (as typical for supertubes), and might even grow as fast as $\sqrt{Q^3}$, as typical for black holes in five dimensions.

To achieve such a vast enhancement requires a very strong magnetic dipole-dipole interaction and this means that multiple magnetic fluxes must be present in the solution. It is *not* sufficient to have a large red-shift: BMPV black holes have infinitely long throats and arbitrarily large red-shifts but have no magnetic dipole moments to enhance the effective charges and thus increase the entropy that may be stored on a given supertube.

Hence, the obvious places to obtain entropy enhancement are solutions with large dipole magnetic fields, such as black ring or bubbling microstate solutions. Since we are focussing on trying to obtain the entropy of black holes from horizonless configurations,

we will focus on the latter. These bubbling solutions are constructed using an ambipolar base GH metric, and near the "critical surfaces," where V vanishes, the term $\frac{K^I}{V}$ in the effective charge diverges. It is therefore natural to expect entropy enhancement for supertubes that localize near the critical ($V = 0$) surfaces.

We also believe that placing supertubes in deep scaling solutions [42, 43, 129] will prove to be an equally crucial ingredient. Indeed, as we will see in the next subsection, in a deep microstate geometry the K^I at the location of the tube can also become large, and hence there will be a double enhancement of the effective charge, both because of the vanishing V in the denominator and because of the very large K^I in the numerator. There is another obvious reason for this: It is only the scaling microstate geometries that have the same quantum numbers as black holes with macroscopic horizons.

This must mean that the simple entropy enhancement one gets from the presence of critical surfaces is not sufficient for matching the black hole entropy. The fundamental reason for this may well be the following: Even if the round supertube can be brought very close to the $V = 0$ surface, once the supertube starts oscillating it will necessarily sample the region around this surface, and the charge enhancement will correspond to the average Q_I^{eff} in that region. For this to be very large the entire region where the supertube oscillates must have a very significant charge enhancement. The only such region in a horizonless solution is the bottom of a deep or scaling throat, where the average of the K^I is indeed very large.

All the issues we have raised here have to do with the details of the entropy enhancement mechanism, and involve some very long and complex calculations that we intend to pursue in future work. We believe their clarification is very important, as it will shed light on how the entropy of black holes can be realized at the level of horizonless configurations.

Our goals in this subsection are rather more modest. We have shown via a Born-Infeld probe calculation that the entropy of supertubes is given by their effective charges, and not by their brane charges, and that these effective charges can be very large. However, because the supertube has been treated as a probe in our calculations, it is logically possible that, once we take into account its back-reaction, the bubble equations may forbid the supertube to get suitably close to the $V = 0$ surfaces, and to have a suitable entropy enhancement.

In principle this is rather unlikely, as we know that in all the examples studied to date, the solutions of the Born-Infeld action of supertubes always correspond to configurations that are smooth and regular in supergravity [130]. However, settling the issue completely is not possible before constructing the full supergravity solutions corresponding to wiggly supertubes. Hence, in the remainder of this subsection we will show that at least for the maximally-spinning supertubes, their effective charges in deep scaling solutions can lead to a black-hole-like enhanced entropy.

11.4 Supertubes in scaling microstate geometries

To find bubbling solutions that contain supertubes with enhanced charges one could look for solutions of the bubble or integrability equations [36, 37, 80]

$$\sum_{\substack{j=1\\ j\neq i}}^{N} \frac{\Gamma_{ij}}{r_{ij}} \;=\; 2\,(\epsilon_0\, m_i - m_0\, q_i) \;+\; \sum_{I=1}^{3} (\ell^I_i \kappa^I_0 - \ell^I_0\, k^I_i) \;, \qquad r_{ij} \equiv |\vec{y}^{(i)} - \vec{y}^{(j)}| \tag{374}$$

that describe scaling solutions where some of the centers are GH points, and the other centers are supertubes. However, it is more convenient to construct such solutions by spectrally flowing multi-center GH solutions, which have been studied much more. The parameters of the equations are then:

$$\Pi^{(I)}_{ij} \;\equiv\; \left(\frac{k^I_j}{q_j} - \frac{k^I_i}{q_i}\right), \qquad\qquad \Gamma_{ij} = q_i\, q_j \Pi^{(1)}_{ij}\Pi^{(2)}_{ij}\Pi^{(3)}_{ij}\,. \tag{375}$$

One obtains a scaling solution when a subset, $\mathcal{S}$, of the GH points approach one another arbitrarily closely, that is, $r_{ij} \to 0$ for $i, j \in \mathcal{S}$. In terms of the physical geometry, these points are remaining at a fixed distance from each other, but are descending a long AdS throat that, in the intermediate region, looks almost identical to the throat of a black hole or black ring (depending upon the total GH charge in $\mathcal{S}$). In particular, in the intermediate regime, one has $Z_I \sim \frac{\hat{Q}_I}{4\,r}$, where we have taken $\mathcal{S}$ to be centered at $r = 0$ and the $\hat{Q}_I$ are the electric charges associated with $\mathcal{S}$. Similarly, if $\mathcal{S}$ has a non-zero total GH charge of $\hat{q}_0$, then one has $V \sim \frac{\hat{q}_0}{r}$. More precisely:

$$Z_I\, V \;=\; l^I_0 V \;+\; \varepsilon_0\,(L_I - \ell^I_0) \;-\; \tfrac{1}{4}\, C_{IJK} \sum_{i,j=1}^{N} \Pi^{(J)}_{ij}\, \Pi^{(K)}_{ij}\, \frac{q_i\, q_j}{r_i\, r_j}\,. \tag{376}$$

Suppose that we perform a spectral flow so that some point, $p \in \mathcal{S}$, becomes a supertube. Let $\widetilde{V}_p$ be the value of $\widetilde{V}$ at p. Then, from (354) and (355), the effective charges of this supertube are dominated by terms from interactions with the magnetic fluxes in the throat:

$$Q^{eff}_I \;\sim\; -\,2\, q_p\, \widetilde{V}_p^{-1}\, C_{IJK} \sum_{j\in\mathcal{S}\,,\, j\neq p} \Pi^{(J)}_{jp}\, \Pi^{(K)}_{jp}\, \frac{q_j}{r_{jp}}\,. \tag{377}$$

However, observe that $\tilde{q}_j = (k^2_p)^{-1} q_p q_j \Pi^{(2)}_{jp}$ and so

$$q_p^{-1}\widetilde{V}_p \;\sim\; (k^2_p)^{-1} \sum_{j\in\mathcal{S}\,,\, j\neq p}^{N} \frac{q_j \Pi^{(2)}_{jp}}{r_{jp}}\,. \tag{378}$$

Therefore the numerator and denominator of (377) have the same naive scaling behavior as $r_{jp} \to 0$ and so, in general, Q^{eff}_I will attain a finite limit that only depends upon the

q_j, k^I_j for $j \in \mathcal{S}$. Indeed, the finite limit of Q^{eff}_I scales as the square of the k's for large k^I_j parameters. This is no different from the typical values of asymptotic electric charges in bubbled geometries.

However, since we are in a bubbled microstate geometry, V and $\widetilde{V}$ change sign throughout the bubbled region. In particular, there are surfaces at the bottom of the throat where $\widetilde{V}$ vanishes and there are regions around them where $\widetilde{V}$ remains finite and bounded as $r_{ij} \to 0$. Suppose that we can arrange for the supertube point p to be in such a region of a scaling throat and at the same time we can arrange that Z_I still diverges as $\frac{1}{r}$. Then, in principle, the effective charges, of the supertube Q^{eff}_I, could become arbitrarily large.

As mentioned above, we expect the entropy of the system to come from wiggly supertubes in throats that are neither very deep (to allow the tubes to wiggle), nor very shallow (to give enhancement). We do not, as yet, know how to take the back-reaction of the wiggly supertubes into account, and hence we do not have any supergravity argument about the length of these throats. However, we can use the *AdS*-CFT correspondence and the fact that we know what the typical CFT microstates are, to argue [42] that the typical bulk microstates are scaling solutions that have GH size r_T given by

$$r_T \;\sim\; \overline{Q}^{\,-1/2} \;\sim\; \frac{1}{\bar{k}}\,, \tag{379}$$

where $\overline{Q}$ is the charge and $\bar{k}$ is the typical flux parameter.

If one takes this *AdS*-CFT result as given, and moreover assumes that the wiggling supertube remains in a region of finite $\widetilde{V}$ in the vicinity of the $\widetilde{V} = 0$ surface, one then has:

$$Q^{eff}_I \;\sim\; (\bar{k})^3 \;\sim\; \overline{Q}^{\,3/2} \tag{380}$$

because $\Pi^{(K)}_{jp} \sim \bar{k}$, and hence the entropy of the fluctuating supertube (373) would depend upon the asymptotic charges as:

$$S \;\sim\; \sqrt{Q^{eff}_1\, Q^{eff}_2} \;\sim\; \overline{Q}^{\,3/2}\,. \tag{381}$$

which is precisely the correct behavior for the entropy of a classical black hole!

These simple arguments indicate that fluctuating supertubes at the bottom of deep scaling microstate geometries can give rise to a black-hole-like macroscopic entropy, provided that they oscillate in a region of bounded $\widetilde{V}$.

Obviously there is a great deal to be checked in this argument, particularly about the effect of the back-reaction of the supertube on its localization near the $\widetilde{V} = 0$ surface. We conclude this subsection by demonstrating that at least maximally spinning tubes, for which we can construct the supergravity solution, have no problem localizing in a region of finite $\widetilde{V}$. As the solution scales, the effective charges diverge, as is needed for entropy enhancement.

11.5 An example

One can construct a very simple deep scaling solution using three Taub-NUT (GH) centers with charges q_1, q_2 and q_3, and fluxes arranged so that the $|\Gamma_{ij}|$, $i, j = 1, 2, 3$, satisfy the triangle inequalities. The GH points then arrange themselves asymptotically as a scaled version of this triangle:

$$r_{ij} \;\to\; \lambda\,|\Gamma_{ij}|\,, \qquad \lambda \to 0\,. \tag{382}$$

One can then take a spectral-flow of this solution so that the second GH point becomes a two-charge supertube. For simplicity, we will choose $q_1\,\Pi^{(2)}_{12} \;=\; q_3\,\Pi^{(2)}_{23}$ so that after the flow the GH charges of the remaining two GH points will be equal and opposite:

$$\tilde{q}_1 \;=\; -\,\tilde{q}_3\,. \tag{383}$$

For $\widetilde{V}_p$ to remain finite in the scaling limit, the supertube must approach the plane equidistant from the remaining GH points.

We have performed a detailed analysis of such solutions and used the absence of CTC's close to the GH points, in the intermediate throat and in the asymptotic region to constrain the possible fluxes. We have found a number of such solutions that have the desired scaling properties for Q_I^{eff} and we have performed extensive numerical analysis to check that there are no regions with CTC's. In particular, we checked numerically that the inverse metric component, g^{tt}, is globally negative and thus the metric is stably causal. We will simply present one example here.

Consider the asymptotically Taub-NUT solution with:

$$q_1 \;=\; 16\,, \qquad q_2 \;=\; 96\,, \qquad q_3 \;=\; -40\,, \qquad \epsilon_0 \;=\; 1\,, \qquad Q_0 \;\equiv\; q_1{+}q_2{+}q_3 \;=\; 72 \tag{384}$$

and

$$k^I_1 \;=\; (8, -88, 8)\,, \qquad k^I_2 \;=\; (0, 96, 0)\,, \qquad k^I_3 \;=\; (20, 64, 20)\,, \tag{385}$$

where Q_0 is the KK monopole charge of the solution. With these parameters one has the following fluxes:

$$\Pi^{(I)}_{12} \;=\; (-\tfrac{1}{2}, \tfrac{13}{2}, -\tfrac{1}{2})\,, \qquad \Pi^{(I)}_{23} \;=\; (-\tfrac{1}{2}, -\tfrac{13}{5}, -\tfrac{1}{2})\,, \qquad \Pi^{(I)}_{13} \;=\; (-1, \tfrac{39}{10}, -1)\,, \tag{386}$$

and

$$\Gamma_{12} \;=\; \Gamma_{23} \;=\; \Gamma_{31} \;=\; 2496\,. \tag{387}$$

In this scaling solution the GH points form an equilateral triangle and thus, after the spectral flow, the supertube will tend to be equidistant from the two GH points of equal and opposite charges (383), and therefore will approach the surface where $\widetilde{V} = 0$.

The solution to the bubble equations yields

$$r_{12} \;=\; \frac{11232\,r_{13}}{11232 + 359\,r_{13}}\,, \qquad r_{23} \;=\; \frac{11232\,r_{13}}{11232 + 731\,r_{13}}\,, \tag{388}$$

which satisfies the triangle inequalities for $r_{13} \leq \frac{11232}{\sqrt{262429}} \approx 21.9$. After spectral flow the value of $\widetilde{V}$ at the location of the supertube (point 2) is

$$\widetilde{V}_2 \;=\; 1 \;+\; \frac{104}{r_{12}} \;-\; \frac{104}{r_{23}} \;=\; -\,\frac{22}{9}\,, \tag{389}$$

independent of r_{13}. In particular, it remains finite and bounded as the three points scale and the distances between them go to zero. The effective charges of the supertube are given by

$$Q_1^{eff} \;=\; Q_3^{eff} \;=\; 384\,\widetilde{V}_2^{-1}\Big(1 \;+\; \frac{52}{r_{12}} \;+\; \frac{52}{r_{23}}\Big)\,, \tag{390}$$

and scale as λ^{-1} as $\lambda \to 0$ in (382). We thus have effective charges that naively scale to arbitrarily large values. As described earlier, we expect this scaling to stop as the supertubes become more and more wiggly, and we expect the entropy to come from configurations of intermediate throat depth.

Finally, this configuration has asymptotic electric, and Kaluza-Klein charges:

$$Q_1 \;=\; 416\,, \qquad Q_2 \;=\; \frac{608}{9}\,, \qquad Q_3 \;=\; 416\,, \qquad J_R \;=\; Q^E_{KK} \;=\; \frac{5824}{9}\,, \qquad Q_0 \;=\; Q^M_{KK} \;=\; 72\,. \tag{391}$$

and is thus a microstate of a Taub-NUT black hole with a finite extremality parameter and a macroscopic horizon:

$$\frac{Q_0\,Q_1\,Q_2\,Q_3 - \frac{1}{4}\,Q_0^2\,J_R^2}{Q_0\,Q_1\,Q_2\,Q_3} \;=\; \frac{27}{76} \;\approx\; 36\%\,. \tag{392}$$

The most important result presented in this section is that the entropy of a supertube in a given background is not determined by its charges, but rather by its "effective charges," which receive a contribution from the interaction of the magnetic dipole moment of the tube with the magnetic fluxes in the background. As a result, one can get very dramatic *entropy enhancement* if a supertube is placed in a suitable background. We have argued that this enhancement can give rise to a macroscopic (black-hole-like) entropy, coming entirely from smooth horizonless configurations.

Three ingredients are needed for this dramatic entropy enhancement:

(i) Deep or scaling solutions

(ii) Ambi-polar base metrics

(iii) BPS fluctuations that localize near the critical ($V = 0$) surfaces of the ambi-polar metrics

These are also precisely the ingredients that have emerged from recent developments in the study of finite-sized black-hole microstates in the regime of parameters where the

gravitational back-reaction of some of the branes is negligible. Indeed, deep scaling ambi-polar configurations are needed both to get a macroscopic entropy in the "quiver quantum mechanics regime" [129], and to get smooth microstates of black holes with macroscopic horizons [42]. Furthermore, the D0 branes that can give a black-hole-like entropy in a D6-$\overline{\text{D6}}$ background [118, 119] must localize near the critical surface of the ambi-polar base, much like the supertubes in our analysis. It would be fascinating to find a link between the microscopic configurations constructed in these papers, and those we consider here.

Acknowledgements

I would like to thank my collaborators, Per Kraus Chih-Wei Wang, Nikolay Bobev, Clément Ruef, and especially Nick Warner, who played instrumental roles in much of the research presented here. I would also like to thank Jan de Boer, Thibault Damour, Gary Gibbons, Eric Gimon, Stefano Giusto, Gary Horowitz, Don Marolf, Samir Mathur, Simon Ross, Kostas Skenderis, Marika Taylor and Eric Verlinde, for interesting discussions that have helped clarify many of the things presented here.

References

[1] S. W. Hawking, "Breakdown Of Predictability In Gravitational Collapse," Phys. Rev. D **14**, 2460 (1976).

"Particle Creation By Black Holes," Commun. Math. Phys. **43**, 199 (1975) [Erratum-ibid. **46**, 206 (1976)].

[2] A. Strominger and C. Vafa, "Microscopic Origin of the Bekenstein-Hawking Entropy," Phys. Lett. B **379**, 99 (1996) [arXiv:hep-th/9601029].

[3] J. M. Maldacena, "The large N limit of superconformal field theories and supergravity," Adv. Theor. Math. Phys. **2**, 231 (1998) [Int. J. Theor. Phys. **38**, 1113 (1999)] [arXiv:hep-th/9711200].

S. S. Gubser, I. R. Klebanov and A. M. Polyakov, "Gauge theory correlators from non-critical string theory," Phys. Lett. B **428**, 105 (1998) [arXiv:hep-th/9802109].

E. Witten, "Anti-de Sitter space and holography," Adv. Theor. Math. Phys. **2**, 253 (1998) [arXiv:hep-th/9802150].

[4] M. Cvetic and A. A. Tseytlin, "Solitonic strings and BPS saturated dyonic black holes," Phys. Rev. D **53**, 5619 (1996) [arXiv:hep-th/9512031]. See also: M. Cvetic and D. Youm, "Dyonic BPS saturated black holes of heterotic string on a six torus," Phys. Rev. D **53** (1996) 584 [arXiv:hep-th/9507090].

[5] O. Lunin and S. D. Mathur, "AdS/CFT duality and the black hole information paradox," Nucl. Phys. B **623**, 342 (2002) [arXiv:hep-th/0109154].

[6] O. Lunin and S. D. Mathur, "Statistical interpretation of Bekenstein entropy for systems with a stretched horizon," Phys. Rev. Lett. **88**, 211303 (2002) [arXiv:hep-th/0202072].

[7] O. Lunin, J. M. Maldacena and L. Maoz, "Gravity solutions for the D1-D5 system with angular momentum," arXiv:hep-th/0212210.

[8] O. Lunin and S. D. Mathur, "The slowly rotating near extremal D1-D5 system as a 'hot tube'," Nucl. Phys. B **615**, 285 (2001) [arXiv:hep-th/0107113].

L. F. Alday, J. de Boer and I. Messamah, "The gravitational description of coarse grained microstates," arXiv:hep-th/0607222.

A. Donos and A. Jevicki, "Dynamics of chiral primaries in AdS(3) x S**3 x T**4," Phys. Rev. D **73**, 085010 (2006) [arXiv:hep-th/0512017].

L. F. Alday, J. de Boer and I. Messamah, "What is the dual of a dipole?," Nucl. Phys. B **746**, 29 (2006) [arXiv:hep-th/0511246].

S. Giusto, S. D. Mathur and Y. K. Srivastava, "Dynamics of supertubes," Nucl. Phys. B **754**, 233 (2006) [arXiv:hep-th/0510235].

M. Taylor, "General 2 charge geometries," JHEP **0603**, 009 (2006) [arXiv:hep-th/0507223].

K. Skenderis and M. Taylor, "Fuzzball solutions and D1-D5 microstates," arXiv:hep-th/0609154.

N. Iizuka and M. Shigemori, "A note on D1-D5-J system and 5D small black ring," JHEP **0508**, 100 (2005) [arXiv:hep-th/0506215].

M. Boni and P. J. Silva, "Revisiting the D1/D5 system or bubbling in AdS(3)," JHEP **0510**, 070 (2005) [arXiv:hep-th/0506085].

D. Martelli and J. F. Morales, "Bubbling AdS(3)," JHEP **0502**, 048 (2005) [arXiv:hep-th/0412136].

Y. K. Srivastava, "Bound states of KK monopole and momentum," arXiv:hep-th/0611124.

[9] D. Z. Freedman, S. D. Mathur, A. Matusis and L. Rastelli, "Correlation functions in the CFT(d)/AdS($d+1$) correspondence," Nucl. Phys. B **546**, 96 (1999) [arXiv:hep-th/9804058].

[10] V. Balasubramanian, P. Kraus and M. Shigemori, "Massless black holes and black rings as effective geometries of the D1-D5 system," Class. Quant. Grav. **22**, 4803 (2005) [arXiv:hep-th/0508110].

[11] I. Kanitscheider, K. Skenderis and M. Taylor, "Holographic anatomy of fuzzballs," arXiv:hep-th/0611171.

[12] I. Kanitscheider, K. Skenderis and M. Taylor, "Fuzzballs with internal excitations," arXiv:0704.0690 [hep-th].

[13] A. A. Tseytlin, "Extreme dyonic black holes in string theory," Mod. Phys. Lett. A **11**, 689 (1996) [arXiv:hep-th/9601177].

A. A. Tseytlin, "Extremal black hole entropy from conformal string sigma model," Nucl. Phys. B **477**, 431 (1996) [arXiv:hep-th/9605091].

[14] S. D. Mathur, "The fuzzball proposal for black holes: An elementary review," Fortsch. Phys. **53**, 793 (2005) [arXiv:hep-th/0502050].

S. D. Mathur, "The quantum structure of black holes," Class. Quant. Grav. **23**, R115 (2006) [arXiv:hep-th/0510180].

[15] I. Bena and N. P. Warner, "Black holes, black rings and their microstates," arXiv:hep-th/0701216.

[16] K. Skenderis and M. Taylor, "The fuzzball proposal for black holes," arXiv:0804.0552 [hep-th].

[17] V. Balasubramanian, J. de Boer, S. El-Showk and I. Messamah, "Black Holes as Effective Geometries," Class. Quant. Grav. **25**, 214004 (2008) [arXiv:0811.0263 [hep-th]].

[18] W. G. Unruh and R. M. Wald, 'Acceleration Radiation And Generalized Second Law Of Thermodynamics," Phys. Rev. D **25**, 942 (1982).

[19] W. G. Unruh and R. M. Wald, "Entropy Bounds, Acceleration Radiation, And The Generalized Second Law," Phys. Rev. D **27**, 2271 (1983).

[20] D. Marolf and R. Sorkin, "Perfect mirrors and the self-accelerating box paradox," Phys. Rev. D **66**, 104004 (2002) [arXiv:hep-th/0201255].

[21] B. C. Palmer and D. Marolf, "Counting supertubes," JHEP **0406**, 028 (2004) [arXiv:hep-th/0403025].

V. S. Rychkov, "D1-D5 black hole microstate counting from supergravity," JHEP **0601**, 063 (2006) [arXiv:hep-th/0512053].

D. Bak, Y. Hyakutake and N. Ohta, "Phase moduli space of supertubes," Nucl. Phys. B **696**, 251 (2004) [arXiv:hep-th/0404104].

D. Bak, Y. Hyakutake, S. Kim and N. Ohta, "A geometric look on the microstates of supertubes," Nucl. Phys. B **712**, 115 (2005) [arXiv:hep-th/0407253].

[22] D. Mateos and P. K. Townsend, "Supertubes," Phys. Rev. Lett. **87**, 011602 (2001) [arXiv:hep-th/0103030].

[23] D. Mateos, S. Ng and P. K. Townsend, "Supercurves," Phys. Lett. B **538**, 366 (2002) [arXiv:hep-th/0204062].

[24] R. Emparan, D. Mateos and P. K. Townsend, "Supergravity supertubes," JHEP **0107**, 011 (2001) [arXiv:hep-th/0106012].

[25] O. Lunin and S. D. Mathur, "Metric of the multiply wound rotating string," Nucl. Phys. B **610**, 49 (2001) [arXiv:hep-th/0105136].

[26] A. Sen, "Extremal black holes and elementary string states," Mod. Phys. Lett. A **10**, 2081 (1995) [arXiv:hep-th/9504147].

[27] I. Bena and P. Kraus, "Three charge supertubes and black hole hair," Phys. Rev. D **70**, 046003 (2004) [arXiv:hep-th/0402144].

[28] J. R. David, G. Mandal and S. R. Wadia, "Microscopic formulation of black holes in string theory," Phys. Rept. **369**, 549 (2002) [arXiv:hep-th/0203048].

[29] O. Aharony, S. S. Gubser, J. M. Maldacena, H. Ooguri and Y. Oz, "Large N field theories, string theory and gravity," Phys. Rept. **323**, 183 (2000) [arXiv:hep-th/9905111].

[30] S. Giusto, S. D. Mathur and A. Saxena, "Dual geometries for a set of 3-charge microstates," Nucl. Phys. B **701**, 357 (2004) [arXiv:hep-th/0405017].

[31] S. Giusto, S. D. Mathur and A. Saxena, "3-charge geometries and their CFT duals," Nucl. Phys. B **710**, 425 (2005) [arXiv:hep-th/0406103].

[32] S. Giusto and S. D. Mathur, "Geometry of D1-D5-P bound states," Nucl. Phys. B **729**, 203 (2005) [arXiv:hep-th/0409067].

[33] S. Giusto, S. D. Mathur and Y. K. Srivastava, "A microstate for the 3-charge black ring," arXiv:hep-th/0601193.

[34] O. Lunin, "Adding momentum to D1-D5 system," JHEP **0404**, 054 (2004) [arXiv:hep-th/0404006].

[35] I. Bena and P. Kraus, "Microstates of the D1-D5-KK system," Phys. Rev. D **72**, 025007 (2005) [arXiv:hep-th/0503053].

[36] I. Bena and N. P. Warner, "Bubbling supertubes and foaming black holes," Phys. Rev. D **74**, 066001 (2006) [arXiv:hep-th/0505166].

[37] P. Berglund, E. G. Gimon and T. S. Levi, "Supergravity microstates for BPS black holes and black rings," JHEP **0606**, 007 (2006) [arXiv:hep-th/0505167].

[38] A. Saxena, G. Potvin, S. Giusto and A. W. Peet, "Smooth geometries with four charges in four dimensions," JHEP **0604** (2006) 010 [arXiv:hep-th/0509214].

[39] S. Giusto, S. D. Mathur and Y. K. Srivastava, "A microstate for the 3-charge black ring," arXiv:hep-th/0601193.

[40] I. Bena, C. W. Wang and N. P. Warner, "The foaming three-charge black hole," arXiv:hep-th/0604110.

[41] V. Balasubramanian, E. G. Gimon and T. S. Levi, "Four dimensional black hole microstates: From D-branes to spacetime foam," arXiv:hep-th/0606118.

[42] I. Bena, C. W. Wang and N. P. Warner, "Mergers and typical black hole microstates," JHEP **0611**, 042 (2006) [arXiv:hep-th/0608217].

[43] I. Bena, C. W. Wang and N. P. Warner, "Plumbing the Abyss: Black Ring Microstates," JHEP **0807**, 019 (2008) [arXiv:0706.3786 [hep-th]].

[44] M. C. N. Cheng, "More bubbling solutions," arXiv:hep-th/0611156.

[45] I. Bena and P. Kraus, "Microscopic description of black rings in AdS/CFT," JHEP **0412**, 070 (2004) [arXiv:hep-th/0408186].

[46] A. Dabholkar, "Exact counting of black hole microstates," Phys. Rev. Lett. **94**, 241301 (2005) [arXiv:hep-th/0409148].

[47] S. Ferrara and R. Kallosh, "Supersymmetry and Attractors," Phys. Rev. D **54**, 1514 (1996) [arXiv:hep-th/9602136].

[48] H. Ooguri, A. Strominger and C. Vafa, "Black hole attractors and the topological string," Phys. Rev. D **70**, 106007 (2004) [arXiv:hep-th/0405146].

[49] P. Kraus, "Lectures on black holes and the AdS(3)/CFT(2) correspondence," arXiv:hep-th/0609074.

B. Pioline, "Lectures on on black holes, topological strings and quantum attractors," Class. Quant. Grav. **23**, S981 (2006) [arXiv:hep-th/0607227].

[50] A. Sen, "How does a fundamental string stretch its horizon?," JHEP **0505**, 059 (2005) [arXiv:hep-th/0411255].

A. Dabholkar, F. Denef, G. W. Moore and B. Pioline, "Precision counting of small black holes," JHEP **0510**, 096 (2005) [arXiv:hep-th/0507014].

A. Dabholkar, F. Denef, G. W. Moore and B. Pioline, "Exact and asymptotic degeneracies of small black holes," JHEP **0508**, 021 (2005) [arXiv:hep-th/0502157].

A. Dabholkar, N. Iizuka, A. Iqubal, A. Sen and M. Shigemori, "Spinning strings as small black rings," arXiv:hep-th/0611166.

A. Dabholkar, A. Sen and S. Trivedi, "Black hole microstates and attractor without supersymmetry," arXiv:hep-th/0611143.

[51] D. Astefanesei, K. Goldstein and S. Mahapatra, "Moduli and (un)attractor black hole thermodynamics," arXiv:hep-th/0611140.

A. Sen, "Black hole entropy function and the attractor mechanism in higher derivative gravity," JHEP **0509**, 038 (2005) [arXiv:hep-th/0506177].

P. Kraus and F. Larsen, "Holographic gravitational anomalies," JHEP **0601**, 022 (2006) [arXiv:hep-th/0508218].

P. Kraus and F. Larsen, "Microscopic black hole entropy in theories with higher derivatives," JHEP **0509**, 034 (2005) [arXiv:hep-th/0506176].

S. Giusto and S. D. Mathur, "Fuzzball geometries and higher derivative corrections for extremal holes," Nucl. Phys. B **738**, 48 (2006) [arXiv:hep-th/0412133].

[52] J. M. Maldacena, J. Michelson and A. Strominger, "Anti-de Sitter fragmentation," JHEP **9902**, 011 (1999) [arXiv:hep-th/9812073].

[53] I. Bena and N. P. Warner, "One ring to rule them all ... and in the darkness bind them?," Adv. Theor. Math. Phys. **9** (2005) 667-701 [arXiv:hep-th/0408106.]

[54] I. Bena, C. W. Wang and N. P. Warner, "Black rings with varying charge density," JHEP **0603**, 015 (2006) [arXiv:hep-th/0411072].

[55] I. Bena, "Splitting hairs of the three charge black hole," Phys. Rev. D **70**, 105018 (2004) [arXiv:hep-th/0404073].

[56] W. I. Taylor, "Adhering 0-branes to 6-branes and 8-branes," Nucl. Phys. B **508**, 122 (1997) [arXiv:hep-th/9705116].

[57] J.D. Jackson, *Classical Electrodynamics,* Wiley, New York, NY, 1975.

[58] J. C. Breckenridge, R. C. Myers, A. W. Peet and C. Vafa, "D-branes and spinning black holes," Phys. Lett. B **391**, 93 (1997) [arXiv:hep-th/9602065].

[59] C. A. R. Herdeiro, "Special properties of five dimensional BPS rotating black holes," Nucl. Phys. B **582**, 363 (2000) [arXiv:hep-th/0003063].

[60] G. T. Horowitz and J. Polchinski, "A correspondence principle for black holes and strings," Phys. Rev. D **55**, 6189 (1997) [arXiv:hep-th/9612146].

[61] H. S. Reall, "Higher dimensional black holes and supersymmetry," Phys. Rev. D **68**, 024024 (2003) [arXiv:hep-th/0211290].

[62] H. Elvang, R. Emparan, D. Mateos and H. S. Reall, "A supersymmetric black ring," Phys. Rev. Lett. **93**, 211302 (2004) [arXiv:hep-th/0407065].

[63] H. Elvang, R. Emparan, D. Mateos and H. S. Reall, "Supersymmetric black rings and three-charge supertubes," Phys. Rev. D **71**, 024033 (2005) [arXiv:hep-th/0408120].

[64] J. P. Gauntlett and J. B. Gutowski, "General concentric black rings," Phys. Rev. D **71**, 045002 (2005) [arXiv:hep-th/0408122].

[65] S. W. Hawking, "Gravitational Instantons," Phys. Lett. A **60**, 81 (1977).

[66] D. Gaiotto, A. Strominger and X. Yin, "New connections between 4D and 5D black holes," JHEP **0602**, 024 (2006) [arXiv:hep-th/0503217].

[67] D. Gaiotto, A. Strominger and X. Yin, "5D black rings and 4D black holes," JHEP **0602**, 023 (2006) [arXiv:hep-th/0504126].

[68] H. Elvang, R. Emparan, D. Mateos and H. S. Reall, "Supersymmetric 4D rotating black holes from 5D black rings," JHEP **0508**, 042 (2005) [arXiv:hep-th/0504125].

[69] I. Bena, P. Kraus and N. P. Warner, "Black rings in Taub-NUT," Phys. Rev. D **72**, 084019 (2005) [arXiv:hep-th/0504142].

[70] I. R. Klebanov and A. A. Tseytlin, "Gravity duals of supersymmetric SU(N) x SU(N+M) gauge theories," Nucl. Phys. B **578**, 123 (2000) [arXiv:hep-th/0002159].

[71] I. R. Klebanov and M. J. Strassler, "Supergravity and a confining gauge theory: Duality cascades and χSB-resolution of naked singularities," JHEP **0008**, 052 (2000) [arXiv:hep-th/0007191].

[72] A. W. Peet, "TASI lectures on black holes in string theory," arXiv:hep-th/0008241.

[73] R. Emparan and H. S. Reall, "Black rings," Class. Quant. Grav. **23**, R169 (2006) [arXiv:hep-th/0608012].

[74] H. Elvang and P. Figueras, "Black Saturn," arXiv:hep-th/0701035.

R. Emparan and H. S. Reall, "A rotating black ring in five dimensions," Phys. Rev. Lett. **88**, 101101 (2002) [arXiv:hep-th/0110260]. R. Emparan, "Rotating circular strings, and infinite non-uniqueness of black rings," JHEP **0403**, 064 (2004) [arXiv:hep-th/0402149].

H. Elvang and R. Emparan, "Black rings, supertubes, and a stringy resolution of black hole non-uniqueness," JHEP **0311**, 035 (2003) [arXiv:hep-th/0310008].

[75] I. Bena, C. W. Wang and N. P. Warner, "Sliding rings and spinning holes," JHEP **0605**, 075 (2006) [arXiv:hep-th/0512157].

[76] G. W. Gibbons and S. W. Hawking, "Gravitational Multi - Instantons," Phys. Lett. B **78**, 430 (1978).

[77] G. W. Gibbons and P. J. Ruback, "The Hidden Symmetries of Multi-Center Metrics," Commun. Math. Phys. **115**, 267 (1988).

[78] J. P. Gauntlett, J. B. Gutowski, C. M. Hull, S. Pakis and H. S. Reall, "All supersymmetric solutions of minimal supergravity in five dimensions," Class. Quant. Grav. **20**, 4587 (2003) [arXiv:hep-th/0209114].

[79] R. Kallosh and B. Kol, "E(7) Symmetric Area of the Black Hole Horizon," Phys. Rev. D **53**, 5344 (1996) [arXiv:hep-th/9602014].

[80] F. Denef, "Supergravity flows and D-brane stability," JHEP **0008**, 050 (2000) [arXiv:hep-th/0005049].

B. Bates and F. Denef, "Exact solutions for supersymmetric stationary black hole composites," arXiv:hep-th/0304094.

F. Denef, "Quantum quivers and Hall/hole halos," JHEP **0210**, 023 (2002) [arXiv:hep-th/0206072].

[81] K. Behrndt, G. Lopes Cardoso and S. Mahapatra, "Exploring the relation between 4D and 5D BPS solutions," Nucl. Phys. B **732**, 200 (2006) [arXiv:hep-th/0506251].

[82] S.W. Hawking and G.F.R. Ellis, *The Large Scale Structure of Space-Time,* Cambridge University Press, 1975.

[83] V. Jejjala, O. Madden, S. F. Ross and G. Titchener, "Non-supersymmetric smooth geometries and D1-D5-P bound states," Phys. Rev. D **71**, 124030 (2005) [arXiv:hep-th/0504181].

[84] V. Cardoso, O. J. C. Dias, J. L. Hovdebo and R. C. Myers, "Instability of non-supersymmetric smooth geometries," Phys. Rev. D **73**, 064031 (2006) [arXiv:hep-th/0512277].

[85] J. P. Gauntlett and J. B. Gutowski, "Concentric black rings," Phys. Rev. D **71**, 025013 (2005) [arXiv:hep-th/0408010].

[86] M. Cyrier, M. Guica, D. Mateos and A. Strominger, "Microscopic entropy of the black ring," Phys. Rev. Lett. **94**, 191601 (2005) [arXiv:hep-th/0411187].

[87] J. M. Maldacena, A. Strominger and E. Witten, "Black hole entropy in M-theory," JHEP **9712**, 002 (1997) [arXiv:hep-th/9711053].

[88] M. Bertolini and M. Trigiante, "Microscopic entropy of the most general four-dimensional BPS black hole," JHEP **0010**, 002 (2000) [arXiv:hep-th/0008201].

[89] R. Dijkgraaf, J. M. Maldacena, G. W. Moore and E. P. Verlinde, "A black hole farey tail," arXiv:hep-th/0005003. P. Kraus and F. Larsen, "Partition functions and elliptic genera from supergravity," arXiv:hep-th/0607138. J. de Boer, M. C. N. Cheng, R. Dijkgraaf, J. Manschot and E. Verlinde, "A farey tail for attractor black holes," JHEP **0611**, 024 (2006) [arXiv:hep-th/0608059].

[90] G. T. Horowitz and H. S. Reall, "How hairy can a black ring be?," Class. Quant. Grav. **22**, 1289 (2005) [arXiv:hep-th/0411268].

[91] M. Guica, L. Huang, W. Li and A. Strominger, JHEP **0610**, 036 (2006) [arXiv:hep-th/0505188].

[92] I. Bena and P. Kraus, "R**2 corrections to black ring entropy," arXiv:hep-th/0506015.

[93] R. Gopakumar and C. Vafa, "On the gauge theory/geometry correspondence," Adv. Theor. Math. Phys. **3**, 1415 (1999) [arXiv:hep-th/9811131].

[94] C. Vafa, "Superstrings and topological strings at large N," J. Math. Phys. **42**, 2798 (2001) [arXiv:hep-th/0008142].

[95] H. Lin, O. Lunin and J. M. Maldacena, "Bubbling AdS space and 1/2 BPS geometries," JHEP **0410**, 025 (2004) [arXiv:hep-th/0409174].

[96] F. Cachazo, K. A. Intriligator and C. Vafa, "A large N duality via a geometric transition," Nucl. Phys. B **603**, 3 (2001) [arXiv:hep-th/0103067].

[97] M. Cvetic and F. Larsen, "Near horizon geometry of rotating black holes in five dimensions," Nucl. Phys. B **531**, 239 (1998) [arXiv:hep-th/9805097].

[98] J. M. Maldacena and L. Susskind, "D-branes and Fat Black Holes," Nucl. Phys. B **475**, 679 (1996) [arXiv:hep-th/9604042].

[99] J. Polchinski and M. J. Strassler, "The string dual of a confining four-dimensional gauge theory," arXiv:hep-th/0003136.

[100] L. Girardello, M. Petrini, M. Porrati and A. Zaffaroni, "The supergravity dual of N = 1 super Yang-Mills theory," Nucl. Phys. B **569**, 451 (2000) [arXiv:hep-th/9909047].

[101] K. Pilch and N. P. Warner, "N = 1 supersymmetric renormalization group flows from IIB supergravity," Adv. Theor. Math. Phys. **4**, 627 (2002) [arXiv:hep-th/0006066].

[102] J. McGreevy, L. Susskind and N. Toumbas, "Invasion of the giant gravitons from anti-de Sitter space," JHEP **0006**, 008 (2000) [arXiv:hep-th/0003075]. M. T. Grisaru, R. C. Myers and O. Tafjord, "SUSY and Goliath," JHEP **0008** (2000) 040 [arXiv:hep-th/0008015]. S. R. Das, A. Jevicki and S. D. Mathur, "Giant gravitons, BPS bounds and noncommutativity," Phys. Rev. D **63**, 044001 (2001) [arXiv:hep-th/0008088].

A. Hashimoto, S. Hirano and N. Itzhaki, "Large branes in AdS and their field theory dual," JHEP **0008**, 051 (2000) [arXiv:hep-th/0008016].

[103] I. Bena and D. J. Smith, "Towards the solution to the giant graviton puzzle," Phys. Rev. D **71**, 025005 (2005) [arXiv:hep-th/0401173].

[104] I. Bena and C. Ciocarlie, "Exact N = 2 supergravity solutions with polarized branes," Phys. Rev. D **70**, 086005 (2004) [arXiv:hep-th/0212252]. I. Bena and R. Roiban, "N = 1* in 5 dimensions: Dijkgraaf-Vafa meets Polchinski-Strassler," JHEP **0311**, 001 (2003) [arXiv:hep-th/0308013].

[105] Y. K. Srivastava, "Perturbations of supertube in KK monopole background," arXiv:hep-th/0611320.

[106] Ashish Saxena, General 3-charge geometries in 4 dimensions (to appear)

[107] S. R. Das and S. D. Mathur, "Excitations of D-strings, Entropy and Duality," Phys. Lett. B **375**, 103 (1996) [arXiv:hep-th/9601152].

[108] J. M. Maldacena and L. Susskind, "D-branes and Fat Black Holes," Nucl. Phys. B **475**, 679 (1996) [arXiv:hep-th/9604042].

[109] C. G. . Callan and J. M. Maldacena, "D-brane Approach to Black Hole Quantum Mechanics," Nucl. Phys. B **472**, 591 (1996) [arXiv:hep-th/9602043].

J. M. Maldacena, "Statistical Entropy of Near Extremal Five-branes," Nucl. Phys. B **477**, 168 (1996) [arXiv:hep-th/9605016].

[110] U. H. Danielsson, A. Guijosa and M. Kruczenski, "Brane-antibrane systems at finite temperature and the entropy of black branes," JHEP **0109**, 011 (2001) [arXiv:hep-th/0106201].

[111] R. Emparan and G. T. Horowitz, "Microstates of a neutral black hole in M theory," Phys. Rev. Lett. **97**, 141601 (2006) [arXiv:hep-th/0607023].

[112] B. D. Chowdhury and S. D. Mathur, "Fractional brane state in the early universe," arXiv:hep-th/0611330.

[113] R. Gregory and R. Laflamme, "Black strings and p-branes are unstable," Phys. Rev. Lett. **70**, 2837 (1993) [arXiv:hep-th/9301052]. For a review see: T. Harmark, V. Niarchos and N. A. Obers, "Instabilities of black strings and branes," arXiv:hep-th/0701022.

[114] B. D. Chowdhury, S. Giusto and S. D. Mathur, "A microscopic model for the black hole - black string phase transition," arXiv:hep-th/0610069.

[115] T. Harmark, K. R. Kristjansson, N. A. Obers and P. B. Ronne, "Three-charge black holes on a circle," arXiv:hep-th/0606246.

[116] J. M. Maldacena, "Eternal black holes in Anti-de-Sitter," JHEP **0304**, 021 (2003) [arXiv:hep-th/0106112].

[117] V. Balasubramanian, B. Czech, V. Hubeny, K. Larjo, M. Rangamani and J. Simon, "Typicality versus thermality: An analytic distinction," arXiv:hep-th/0701122. V. Balasubramanian, J. de Boer, V. Jejjala and J. Simon, "The library of Babel: On the origin of gravitational thermodynamics," JHEP **0512**, 006 (2005) [arXiv:hep-th/0508023].

[118] F. Denef, D. Gaiotto, A. Strominger, D. Van den Bleeken and X. Yin, "Black hole deconstruction," arXiv:hep-th/0703252.

[119] E. G. Gimon and T. S. Levi, "Black Ring Deconstruction," arXiv:0706.3394 [hep-th].

[120] P. O. Mazur and E. Mottola, "Gravitational condensate stars," arXiv:gr-qc/0109035.

P. O. Mazur and E. Mottola, "Gravitational vacuum condensate stars," Proc. Nat. Acad. Sci. **101** (2004) 9545 [arXiv:gr-qc/0407075].

[121] A. Ashtekar and M. Bojowald, "Black hole evaporation: A paradigm," Class. Quant. Grav. **22**, 3349 (2005) [arXiv:gr-qc/0504029].

[122] J. de Boer, S. El-Showk, I. Messamah and D. V. d. Bleeken, "Quantizing N=2 Multicenter Solutions," arXiv:0807.4556 [hep-th].

[123] I. Bena, N. Bobev, C. Ruef and N. P. Warner, "Entropy Enhancement and Black Hole Microstates," arXiv:0804.4487 [hep-th].

[124] B. C. Palmer and D. Marolf, "Counting supertubes," JHEP **0406**, 028 (2004) [arXiv:hep-th/0403025].

[125] D. Bak, Y. Hyakutake, S. Kim and N. Ohta, "A geometric look on the microstates of supertubes," Nucl. Phys. B **712**, 115 (2005) [arXiv:hep-th/0407253].

[126] V. S. Rychkov, "D1-D5 black hole microstate counting from supergravity," JHEP **0601**, 063 (2006) [arXiv:hep-th/0512053].

[127] I. Bena, N. Bobev and N. P. Warner, "Spectral Flow, and the Spectrum of Multi-Center Solutions," Phys. Rev. D **77**, 125025 (2008) [arXiv:0803.1203 [hep-th]].

[128] J. Ford, S. Giusto and A. Saxena, "A class of BPS time-dependent three-charge microstates from spectral flow," Nucl. Phys. B **790**, 258 (2008) [arXiv:hep-th/0612227].

[129] F. Denef and G. W. Moore, "Split states, entropy enigmas, holes and halos," arXiv:hep-th/0702146.

[130] I. Bena, N. Bobev, C. Ruef and N. P. Warner, "Supertubes in Bubbling Backgrounds: Born-Infeld Meets Supergravity," arXiv:0812.2942 [hep-th].